10/04-15 - INRIA - Sophia-Antipolis

Journées Alain Dervieux - INRIA

Modélisation et simulation de la turbulence

par

Marianna BRAZA

Directrice de Recherche CNRS
Institut de Mécanique des Fluides de Toulouse UMR-CNRS-5502

Contribution:

G. Harran, D. Szubert, F. Grossi, T. Deloze, Y. Hoarau, I. Asproulias, E. Deri, H. Ouvrard

Turbulence modelling and simulation involving Fluid Structure Interaction
Applications in:

Aeronautics
Marine hydrodynamics,
Nuclear Eng., Gas & Oil Eng.

National Projects: ANR-*ECINADS**

Ecoulements instationnaires turbulents et adjoints par Simulation Numérique de Haute Performance

EU Projects in aeronautics

FLOMANIA DESider UFAST ATAAC SEVENTH FRAMEWORK PROGRAMME

TFAST ***ETMA**** ***ECARP*** UNSI

* *Coordinated by Alain Dervieux*

Exemples : génie nucléaire

Dans les réacteurs à eau préssurisé, une grappe de tube (contenant des pastilles de combustibles) est utilisé pour contrôler la vitesse de la récation en chaîne et donc la puissane dégagée : tubes déformables dans un écoulement mulphasique très perturbé.

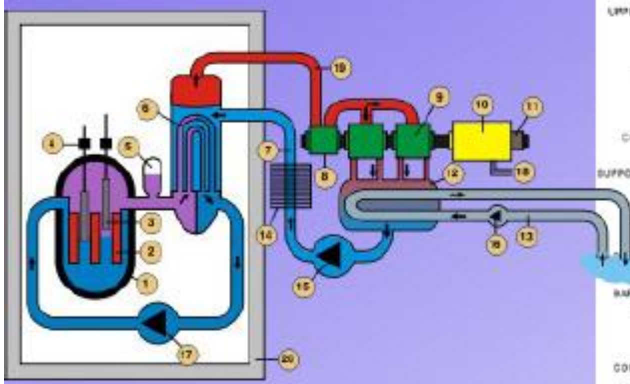

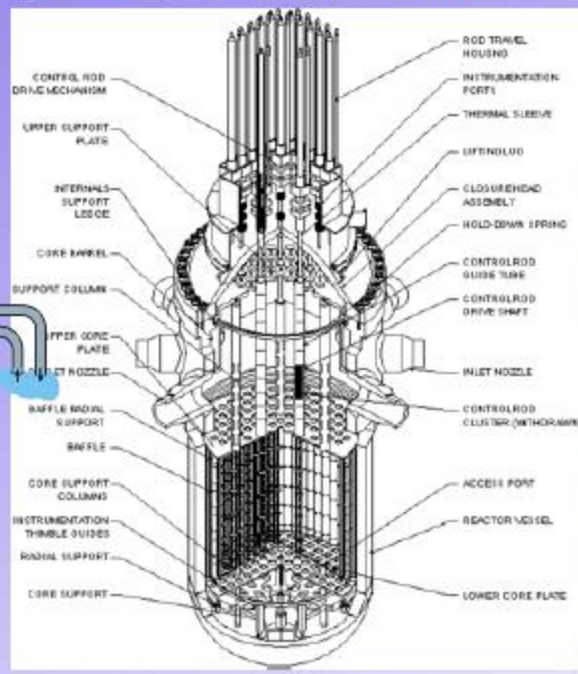

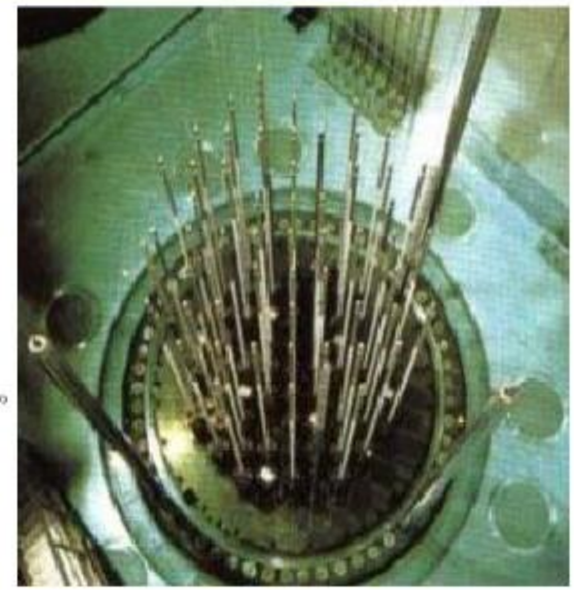

ANR programme BARESAFE « Simulation of Safety Barrier Reliability coordinated by EDF : partners: CEA, AREVA, IMFT, ICUBE

Fluid-Structure interaction in an array of cylinders. Cooling system - heat exchanger - nuclear reactor. IMFT collaboration with EDF, CEA and AREVA - ANR BARESAFE. Inter-tube Reynolds N° ~60 000

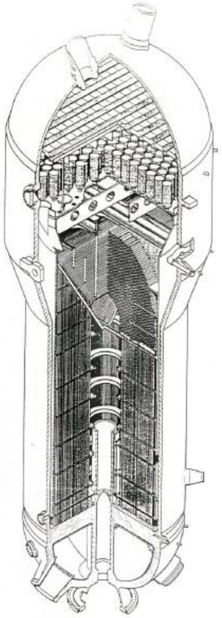

Steam generator : bundle of tubes

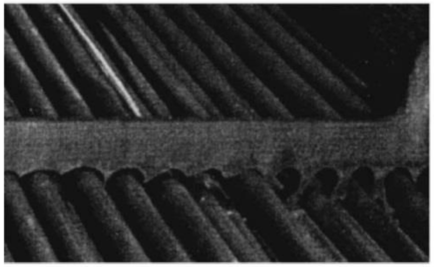

Exemple of tube break

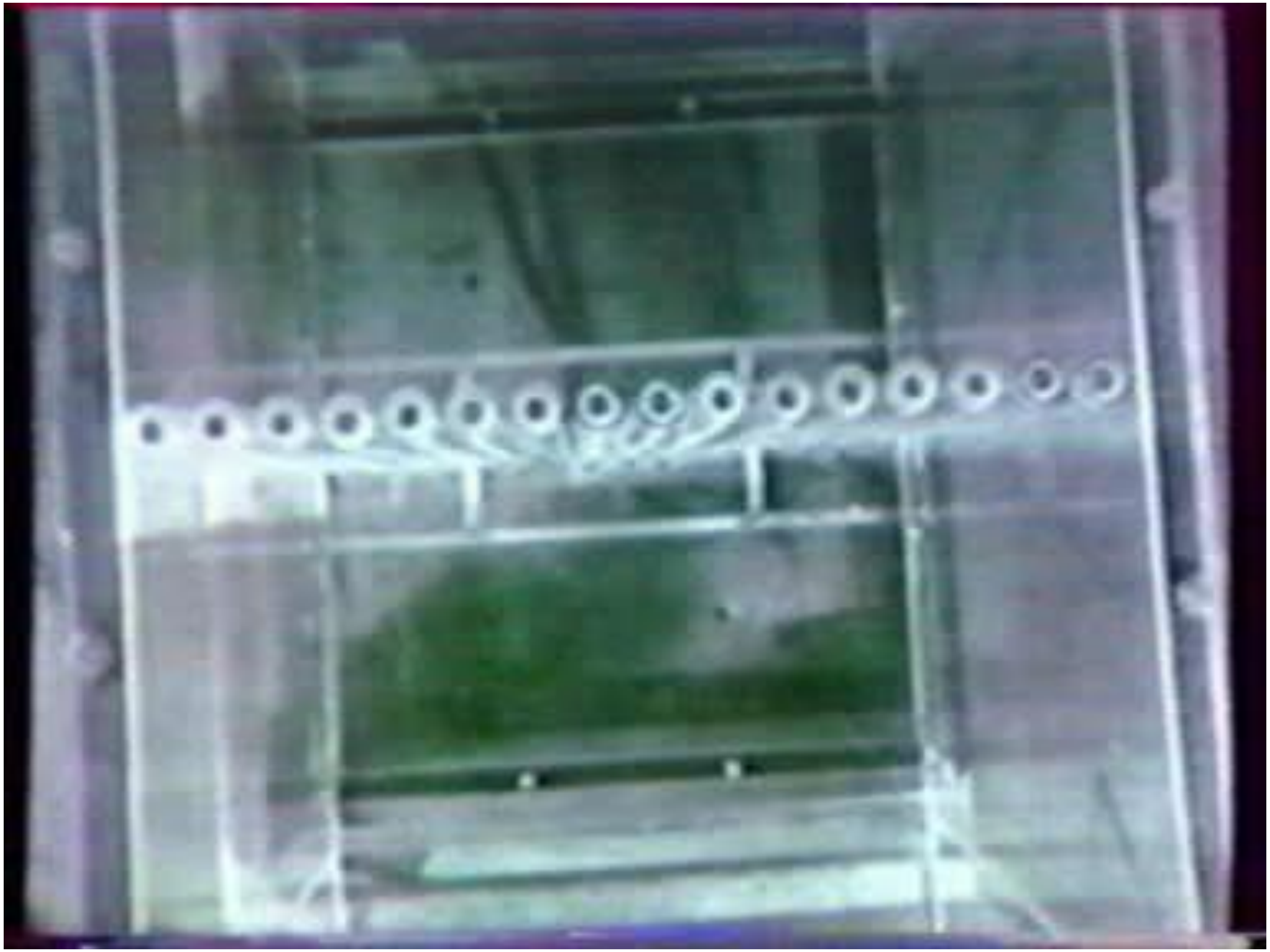

Movie : Courtesy of CEA: Commisariat d’Etudes Atomiques, Experiment ‘DIVA’

Tandem Cylinders for landing gear IMFT participation in EU program ATAAC*

- Generic configuration of the two cylinders of a **landing gear**
- Movement Induced Vibrations
    - Unsteady vortex structures
    - Aerodynamic noise
- Usefulness: future strategies for <u>noise reduction</u> and <u>stability</u> of a landing gear

***Advanced Turbulence simulations for Aerodynamics Applications Challenges**

Applications in aerodynamics

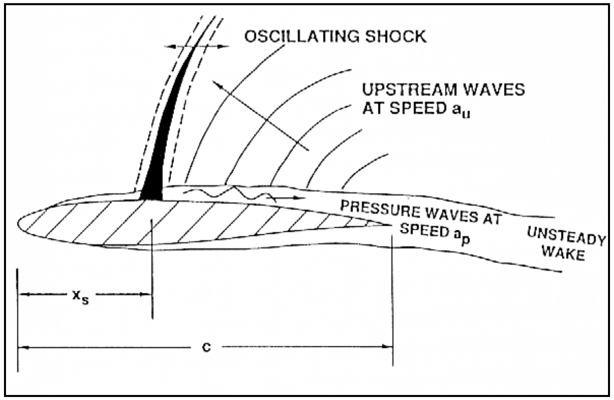

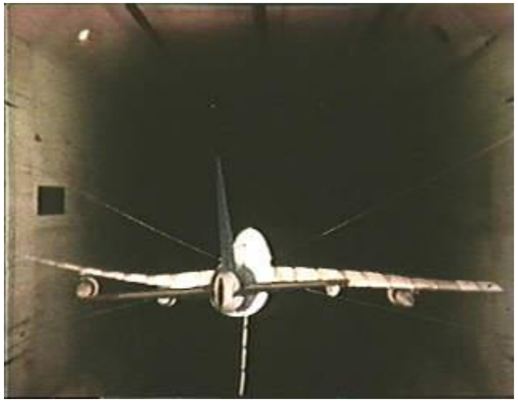

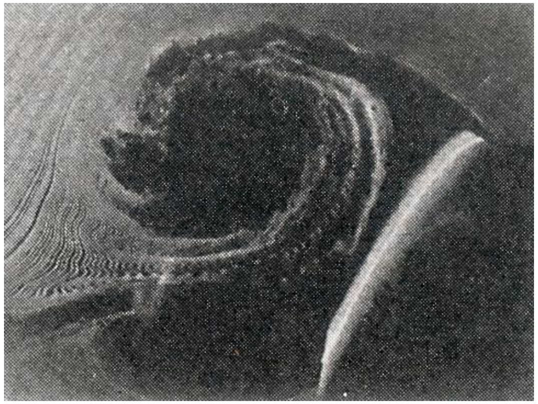

Buffeting	Flutter phenomenon	Dynamic stall
•Drag increase •Vibrations	Structure destruction	Sudden lift loss
• materials fatigue • Reduction of the range of operation	•Structure enforcement •Velocity reduction	• Manoeuvrability limitation •Velocity reduction (helicopter)

Unsteady aerodynamics and aeroelasticity:

High-Reynolds number flows with thin interfaces

rotational/irrotational region

Wall flows:Turbulence onset from near-wall

Near-wake modeling : Decisive for reliability of the overall simulation and for accurate prediction of forces

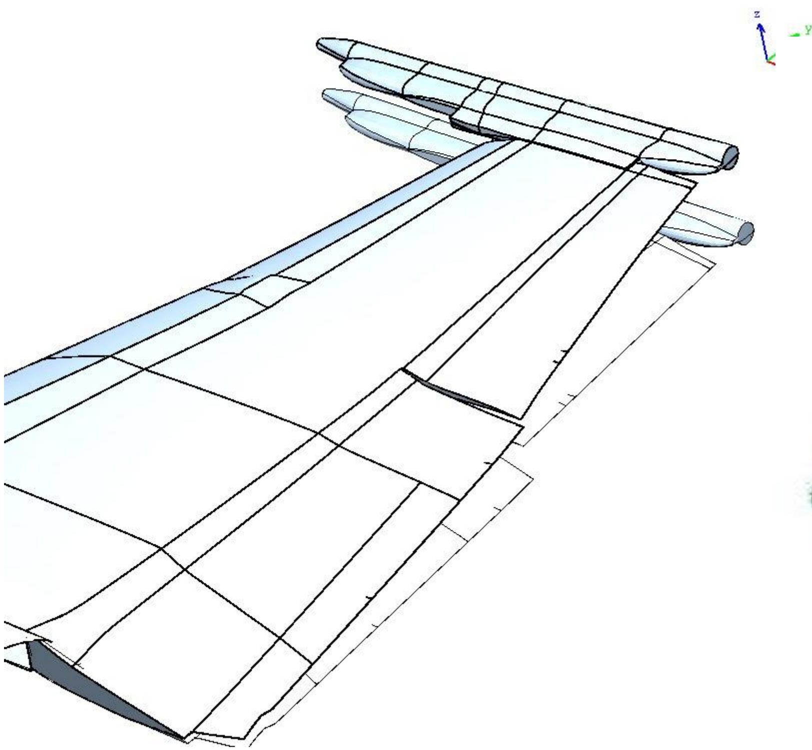

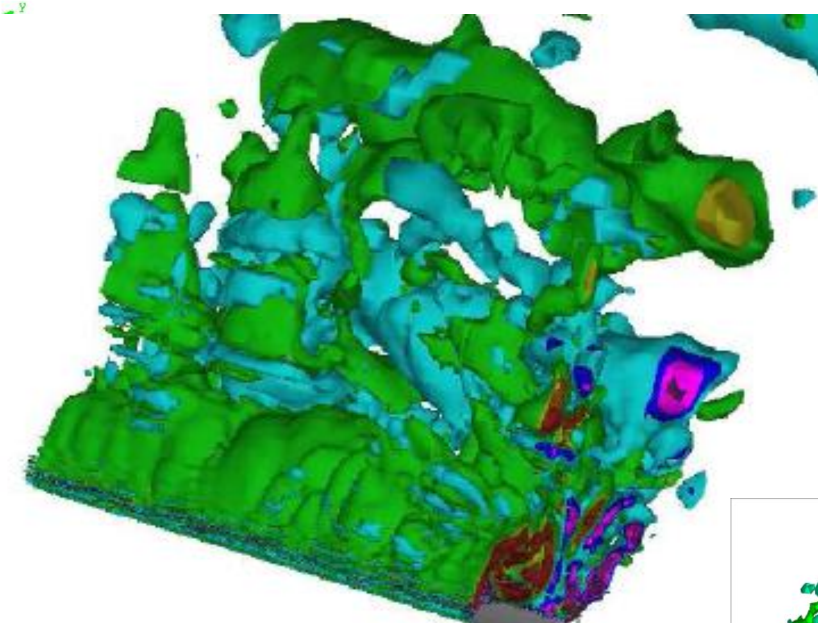

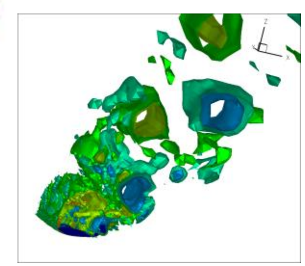

Improved statistical (URANS) and Hybrid (URANS-LES) Turbulence modelling accounting for non - equilibrium turbulence in strongly detached flow regions

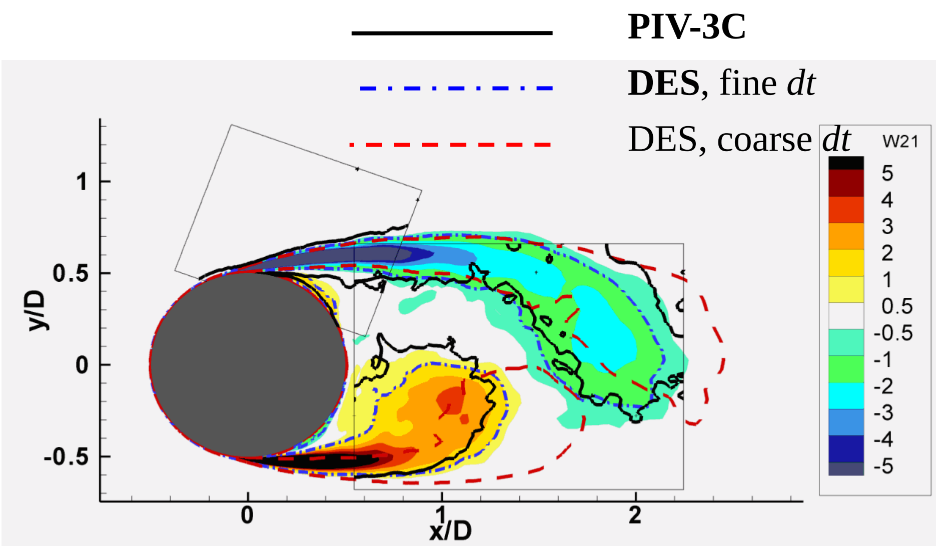

Comparison DES – PIV-3C - movie

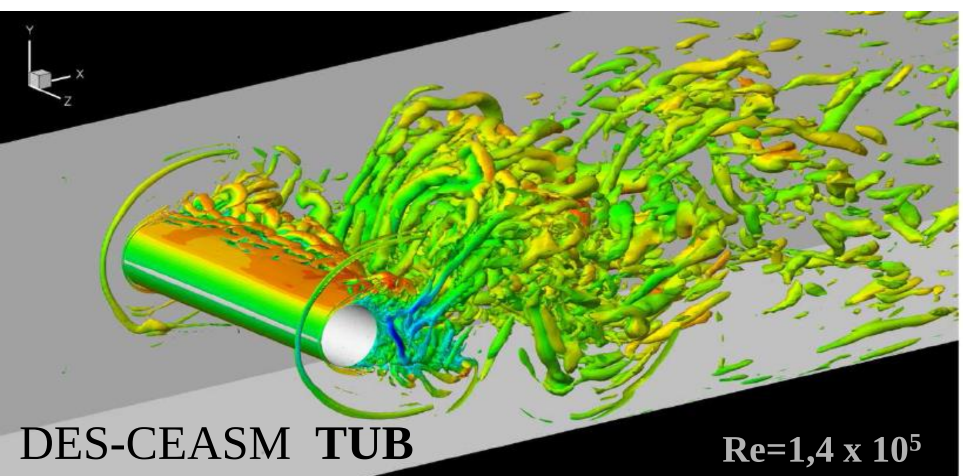

Isosurfaces of λ_2, shaded with streamwise velocity

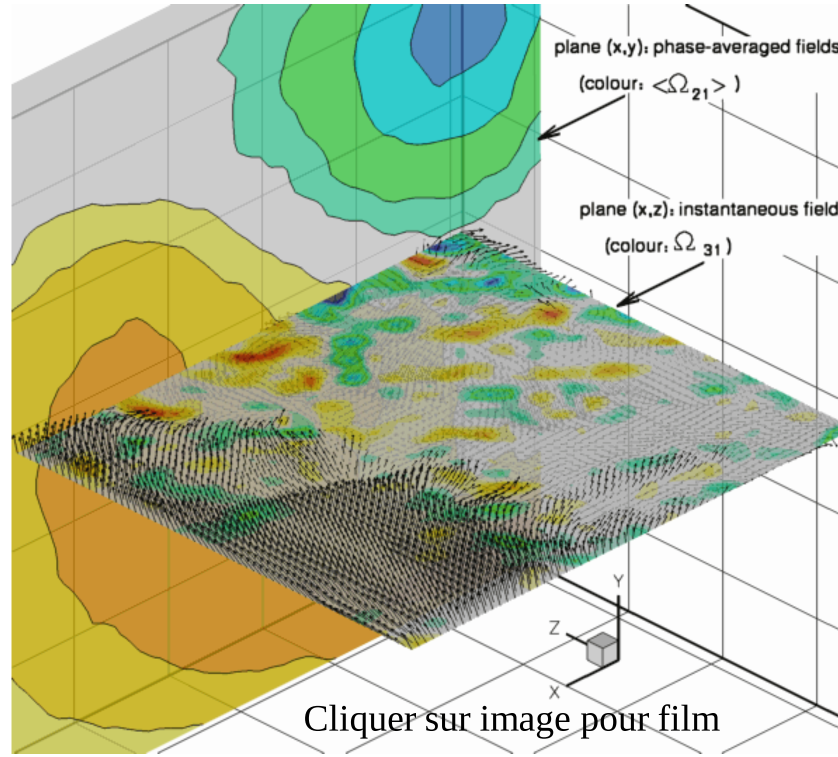

'The IMFT's circular cylinder' test-case

FLOMANIA and DESIDER –EU research programmes

Detailed data base from: simultaneous use of 3C-PIV and of time-resolved TRPIV - R.Perrin PhD '02-05

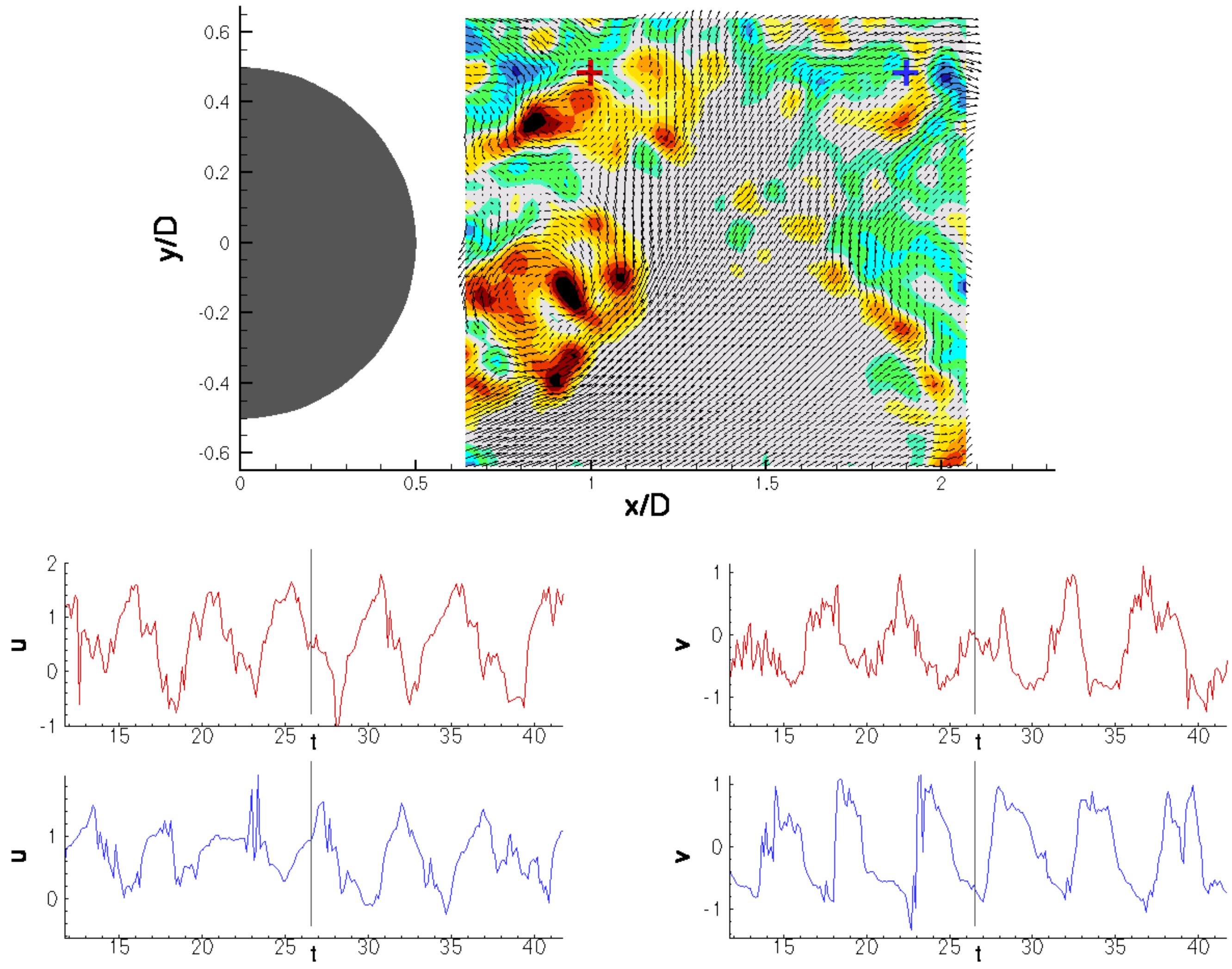

TR-PIV – Re=140,000

S1 and S4 wind tunnels - IMFT

The OES Organised Eddy Simulation
Capturing the organised coherent motion and the random turbulence

FLOMANIA EU Program : « The IMFT Circular cylinder »

Vertical velocity spectrum in a cylinder wake, Re=140 000

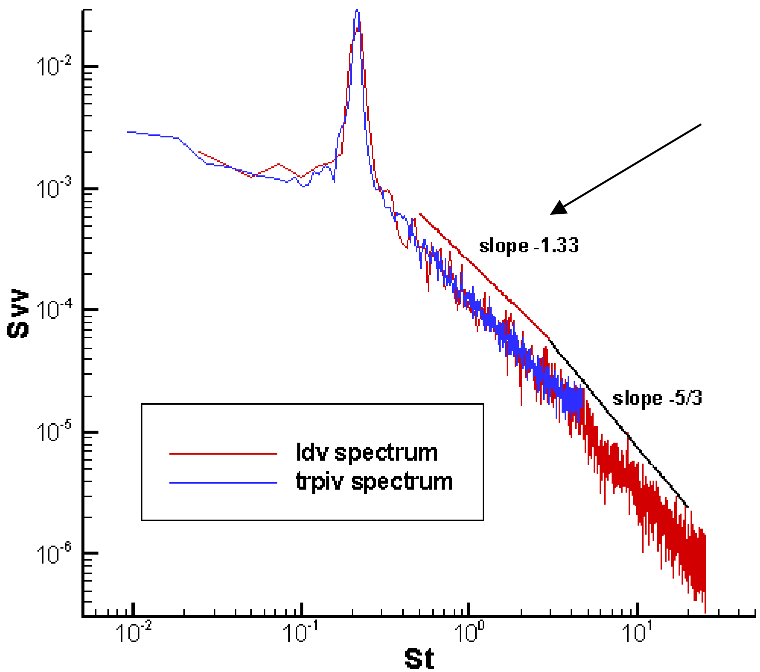

Spectrum from originals signals

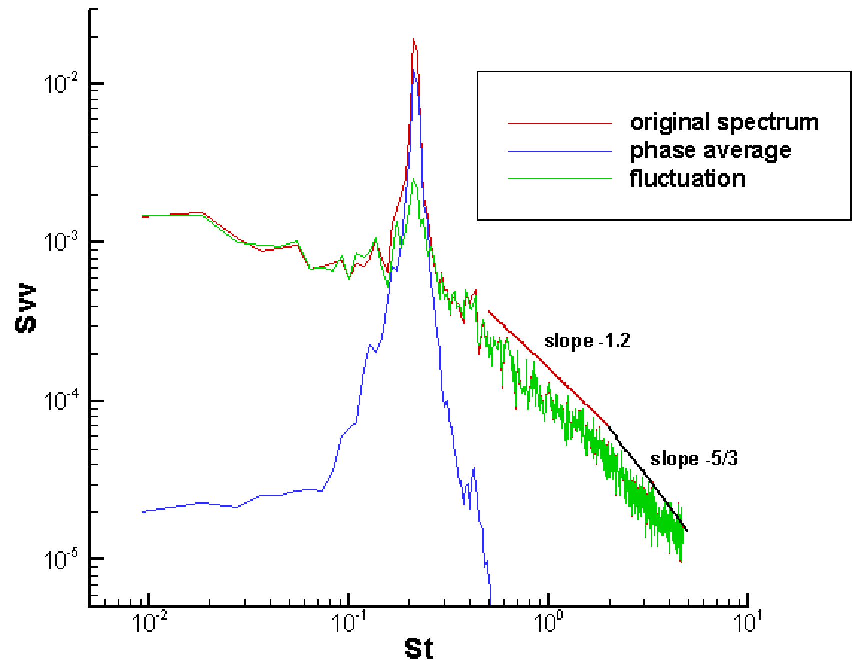

Spectrum from phase-averaged signals

Experimental data from PIV (*M. Braza,R. Perrin, Y. Hoarau, Journal of Fluids and Structure 2006, Exp. Fluids 2007***) and LDV (***Djeridi, Perrin, Braza, Cid, Cazin, JFTAC 2003)*

DESIDER EU Program : « The IMFT Circular cylinder »

Organized Eddy Simulation:

Energy spectrum splitting for

Distinction between the structures to be resolved from those to be modeled based on their organized coherent character

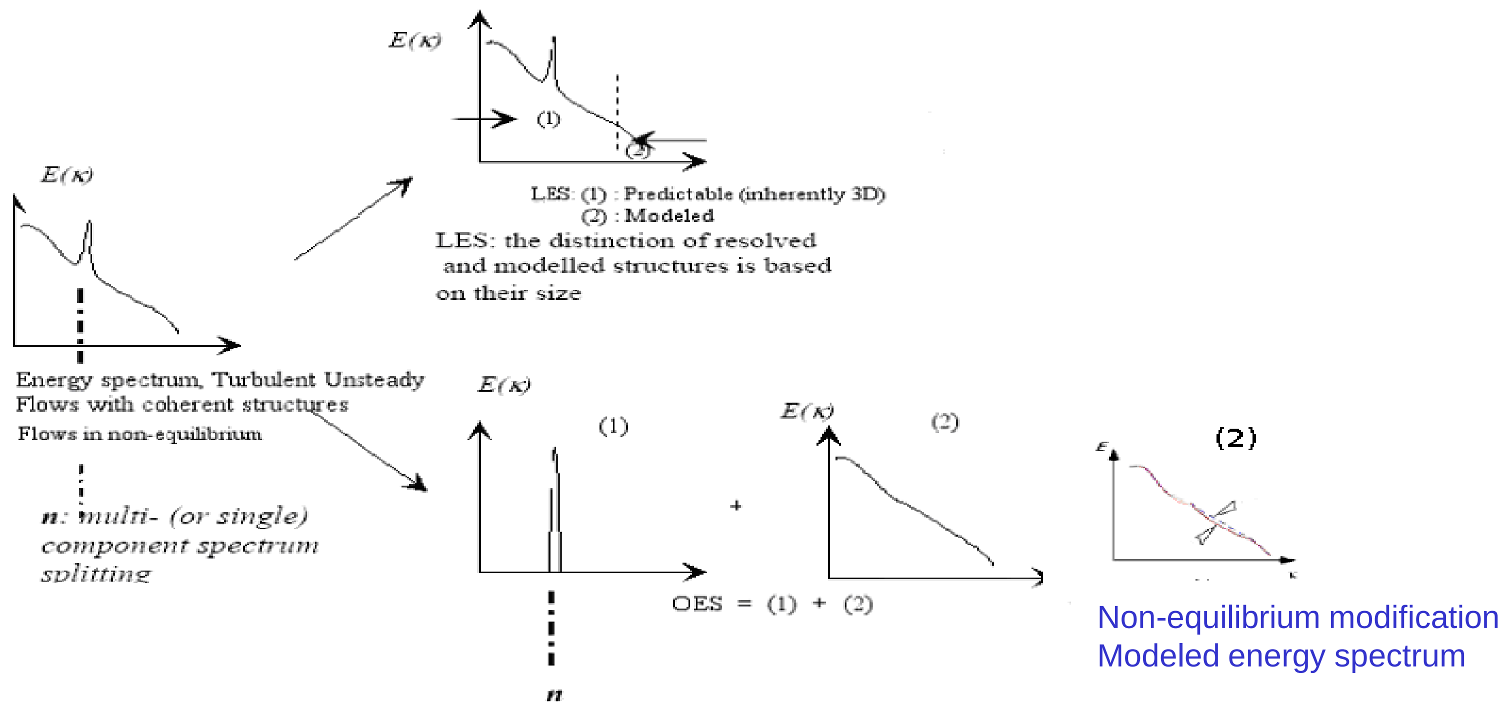

Dervieux, Braza, Dussauge, Notes on Num. Fluid Mech., Vol. 65, 1998
Braza, Perrin, Hoarau, J. Fluids Struct. 2006
Bourguet, Braza, J. Fluids & Struct. 2008
Haase, Braza, Revell, Notes on Num. Fluid Mech. And Multidisciplinary design, Vol. 109
Shinde, Hoarau, Longatte, Braza, J. Fluids & Struct., Vol. 47, 2014

Phase-averaged decomposition – Navier-Stokes equations

$$U_i(x_k,t) = \langle U_i(x_k,t)\rangle + u_i(x_k,t)$$

$$\langle u_i(x_k,t)\rangle = 0 \qquad \langle\langle U_i(x_k,t)\rangle\rangle = \langle U_i(x_k,t)\rangle$$

$$\frac{\partial\langle U_i\rangle}{\partial x_i} = 0$$

$$\frac{\partial\langle U_i\rangle}{\partial t} + \langle U_i\rangle\frac{\partial\langle U_i\rangle}{\partial x_j} = -\frac{1}{\langle\rho\rangle}\frac{\partial\langle P\rangle}{\partial x_i} + \nu\frac{\partial^2\langle U_i\rangle}{\partial x_j\partial x_j} - \frac{\partial\langle\tau_{ij}\rangle}{\partial x_j}$$

$$\langle\tau_{ij}\rangle = \langle u_i u_j\rangle$$

Navier-Stokes equations in phase-averaged decomposition

Modification of modelling $\langle u_i u_j\rangle$ to take into account non-equilibrium

Experimental investigation of 3D **stress-strain misalignment- The IMFT circular cylinder- DESIDER EU-pgm**

Eigenvectors of turbulence stress anisotropy (-a) and of strain rate (S)

rs

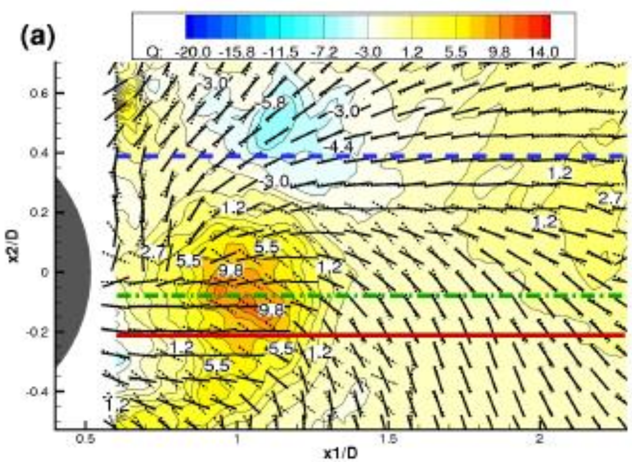

Re=140,000

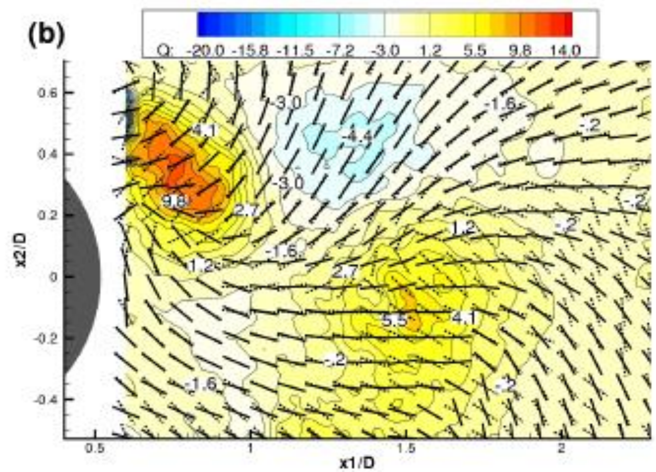

First principal directions of $-a$ and S at phase angle (a) $\varphi = 50^o$ and (b) $\varphi = 140^o$, isocontour of Q criterion

Haase, Braza, Revell, 2009

Bourguet, Braza

J. Fluids and Struct., 2008

Braza, Perrin, JFS 2006

$$-\overline{u_i u_j} + \frac{2}{3}k\delta_{ij} = 2S_{ik}\left(\nu_{tt}\right)_{kj}$$

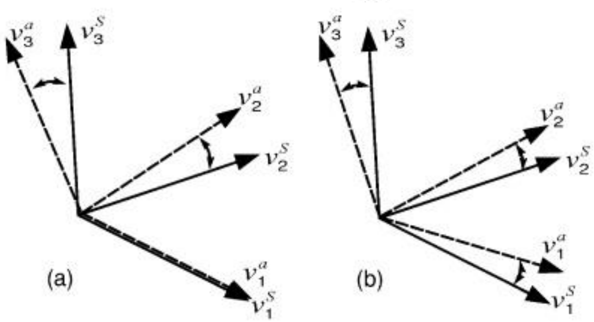

Significant misalignment in coherent structures and in sheared regions

$\longrightarrow$ **anisotropic modulation** of the C_μ eddy-diffusion coefficient in Reynolds stress constitutive law

•OES- Tensorial eddy-viscosity modeling

- Capturing near-wall turbulence stress anisotropy
- Non-equilibrium turbulence – directional 3D stress-strain misalignment
- Projection of the DRSM model on the principal directions of the strain-rate

$$(\nu_{tt})_{ij} = (\nu_{td})_k \left(v_k^S\right)_i \left(v_k^S\right)_j \quad \text{with} \quad (\nu_{td})_i = \frac{C_{Vi}}{2\lambda_i^S} k \,, \quad C_{\mu i} = \frac{C_{Vi}}{2} \frac{\varepsilon}{k\lambda_i^S}$$

C_{Vi} : directional angle between turbulence anisotropy tensor and strain rate

λi : eigenvalues – projection angle between anisotropy and strain-rate tensors

Turbulence constitutive law $-\overline{u_i u_j} + \frac{2}{3} k\delta_{ij} = 2S_{ik} (\nu_{tt})_{kj}$

Momentum equations :

$$\frac{DU_i}{Dt} = \frac{\partial}{\partial x_j} \left(2\nu S_{ij} + 2 (\nu_{tt})_{kj} S_{ik} - \frac{2}{3} k\delta_{ij}\right) - \frac{1}{\rho} \frac{\partial P}{\partial x_i}$$

C_{Vi} : 3 transport equations from DRSM projection on the principal directions of S_{ij}

$$\frac{Dk}{Dt} = \frac{\partial}{\partial x_\alpha} \left(\left(\nu\delta_{\alpha\beta} + \frac{(\nu_{tt})_{\alpha\beta}}{\sigma_k} \right) \frac{\partial k}{\partial x_\beta} \right) + P_k - \varepsilon - \frac{2\nu k}{{y_n}^2},$$

$$\frac{D\varepsilon}{Dt} = \frac{\partial}{\partial x_\alpha} \left(\left(\nu\delta_{\alpha\beta} + \frac{(\nu_{tt})_{\alpha\beta}}{\sigma_\varepsilon} \right) \frac{\partial \varepsilon}{\partial x_\beta} \right) + c_{\varepsilon 1} f_1 \frac{\varepsilon}{k} P_k - c_{\varepsilon 2} f_2 \frac{\varepsilon^2}{k} - \frac{2\nu\varepsilon}{{y_n}^2} \exp\left(-0.5 y^+\right)$$

Directional DRSM

- Transport equations for Cvi projection coefficients, for q = 1,2,3

$$\frac{DC_{V\,q}}{Dt} = -\left(V_q\right)_{ij}\frac{Da_{ij}}{Dt} - a_{ij}\frac{D\left(V_q\right)_{ij}}{Dt}\ ,\ \left(V_q\right)_{ij} = \left(v_q^S\right)_i\left(v_q^S\right)_j$$

- Projection of Speziale, Sarkar and Gatski second order closure scheme

J. Fluid Mech., 227, 1991

$$\begin{aligned}\frac{DC_{V\,q}}{Dt} &= \left(\frac{4}{3} + c_3^* II_a^{\frac{1}{2}} - c_3\right)\left(V_q\right)_{ij}S_{ij} + \left(2 - 2c_4\right)\left(V_q\right)_{ij} a_{ik}S_{jk} - \frac{c_2\varepsilon}{k}\left(V_q\right)_{ij}a_{ik}a_{kj}\\ &+ \left(2 - 2c_5\right)\left(V_q\right)_{ij}a_{ik}\Omega_{jk} + \left(1 - c_1\right)\frac{\varepsilon}{k}C_{V\,q} + \left(1 + c_1^*\right)C_{V\,q}a_{ij}S_{ij} + \frac{c_2 II_a\varepsilon}{3k}\\ &+ \frac{2\left(c_4 - 1\right)}{3}a_{ij}S_{ij} - a_{ij}\frac{D\left(V_q\right)_{ij}}{Dt} + D^{C_{V\,q}}\end{aligned}$$

where c_i and c_i^* are SSG model constants

$$\hat{a}_{ij}\frac{D\left(V_q\right)_{ij}}{Dt} = -C_{V_r}V_r\frac{D\left(V_q\right)_{ij}}{Dt} = 0 \text{ and } D^{C_{V\,q}} = \frac{\partial}{\partial x_i}\left(\left(\nu + \frac{\left(\nu_{tt}\right)_{ij}}{\sigma_{C_{V\,q}}}\right)\frac{\partial C_{V\,q}}{\partial x_j}\right)$$

A tensorial eddy-diffusion coefficient $\boldsymbol{C_{\mu,i}}$ can be derived. For faster computations, can be assumed scalar with equivalent optimum values of order 0.02-0.03

Tensorial eddy-viscosity modeling:

Ability of capturing negative production

of turbulence kinetic energy regions

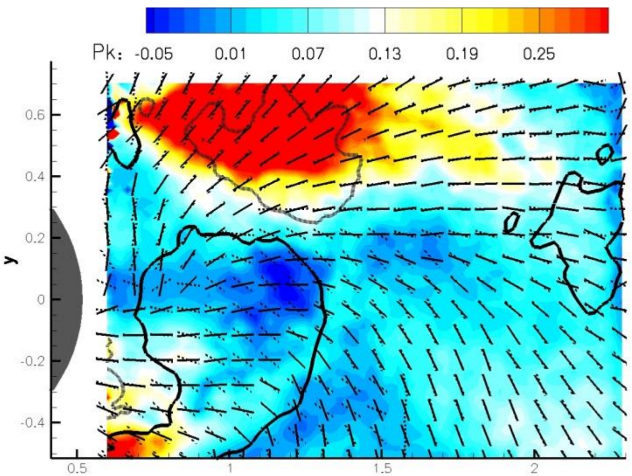

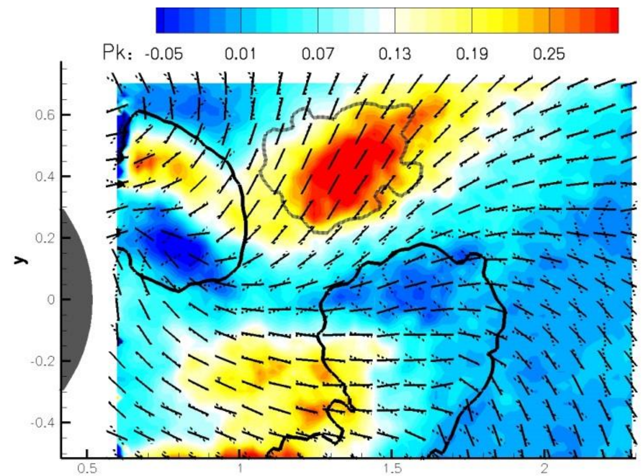

Exp $\mathcal{P}_{ij} = - \langle u_i u_j \rangle \, \partial \langle U_i \rangle / \partial x_j$ Modeled

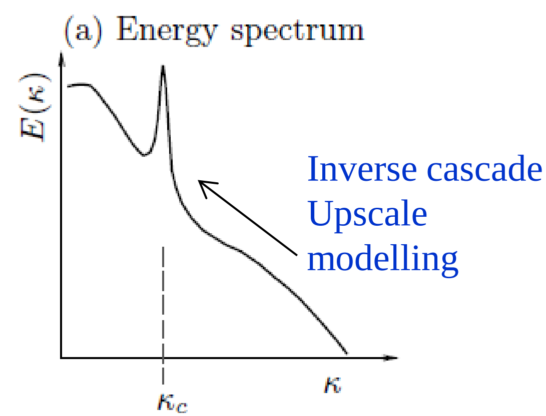

Detached Eddy Simulation

Turbulent length scale: $l_{DES} = \min\left(l_{RANS}, C_{DES} \times \Delta\right)$, $\Delta = \max\left(\Delta x, \Delta y, \Delta z\right)$

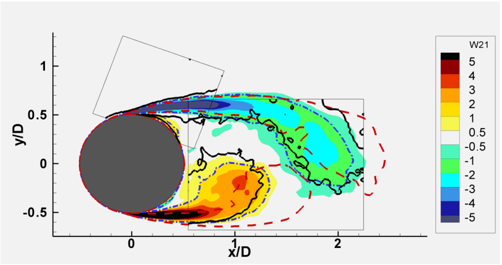

- For *Spalart-Allmaras* model*: $l_{DES} = \min\left(d_w, C_{DES} \times \Delta\right)$

➔Augmentation of the dissipation term in the eddy-viscosity transport equation:

$$\frac{D\tilde{\nu}}{Dt} = c_{b1}(1 - f_{t2})\tilde{S}\tilde{\nu} + \frac{1}{\sigma}\left[\nabla.((\nu + \tilde{\nu})\nabla\tilde{\nu}) + c_{b2}(\nabla\tilde{\nu})^2\right] - \boxed{\left(C_{w1} f_w - \frac{C_{b1}}{\kappa^2} f_{t2}\right)\left(\frac{\tilde{\nu}}{l_{DES}}\right)^2}$$

- For *k-ω** model*: $l_{DES} = \min\left(k^{1/2}/\beta\omega, C_{DES} \times \Delta\right)$

➔Augmentation of the dissipation term in the *k* transport equation:

$$\frac{D\overline{\rho}k}{Dt} = \tau_{ij}\frac{\partial U_j}{\partial x_i} - \boxed{\frac{\rho k^{3/2}}{l_{DES}}} + \frac{\partial}{\partial x_j}\left[\left(\mu + \sigma^* \mu_t\right)\frac{\partial k}{\partial x_j}\right]$$

- Improvement of l_{RANS} adopted from equilibrium turbulence within DES using l_{OES} in inertial regions

$$l_{OES} = \frac{k^{1/2}}{C_\mu \omega}$$

➔➔**DES/OES** approach

DDES – avoid Modeled Stress Depletion

• **Hybrid Turbulence Modelling**

$$l_{DDES} = l_{RANS} - f_d \max(0, l_{RANS} - C_{DES} \times \Delta)$$

$$\Delta = \max(\Delta x, \Delta y, \Delta z)$$

$$f_d = \begin{cases} 0, & \text{close to wall} \\ 1, & \text{far from wall} \end{cases}$$

Delayed Detached Eddy Simulation:

- URANS (near body surface)
- LES (shear layer, detached flow…)

$$r_d = \frac{\nu + \nu_t}{S_{ij} \kappa^2 d^2} \qquad f_d = 1 - tanh[(8 r_d^3)]$$

Turbulence length scale in URANS part : l_{OES}

DDES-OES k-ω-version

$$\frac{Dk}{Dt} = P_k - C_\mu k \omega + \text{div}\left[(\nu + \sigma_k \nu_t)\, \underline{\text{grad}}\, k\right]$$

$$\frac{D\omega}{Dt} = \gamma \frac{P_k \omega}{k} - \beta \omega^2 + \text{div}\left[(\nu + \sigma_\omega \nu_t)\, \underline{\text{grad}}\, \omega\right]$$

$$+2\,(1 - F_1)\, \sigma_{\omega 2} \frac{1}{\omega} \underline{\text{grad}}\, k \cdot \underline{\text{grad}}\, \omega$$

$$\omega = \frac{\varepsilon}{\beta^* k} \qquad \nu_t = \frac{k}{\omega}$$

k: turbulent kinetic energy
1/ω: turbulence time scale

- *SST*: Shear-Stress-Transport limiter of eddy viscosity
- **OES**: Organised Eddy Simulation
- **DDES-OES**

Spalart, Stelets, J. Flow Turb. Combust, 2000 (DES), (DDES) 2004- 2006
Menter, (SST) 1992, Menter & Kunz, (DDES) 2004

Braza, Hoarau (OES) 1998-2000
Braza, Bourguet, Hoarau 2008 - 2012

Stochastic forcing in turbulent transport equations

Upscale turbulence modelling - inverse turbulence casacade - Collaboration with J. Hunt - UCL and IMFT

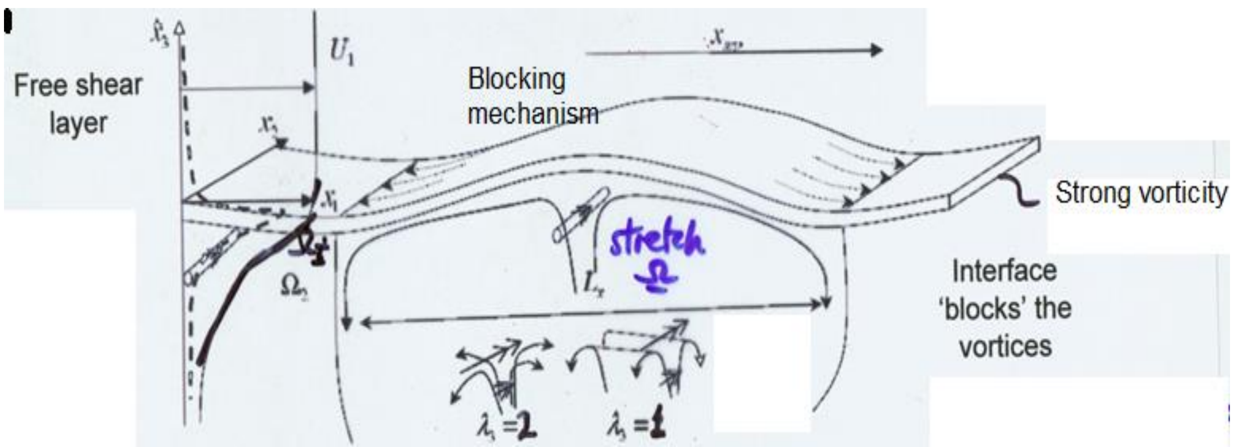

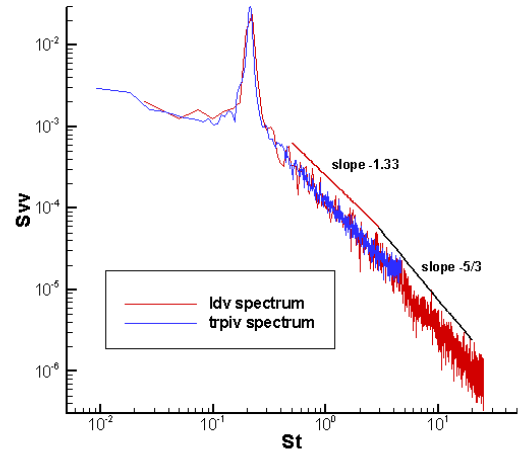

Crucial to predict the instability modes in FSI and acoustics

Buffet instability capturing

Grossi, Braza et al, AIAA J, 2014

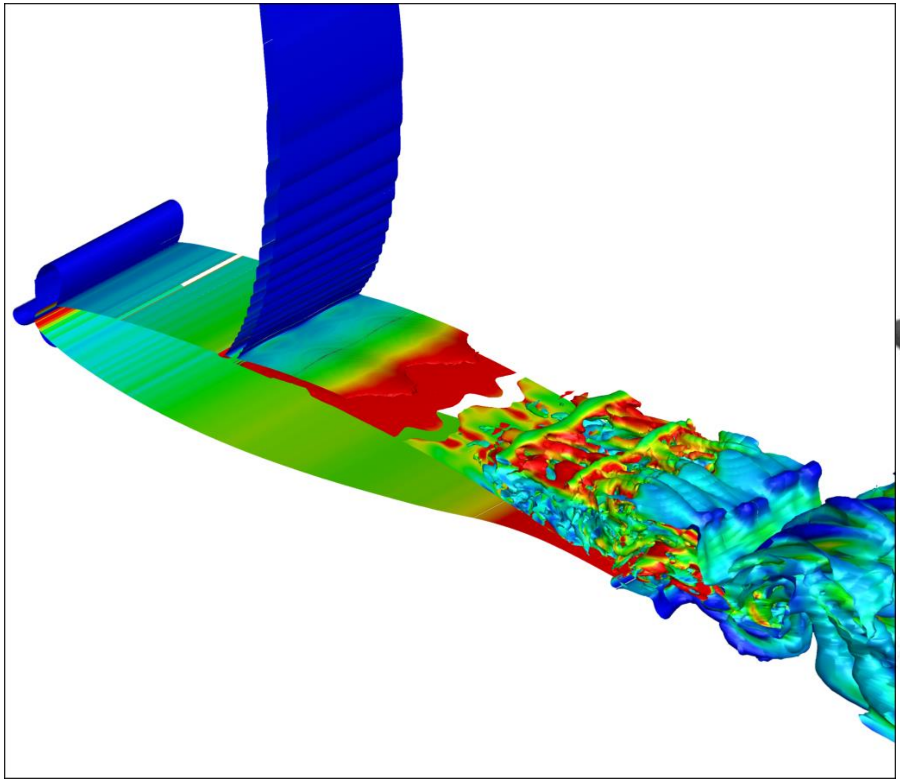

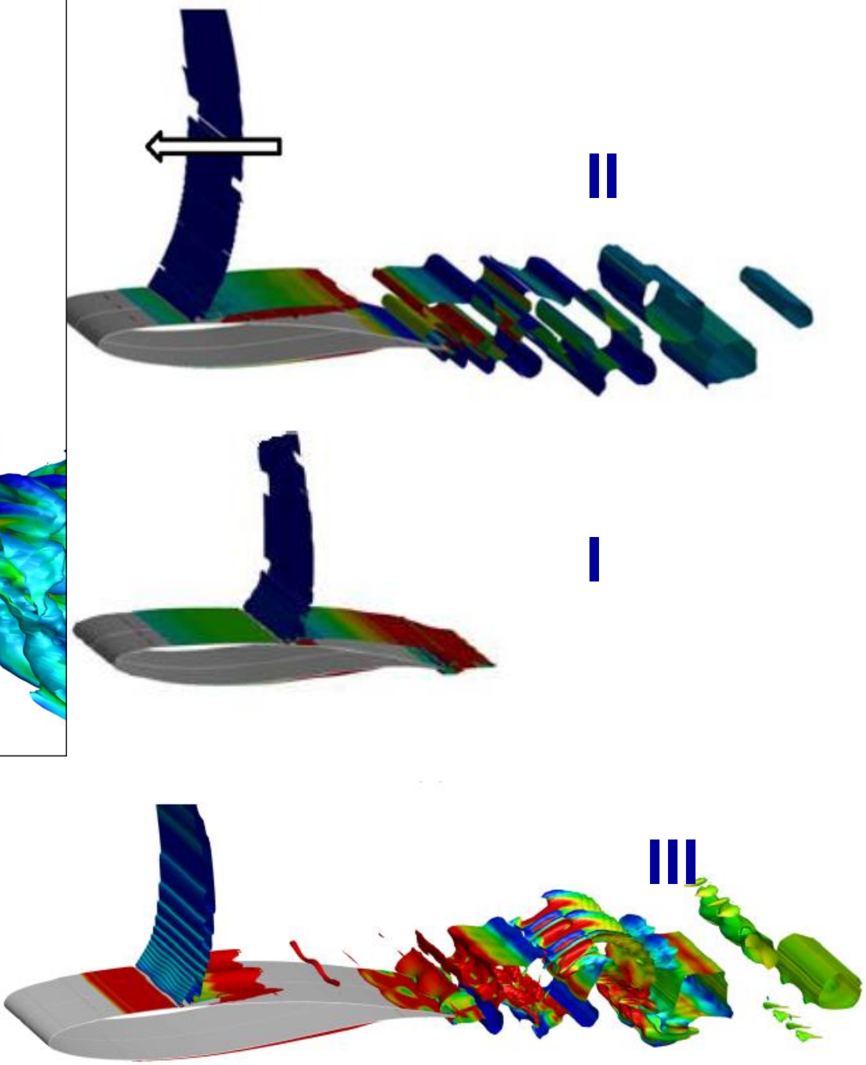

Proper Orthogonal Decomposition

- **Karhunen-Loève expansion** (Karhunen 1946)

$$v(x,t) \approx \sum_{i=1}^{N_{pod}} a_i(t)\Phi_i(x)$$

Time/space separation : stationarity, neglecting correlations at non-zero time-lag

At IMFT : Faghani 1996, Borée 2000, Barthet 2003, Perrin 2005, Favier 2007, El Akoury 2007,... in incompressible case

- Spatial modes $\Phi_i(x)$, iterative solutions of an **optimisation problem**

$$\Phi_{i+1}(x) = \arg \max_{\phi \in L^2(\Omega)} \left\langle (v - \Pi_i v, \phi)^2 \right\rangle \text{ with } \|\phi\|^2 = 1$$

$< \cdot >$ ensemble average (time average, ergodicity), $(\cdot,\cdot)$ spatial inner product, Π_i : projector on span$\{\Phi_1, \ldots, \Phi_i\}$

- **Snapshot POD** (Sirovich 1987) - if $N_x \gg N_t$, N_t, N_x : numbers of snapshots, space points

$$C_t(t,t') = \frac{1}{T}\int_\Omega v(x,t)v(x,t')dx \;\rightarrow\; \text{eigenfunctions } \Psi_i$$

$$\Phi_i(x) = \frac{1}{T\lambda_i^{1/2}}\int_T v(x,t)\Psi_i(t)dt \text{ for } \lambda_i > 0$$

T : sampling time interval, $\lambda_1 \geq \lambda_2 \geq \ldots \geq 0$: C_x and C_t eigenvalues

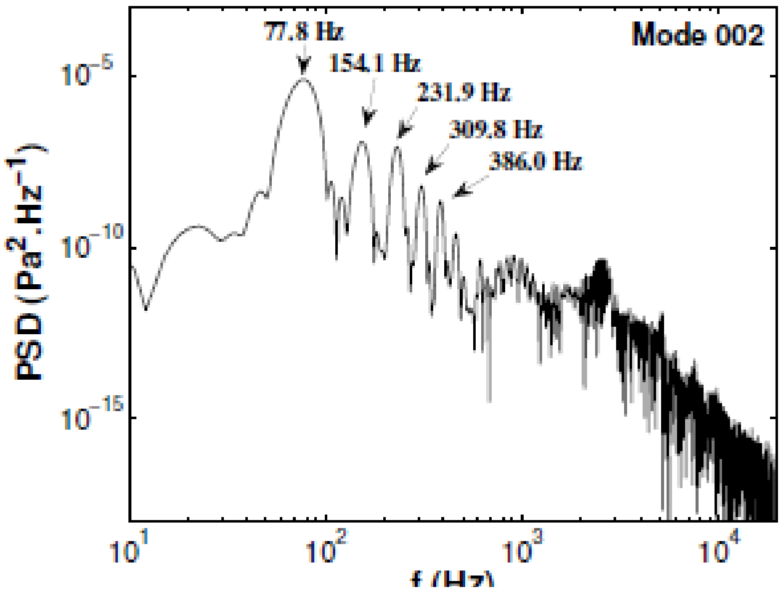
Mode 002
77.8 Hz
154.1 Hz
231.9 Hz
309.8 Hz
386.0 Hz
PSD (Pa².Hz⁻¹)
f (Hz)

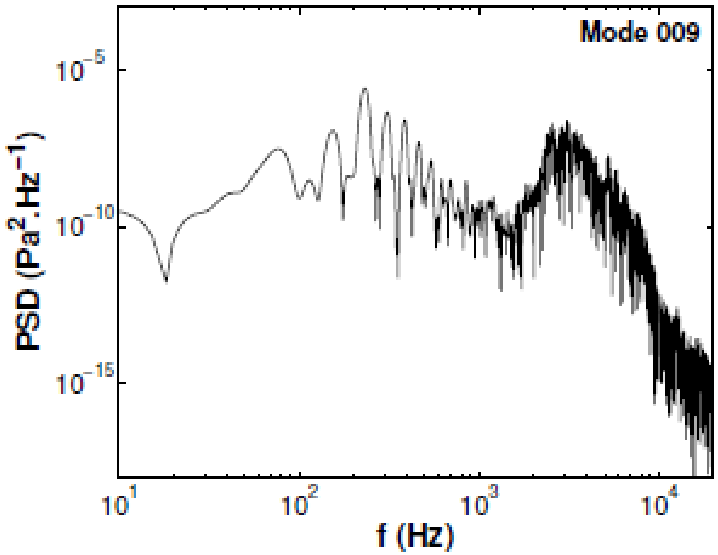
Mode 009
PSD (Pa².Hz⁻¹)
f (Hz)

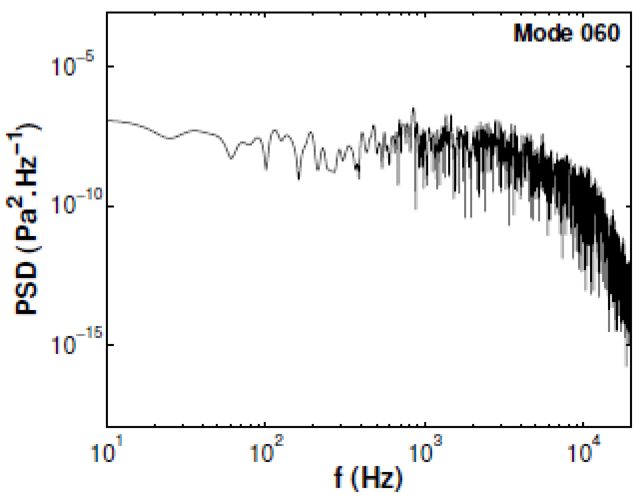
Mode 060
PSD (Pa².Hz⁻¹)
f (Hz)

Phase I: POD modes evaluation

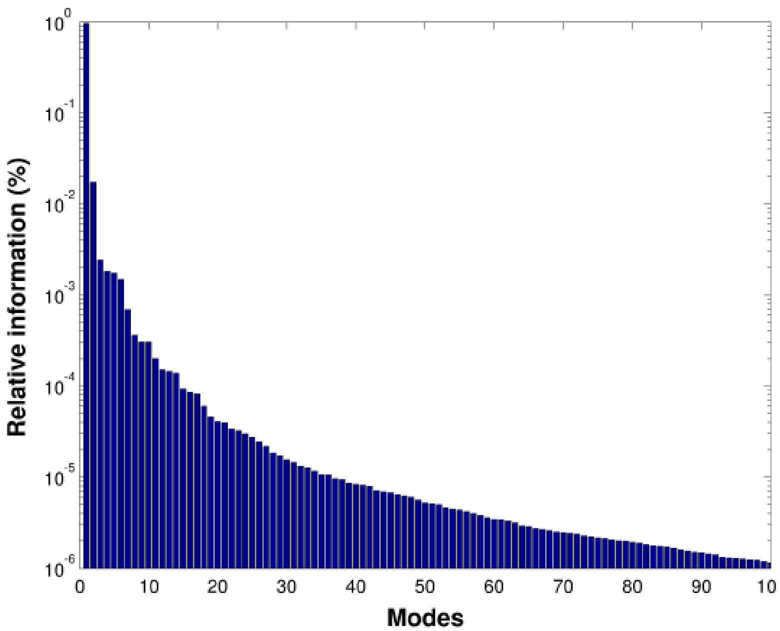

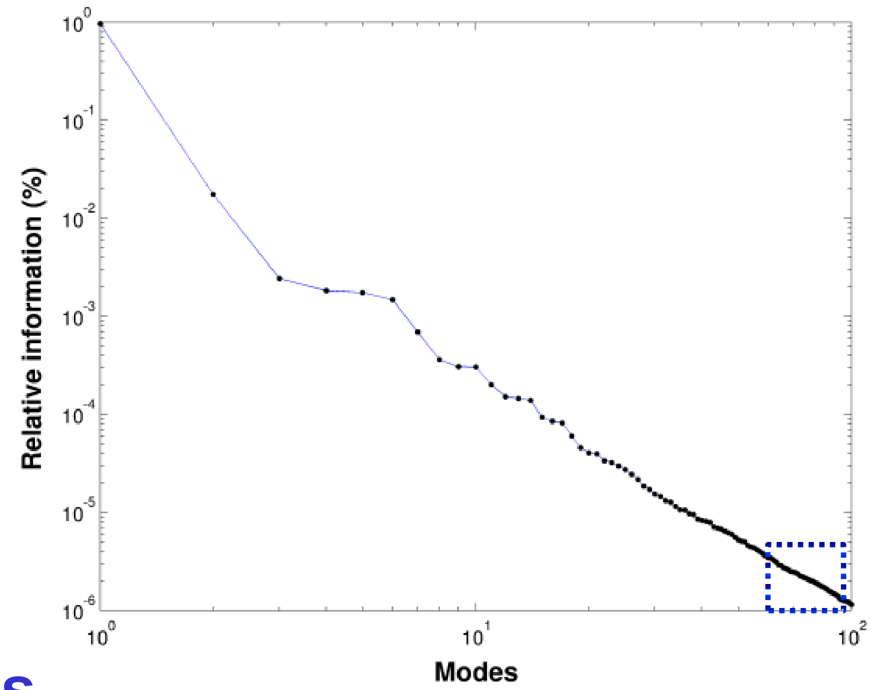

Energy of the POD modes

Selection of the last 30 modes to reconstruct velocity fluctuations

$$u_i(\vec{x},t) = \sum_{n=1}^{30} a^{(n)} \phi_i^{(n)}(\vec{x},t)$$

for the stochastic forcing :

***$\alpha^{(n)}$ (t)* : POD temporal coefficients** ***Φ_i (x,t)* : space functions**

Structure of Modes from low order to high order

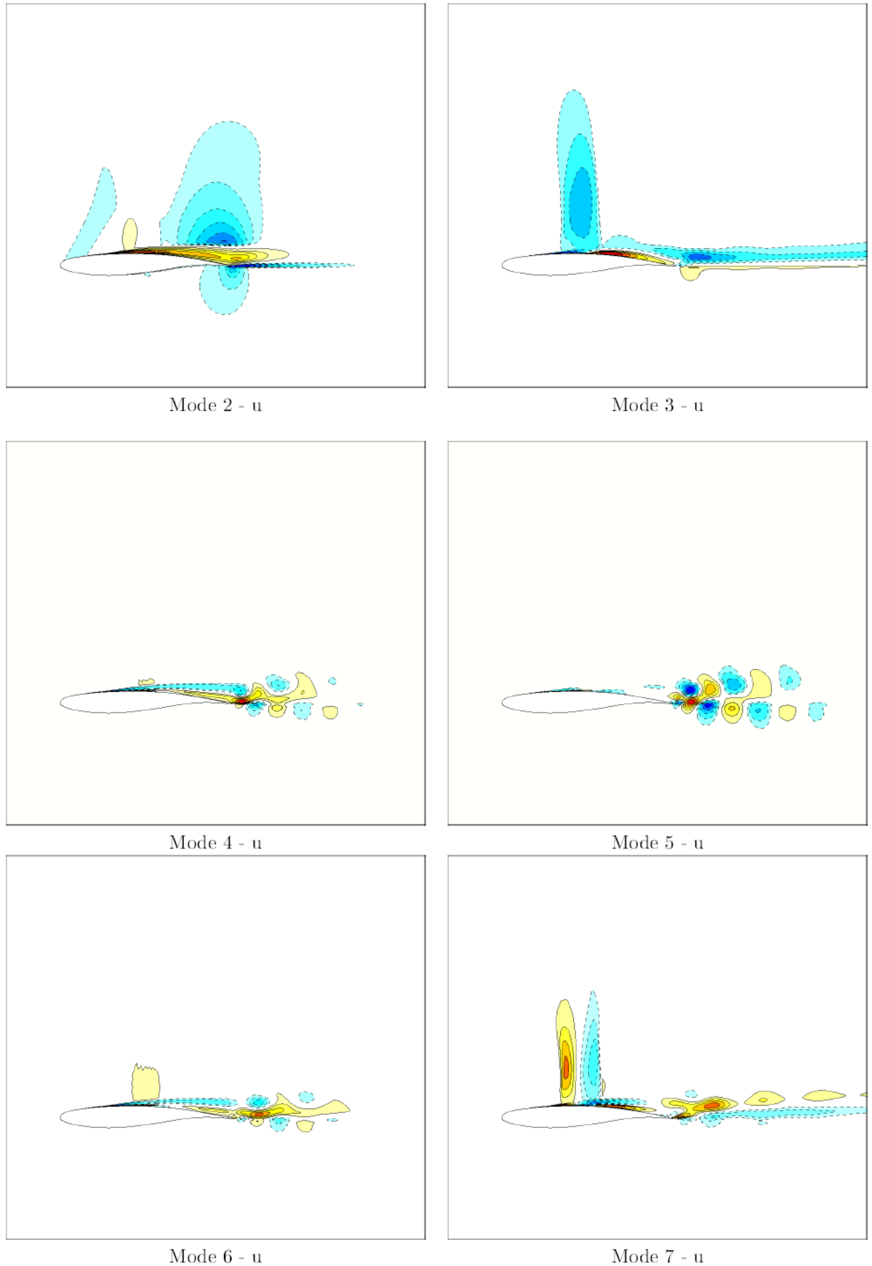

Modes 1-6 : are associated with the organised structures : buffet, von Karman

Low-energy POD modes :

Affect the shear-layers and interact with shock wave (buffet)

Can be used to produce small turbulent kinetic energy – forcing

That will act in the regions of interest and will not affect the irrotational regions

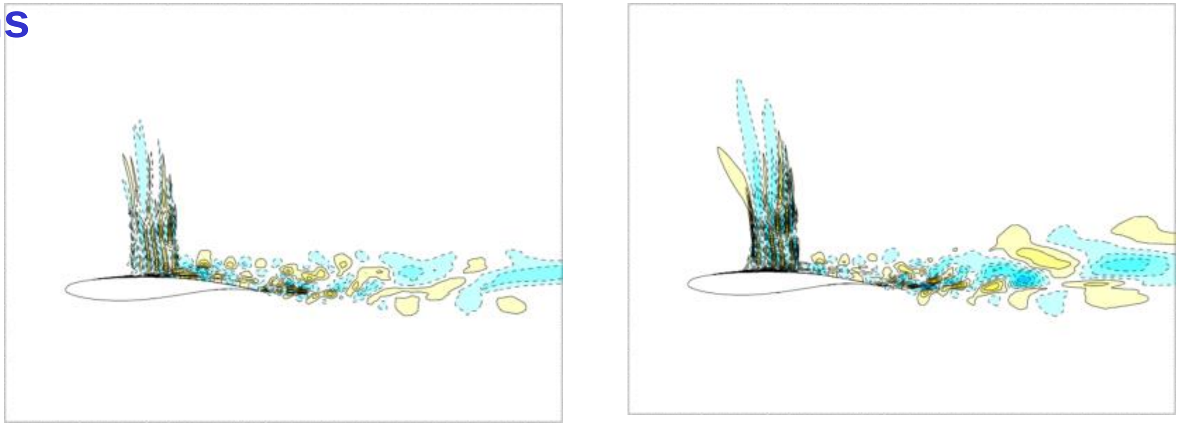

Modes 74 and 75 the filling of the shear-layer by smaller structures and the interaction within the shock

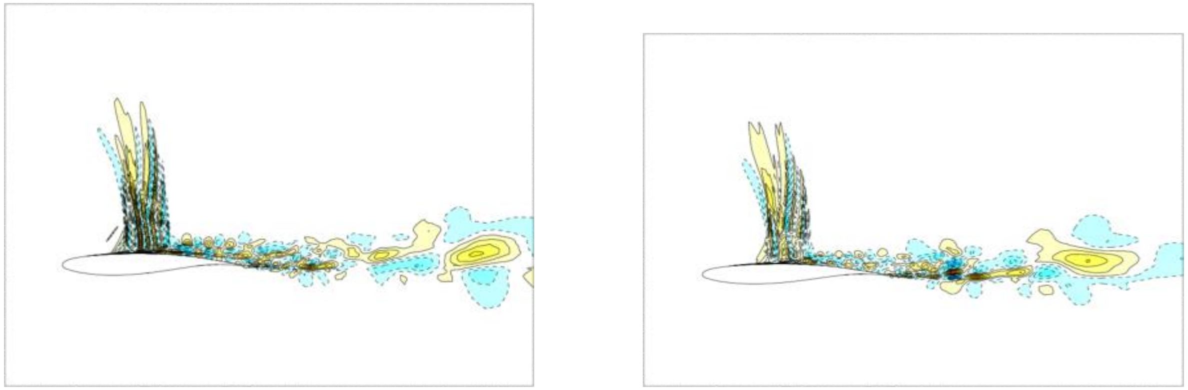

Modes 82 and 83

Stochastic forcing to keep thin the shear layer interfaces

Criterion 1

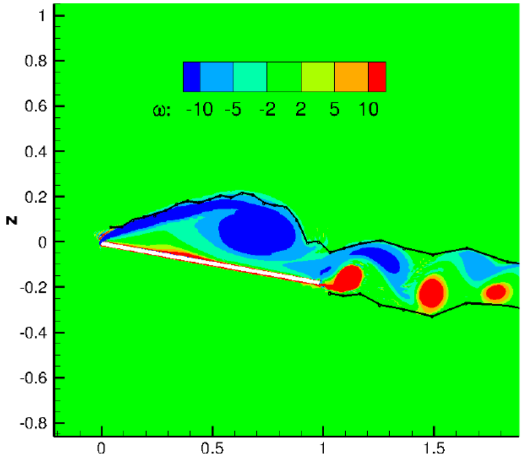

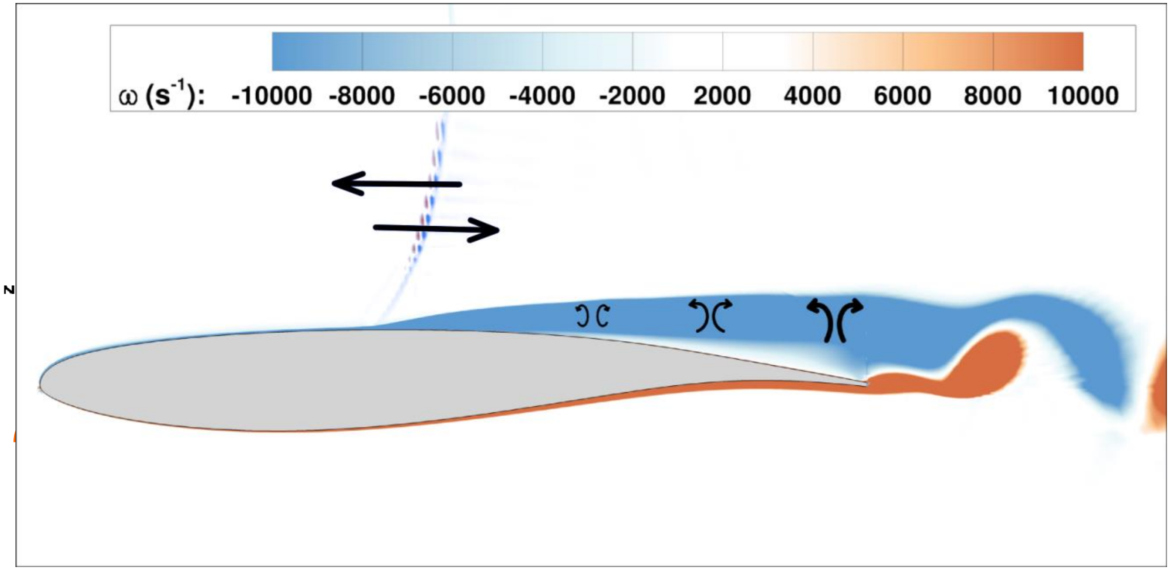

$$\frac{Dk}{Dt} = P - \varepsilon + \frac{\partial}{\partial x_i}\left[\left(\nu + \frac{\nu_t}{\sigma_k}\right)\frac{\partial k}{\partial x_i}\right] + S_{\text{POD}}$$

$$\frac{D\varepsilon}{Dt} = \frac{\varepsilon}{k}(C_{\varepsilon 1}\, P - C_{\varepsilon 2}\, \varepsilon) + \frac{\partial}{\partial x_i}\left[\left(\nu + \frac{\nu_t}{\sigma_\varepsilon}\right)\frac{\partial \varepsilon}{\partial x_i}\right] + \frac{C_{\varepsilon 2}\, S_{\text{POD}}^2}{k_{\text{amb}}}$$

$$S_{\text{POD}} = \tilde{r}\; C_\mu\; (k_{\text{amb}}^2 + k_{\text{POD}}^2)/\nu_{t\infty} \quad k_{\text{amb}} = k_{fs}\; U_\infty^2, \text{ and } k_{fs} = 3/2\ \text{Tu}^2$$

Computations with stochastic forcing: keeps thinner the shear-layers and ensures correct amplitude of shock wave m

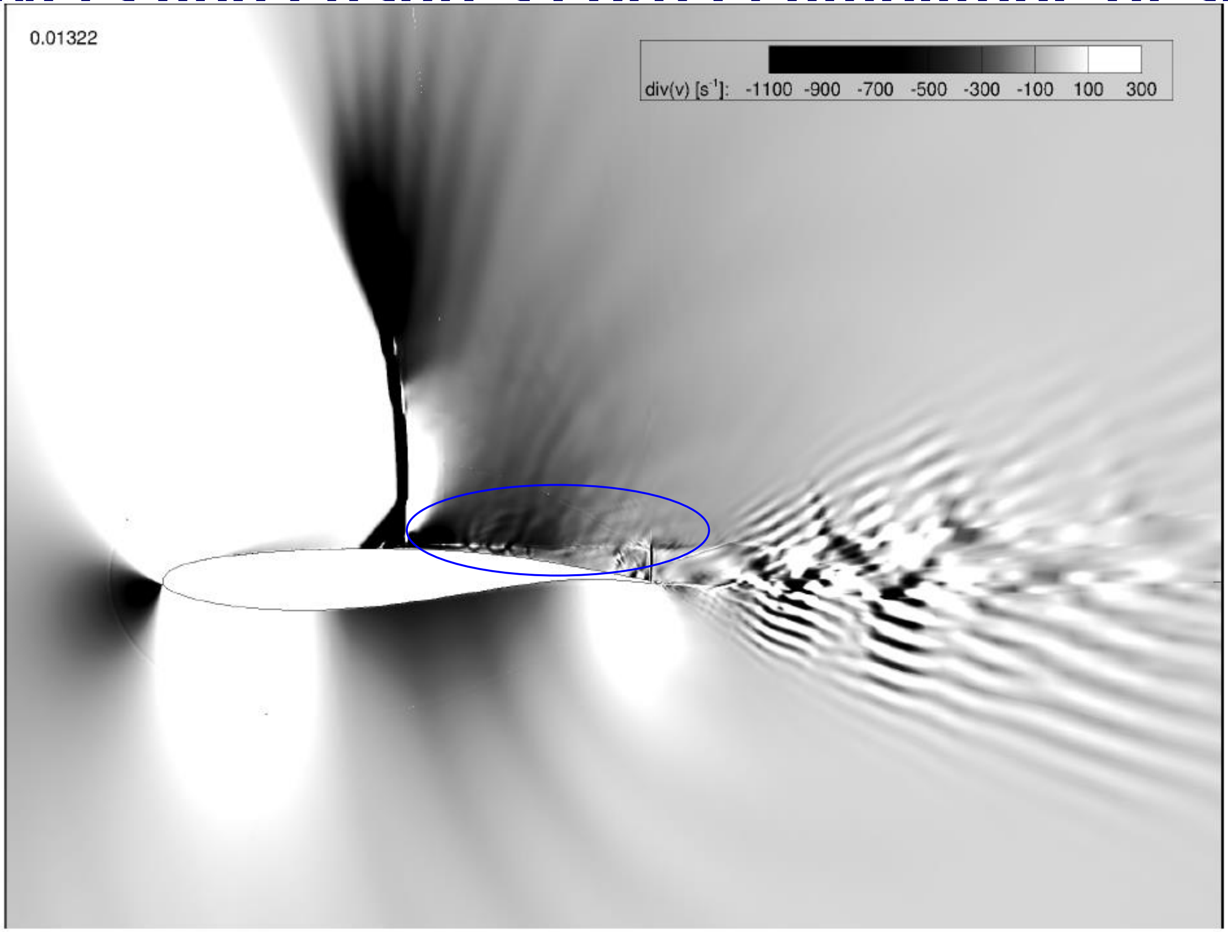

FIGURE 4.4 – Visualisation instantanée de la divergence du champ de vitesse.

Influence of the forcing on the wall pressure averaged coefficient

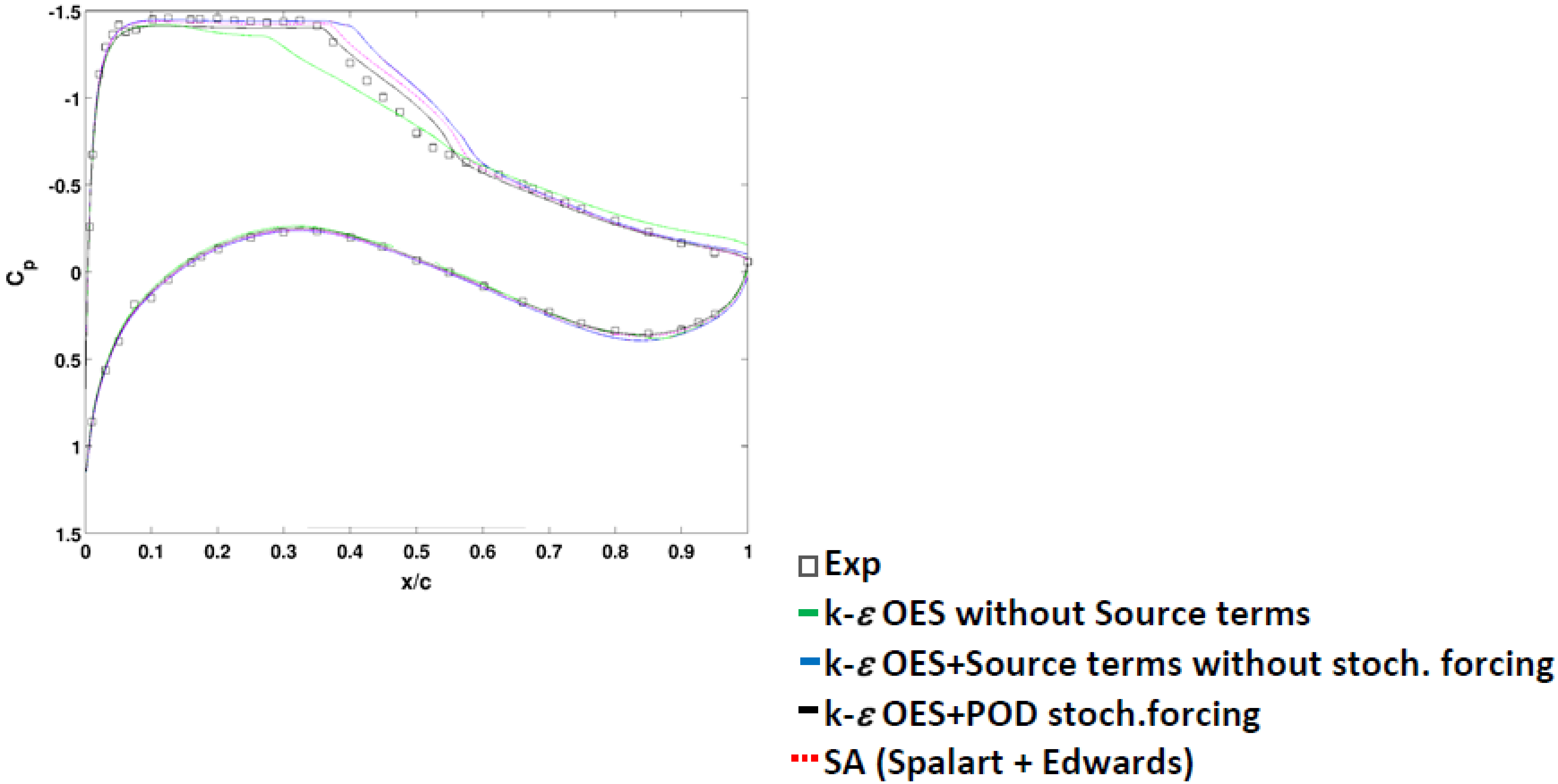

Green line: without forcing: larger amplification of the shock motion

Comparison of the phase-averaged velocity profiles accross the TNT interface : with (red) and without forcing

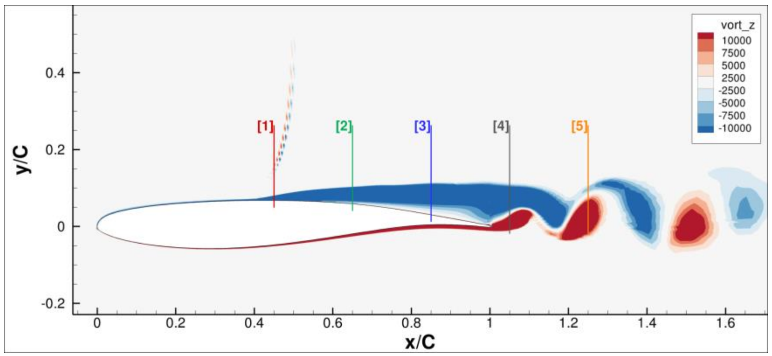

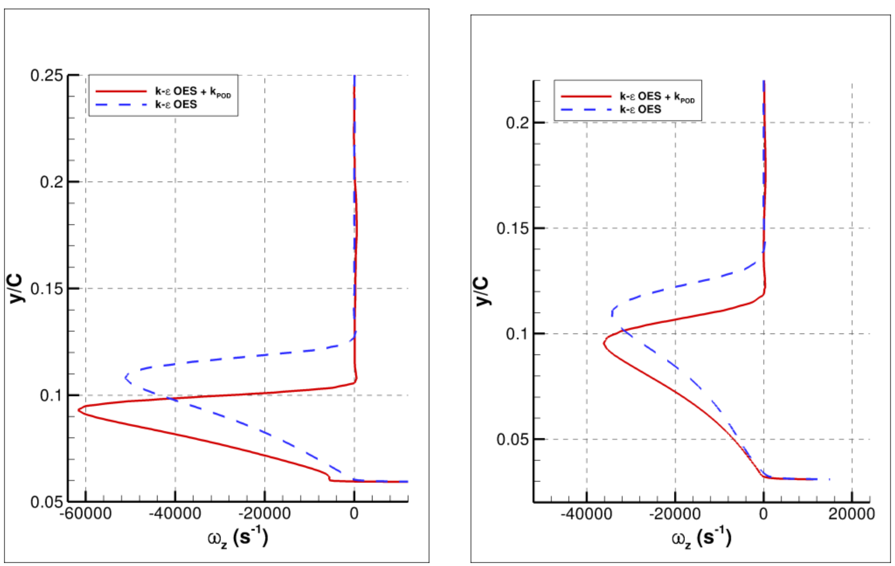

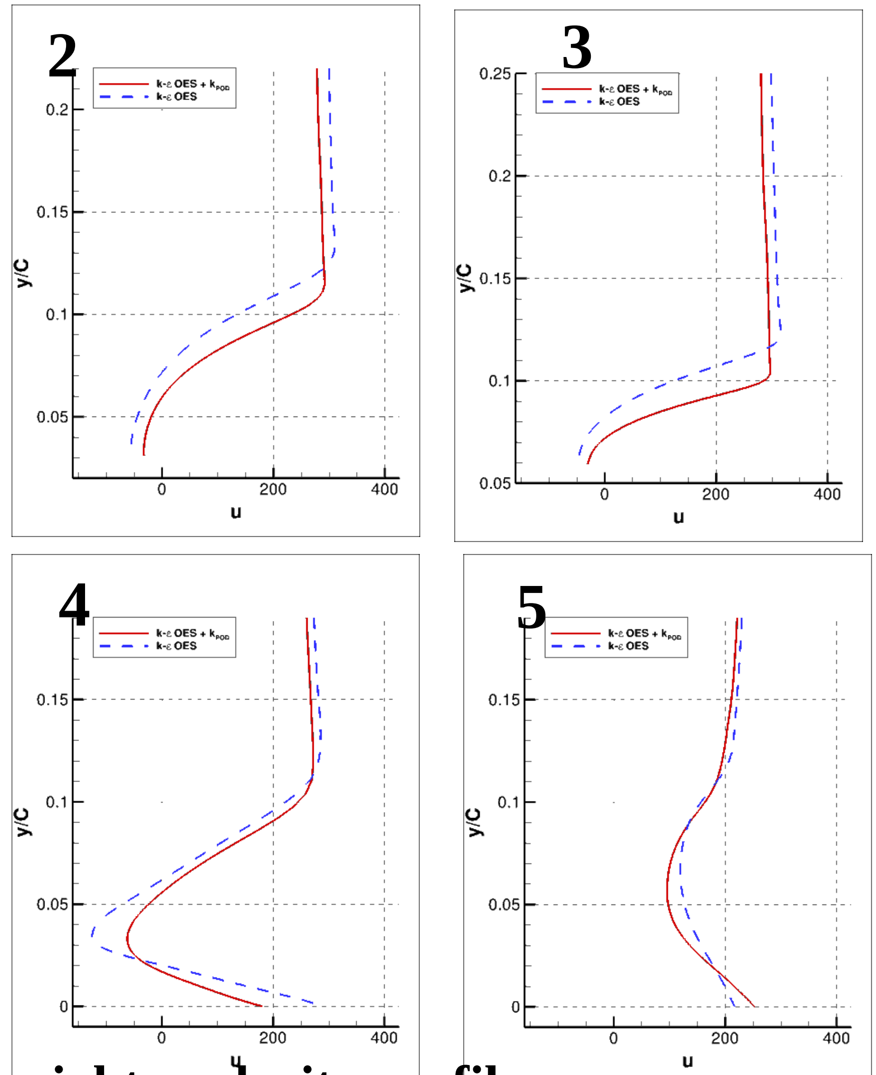

Red curves with forcing. Left: vorticity, right : velocity profiles

Comparison div(V): effect of the stochastic forcing in OES:

- **Correct shock amplitude motion**
- **Thinner interface**

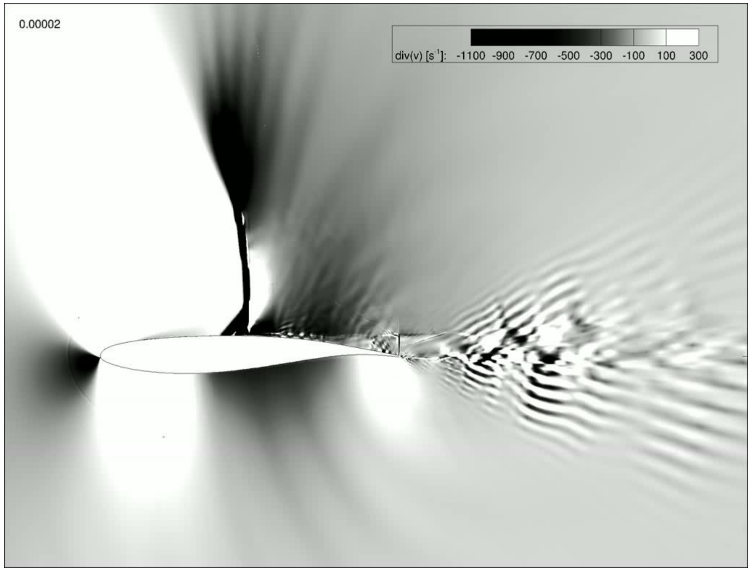

with forcing

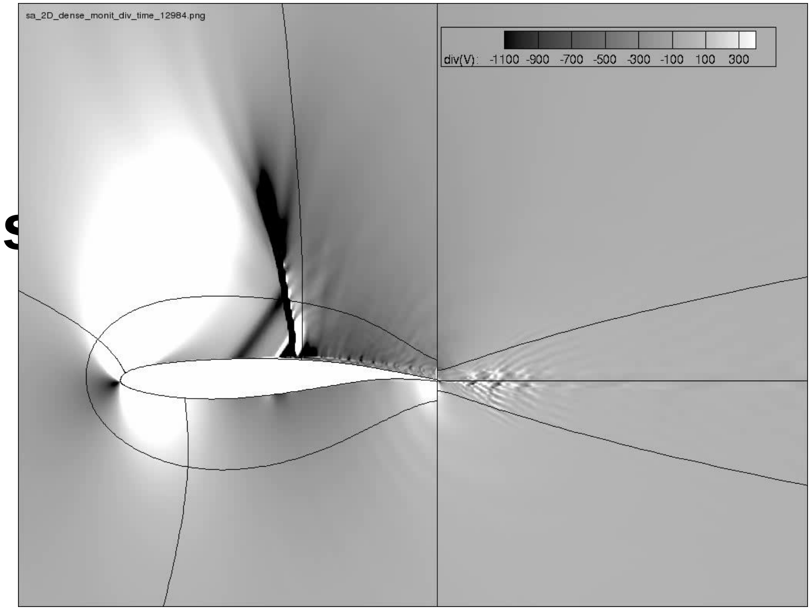

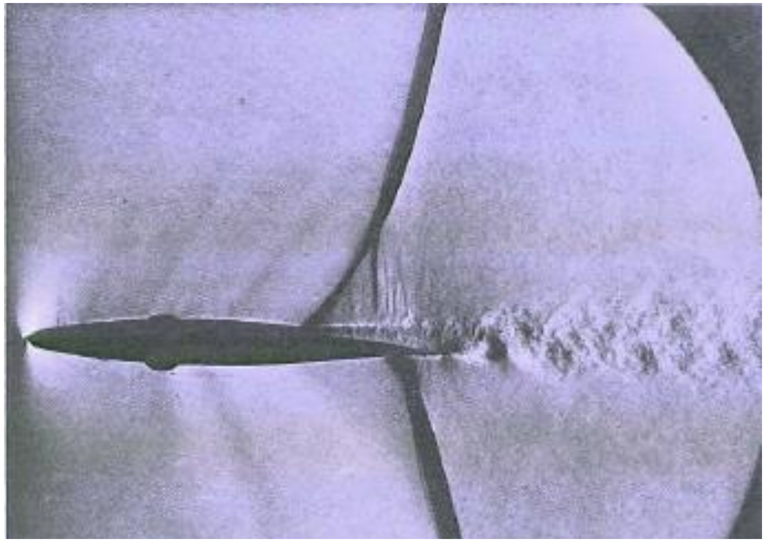

Figure 5: Schlieren photograph of the shock-induced flow separation on (Courtesy of National Physical Laboratory, England; photo by D. W. Holder)

OES modelling: Capturing of buffet frequency, shear-layer and von Karman mode, Re= 3 Million

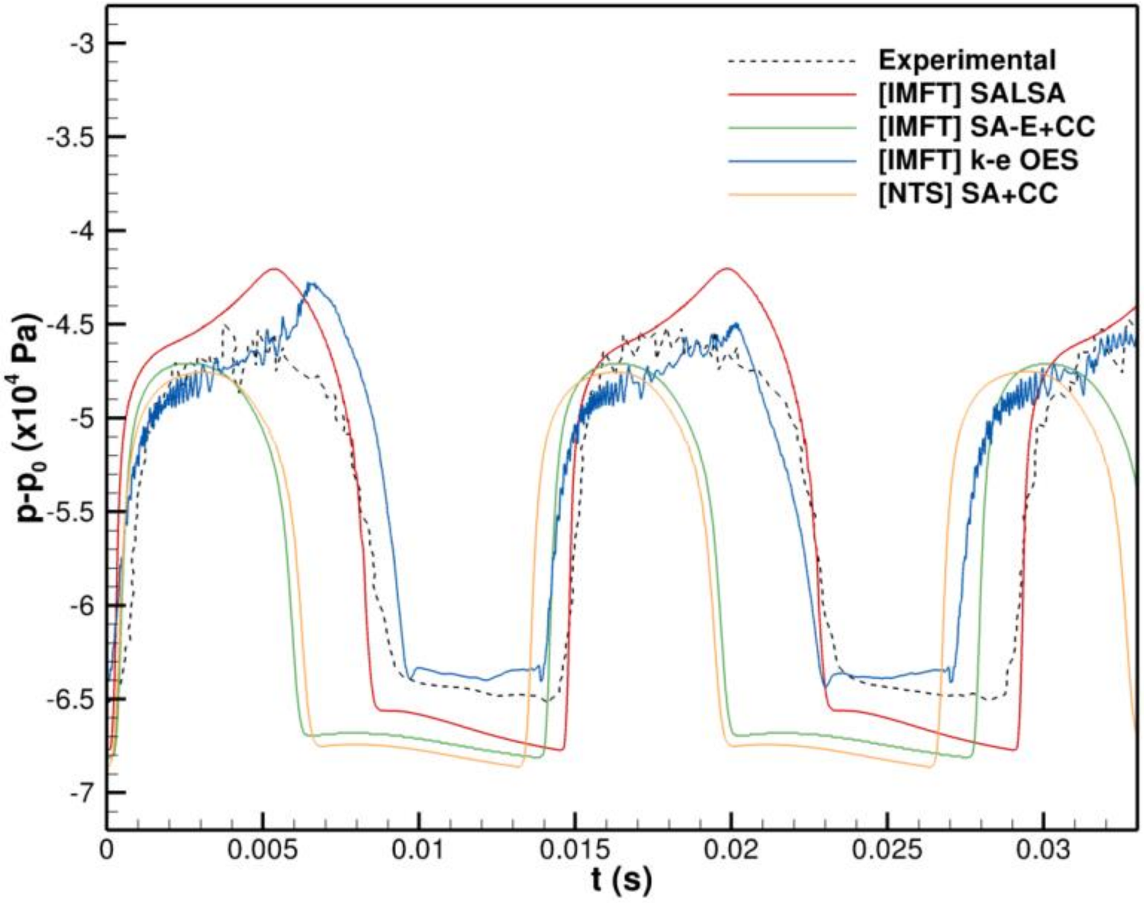

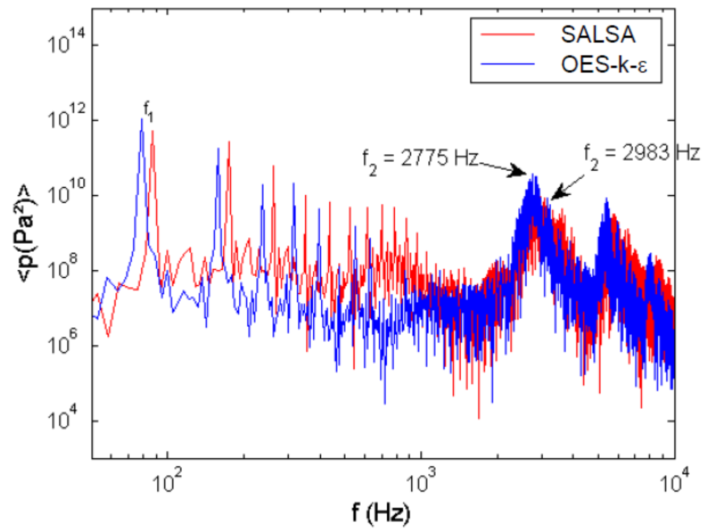

$f_{buffet\,(num)}$ ~73 Hz St=0.10

f_b (exp)~70 Hz - Jacquin et al, AIAA 2009

f_{VK}~35 f_b **~**2600 -2700 Hz

f_{SL}~10^4 Hz

The present stochastic forcing is efficient to keep TNT interfaces thin.

The amplitudes of the low-frequency oscillations and the shock motion (buffet) become closer to the physical experiments

The approach is applicable in hybrid RANS-LES and LES

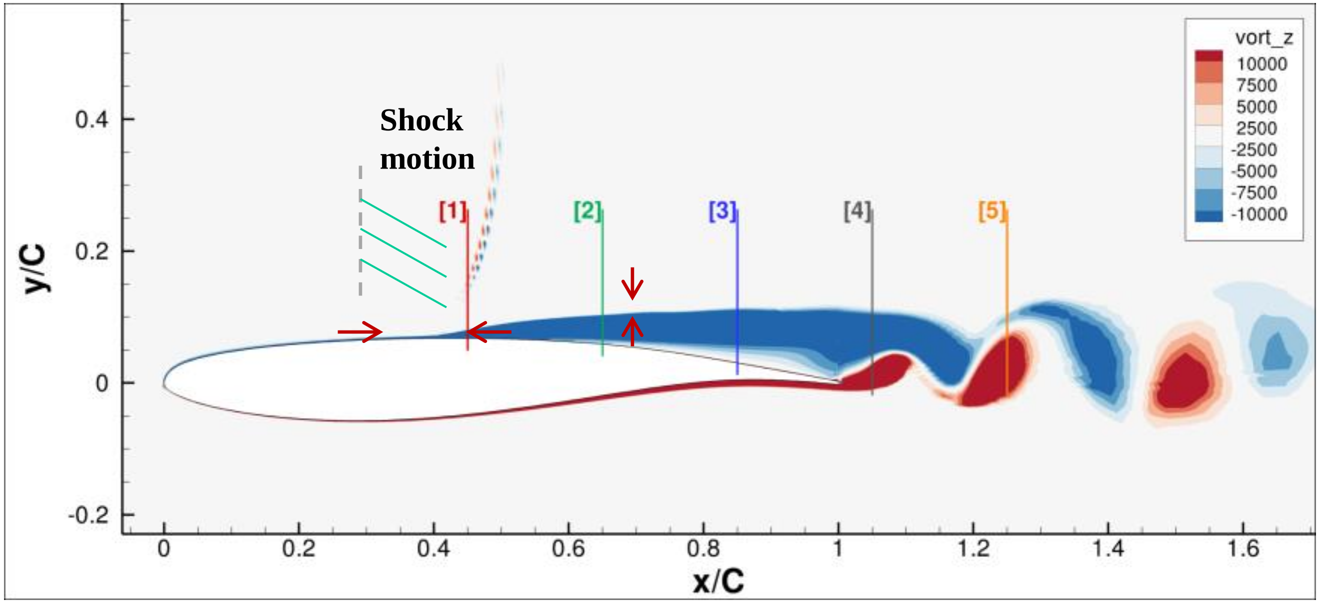

NSMB code - Navier-Stokes Multi-Block

The NSMB consortium

- **Research Institutes:**

  KTH, CFS Eng., EPFL, ETH, Uni Karlsruhe, IMFT, IMFS, CERFACS

- **Industries:**

  AIRBUS-FR, CFS Eng., Ruag Aerospace-Swiss, SMR Eng., SMARTFLOW-FR

- **Governing Equations and Numerical schemes**

- **Compressible and incompressible flows**
- **CHIMERA grids**
- **ALE, Aritrary Lagrangian-Eulerian method for moving/deformable grids**
- **Grid deformation**
- **Interfacing with structural analysis**
- **Numerical schemes : explicit, implicit (dual time-stepping), Mulltigrid**
- **High-order temporal (Runge-Kutta) and spatial schemes (6th-order advective, W-ENO, etc..)**

- **Turbulence modelling:**

NSMB code - Navier-Stokes Multi-Block

- **Turbulence modelling:**

  ***LES, URANS (standard and advanced)**

  ***Hybrid approaches, especially DDES, (Delayed Detached Eddy Simulation)**

  ***Stochastic forcing - inverse turbulence cascade - upstream turbulence modelling capturing thin turbulent/non-turbulent interfaces -collaboration with Prof. J. Hunt, Univ.Coll. Lond./IMFT**

WP5: External Flows-Wing
The V2C configuration by Dassault Aviation

Turbulence modelling and simulation by IMFT:
D. Szubert, F. Grossi, I. Asproulias, Y. Hoarau*, M. Braza

Institut de Mécanique des Fluides de Toulouse - IMFT
UMR CNRS-INPT-UPS 5502

* ICUBE-Strasbourg - visiting fellow IMFT

35

Introduction

V2C Laminar Transonic Airfoil

- Designed by Dassault Aviation.
- Laminar boundary layer over a long distance
  - upstream of the shock-BL-Interaction:
  - Minimisation of drag
- Maximum Lift/Drag.

Objectives

- Transition location effects
  - steady, unsteady shock
  - shock position, shock strength
  - flow separation
  - Lift/Drag
  - URANS-OES versus DDES
- Buffet Dynamics
  - OES, DDES

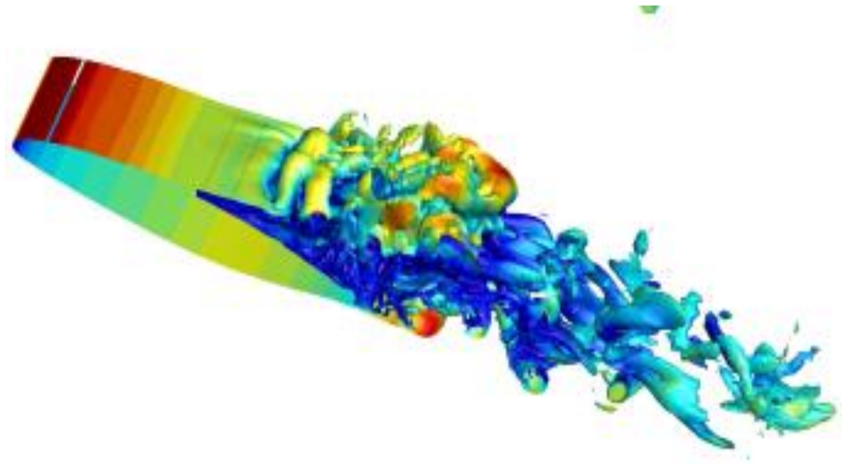

Grid

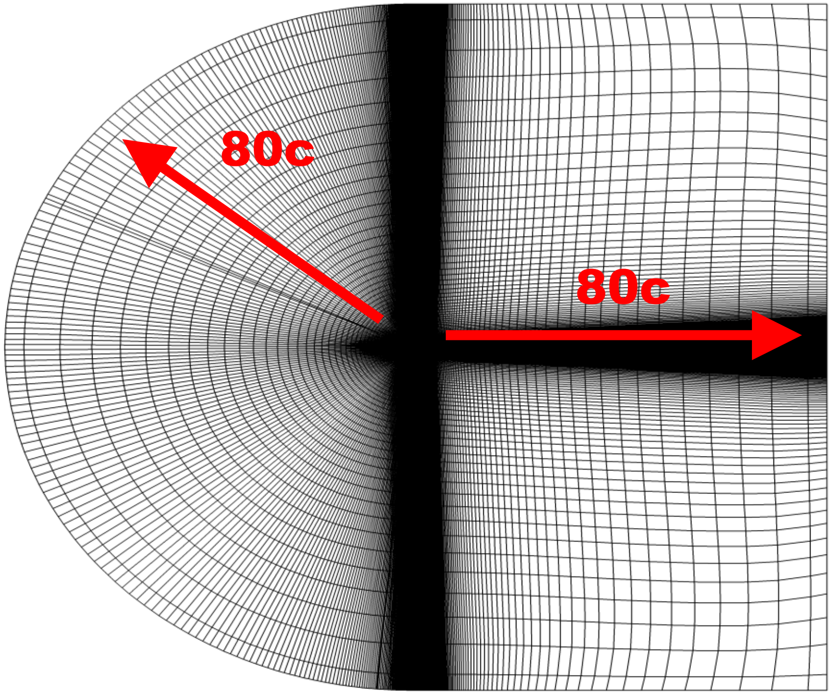

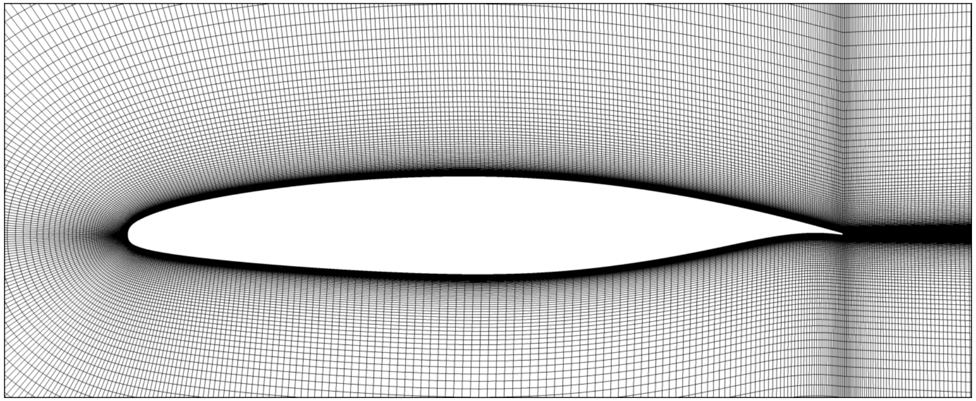

No. cells	
Upper surface	234
Lower surface	192
Trailing edge	42
Normal direction	192
Wake direction	192
Total in (x,y):	**163 584 +128 cells spanwis**

Normal distances	
1st cell height	5e-7 c
y+ average	0.259
y+ maximum	0.535

Buffet Map

2D URANS SST

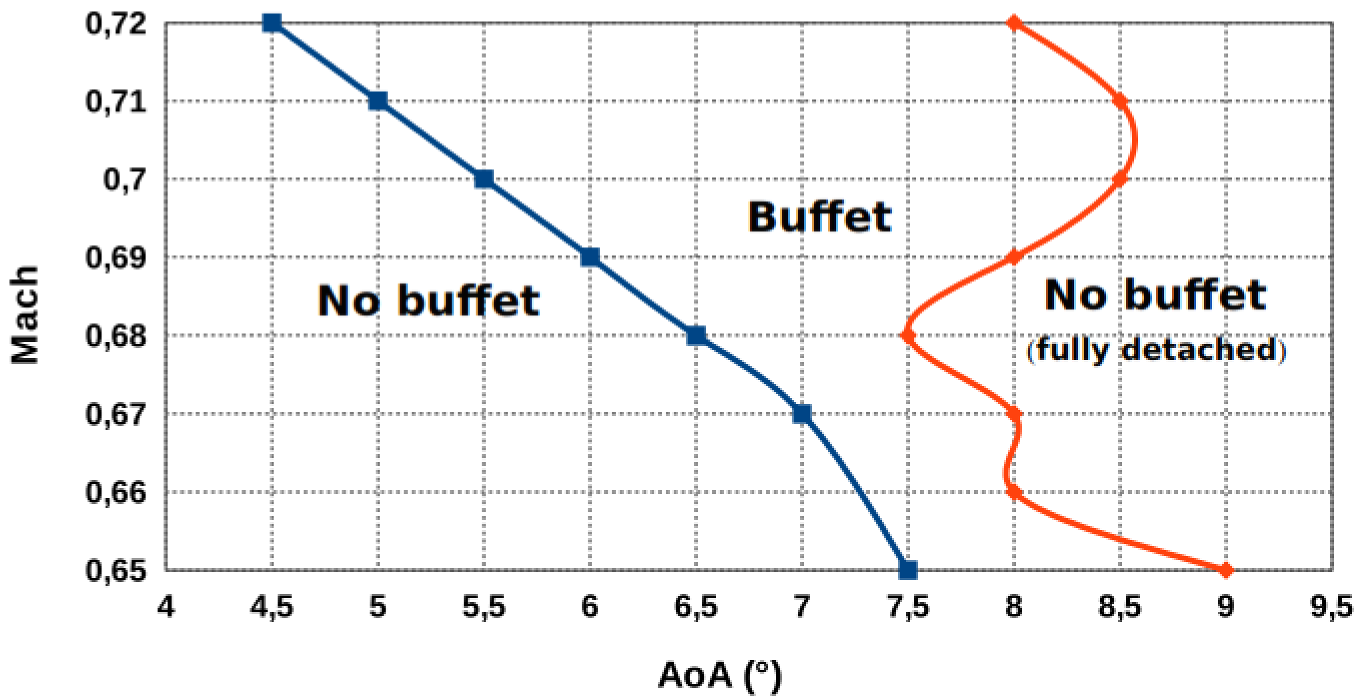

Transition Study-Steady

AoA = 4°

- $Re = 3.245 \times 10^6$
- Mach = 0.70
- k-ω SST

x_t/c	fully turb.	0.10	0.20	0.30	0.40	0.50
x_s/c	0.523	0.532	0.541	0.552	0.564	0.574
x_b/c	0.533	0.541	0.547	0.556	0.566	0.575
l_b/c	0.011	0.024	0.047	0.068	0.085	0.094
x_r/c	0.911	0.925	0.946	0.965	0.566	-
C_L	0.8873	0.9174	0.9556	0.9919	1.029	1.061
C_D x 100	2.080	2.069	2.102	2.171	2.268	2.365
L/D	42.7	44.3	45.5	45.7	45.4	44.9

Transition at 30 % c: optimum lift/drag ra

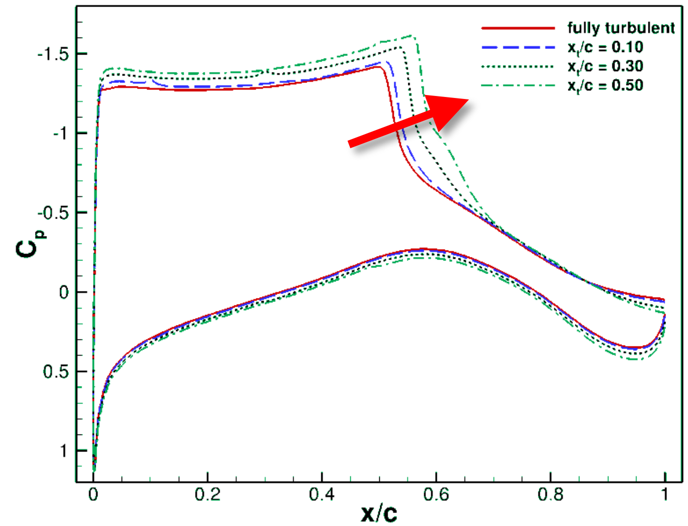

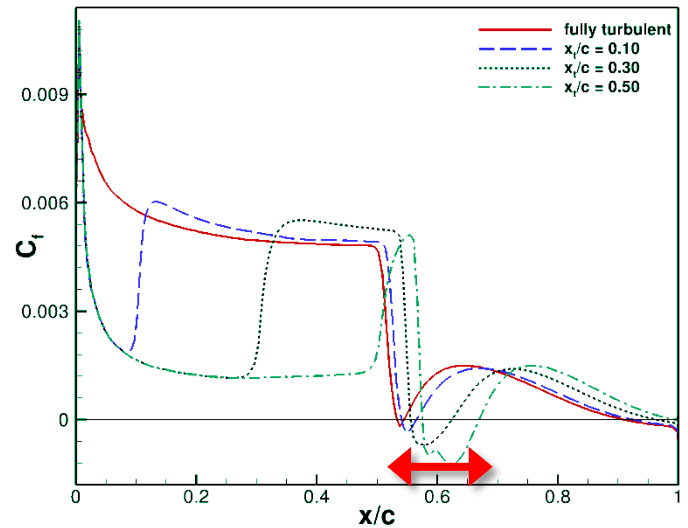

Transition Study-Unsteady

Contours of RMS of pressure fluctuations

- Fully Turb.
- $x_t/c = 0.09$
- $x_t/c = 0.16$
- $x_t/c = 0.24$

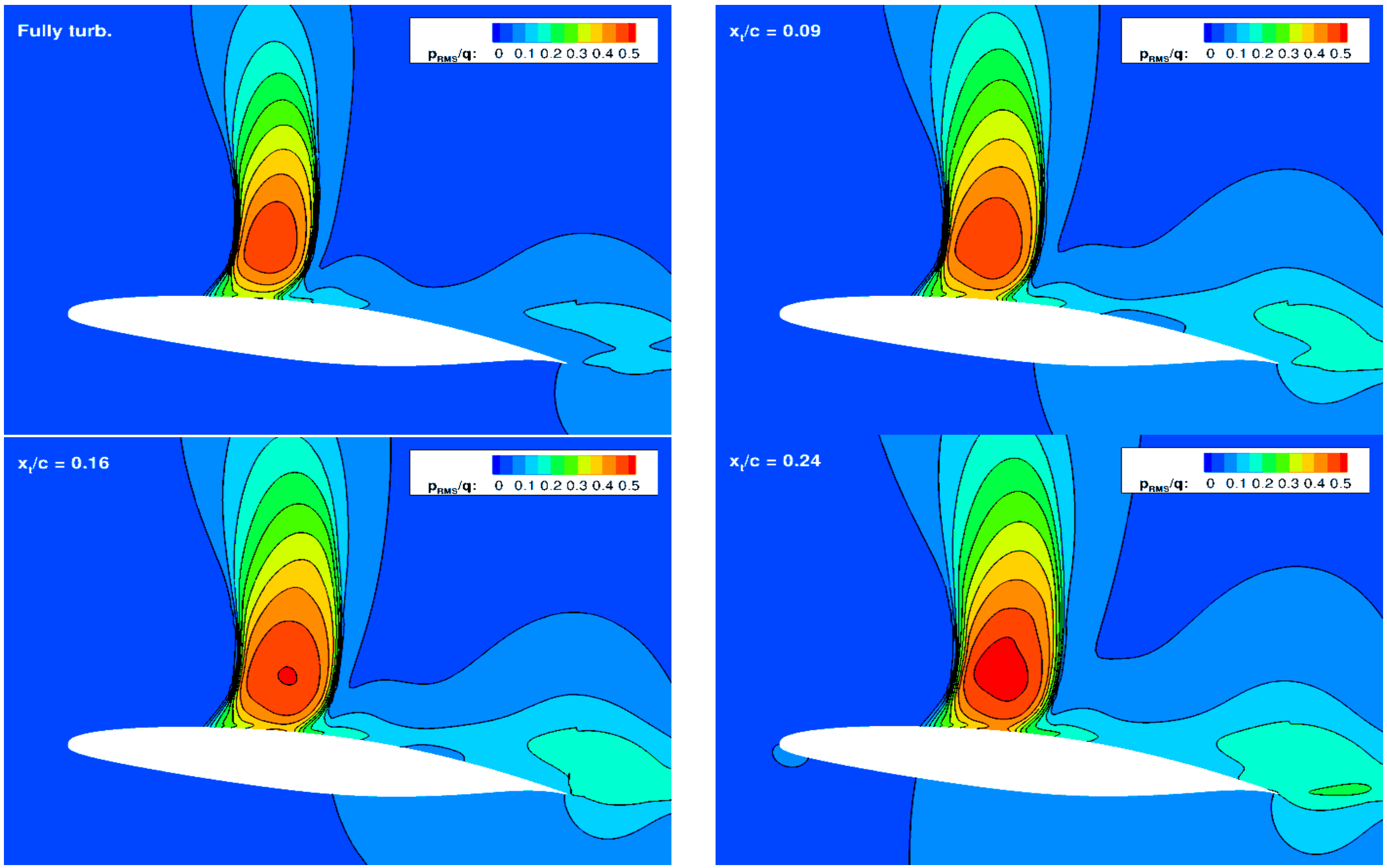

- Delay of transition: increased pressure fluctuation levels within the shock region and near the trailing edge, wider shock-motion range

OPTIMISATION OF THE TRANSITION LOCATION
Collaboration INRIA (R. Duvigneau - J.A. Desideri) avec IMFT

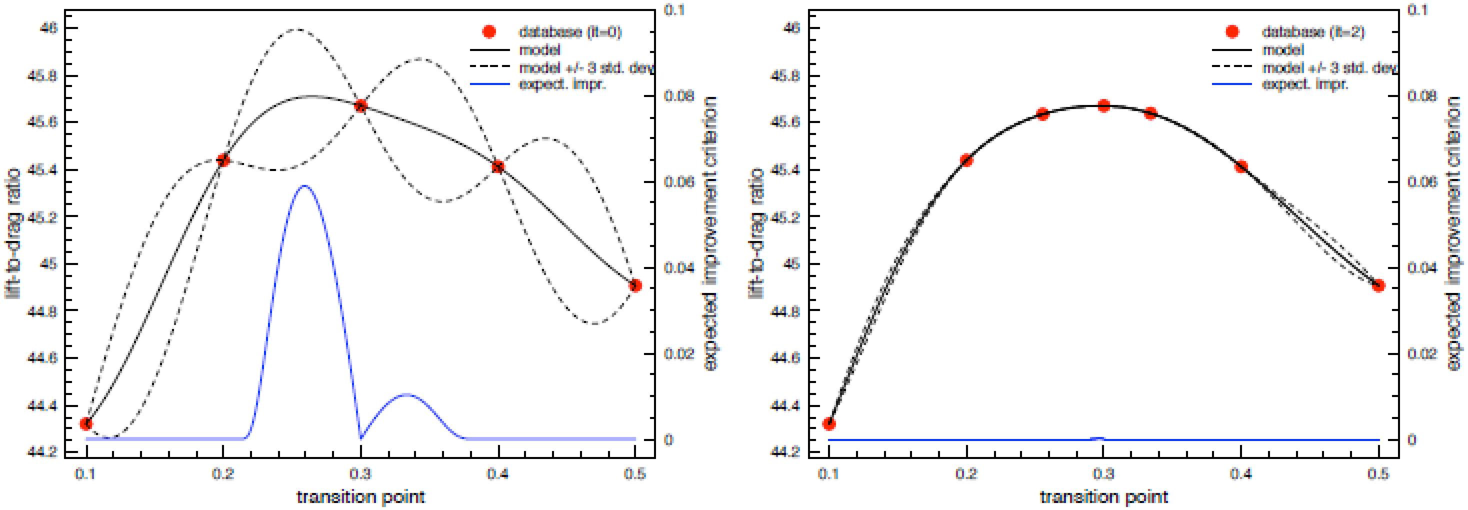

Figure 1: Statistical model for the lift-to-drag ratio w.r.t. the tripping location (steady case), for iteration 0 (left) and iteration 2 (right)

Contribution R. Duvigneau - INRIA avec résultats de simulation IMFT

3D Transonic buffet by DDES

Instantaneous Q-criterion isosurfaces for $Q(c/U)^2 = 75$

Lift_{max}:
$t^* = 0.00$

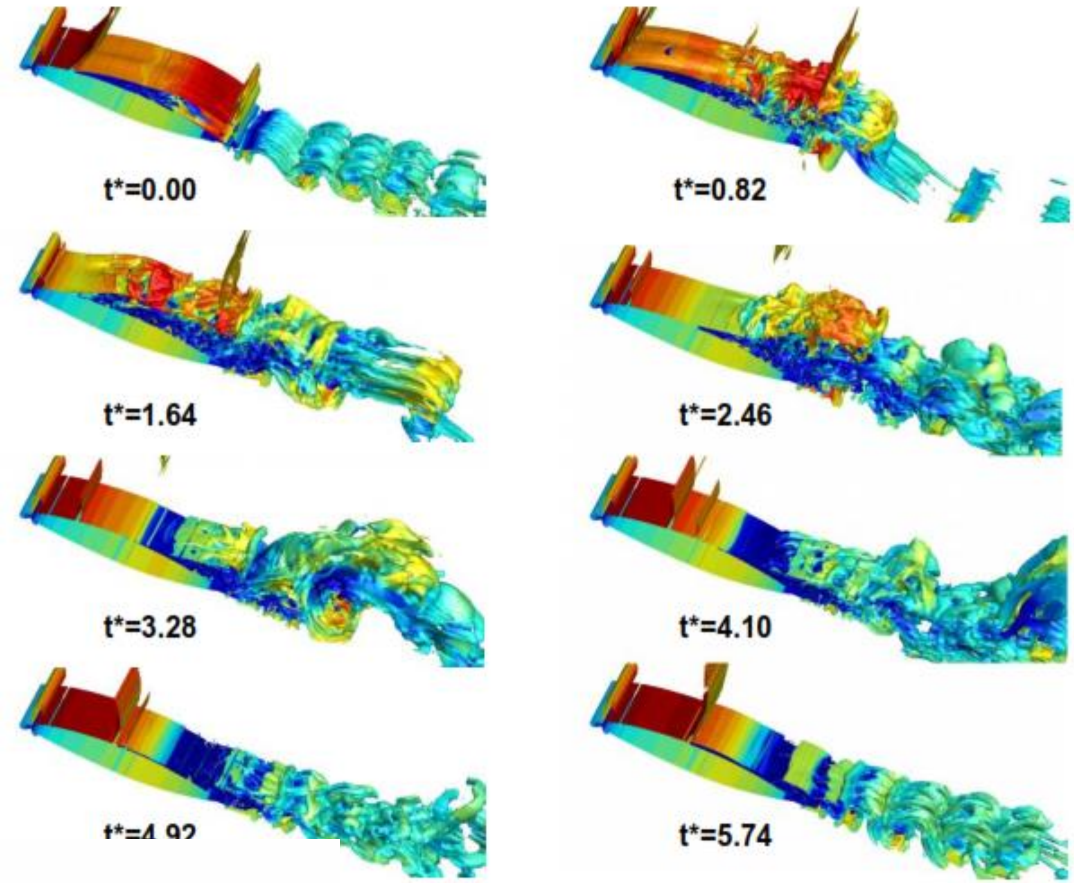

t*=0.00

t*=1.64

t*=3.28

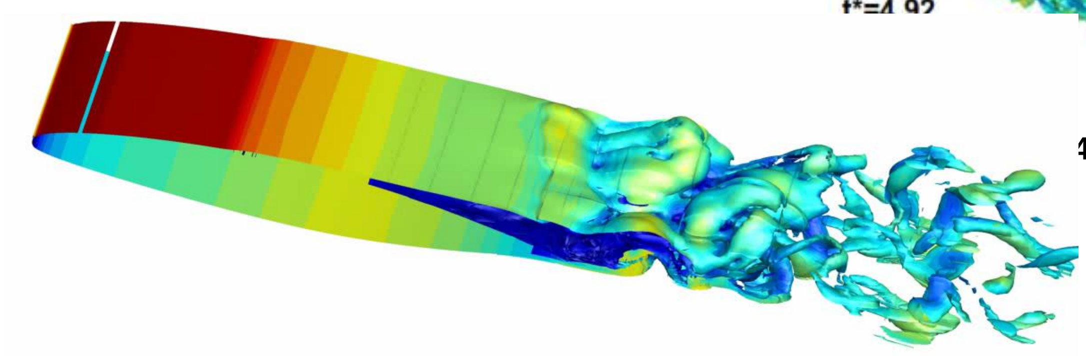

42

Instantaneous contours of divU

Lift$_{max}$:

t*= 0.00

t*=0.00

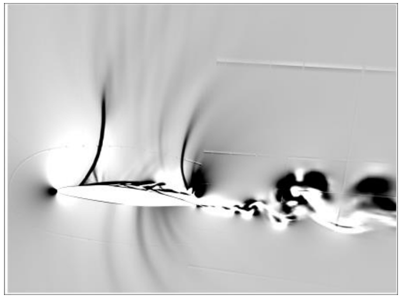

t*=0.82

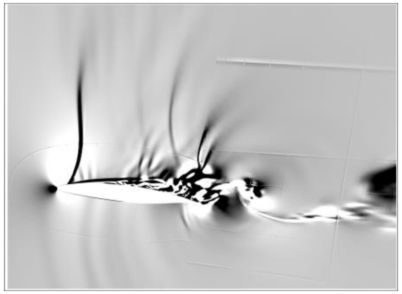

t*=1.64

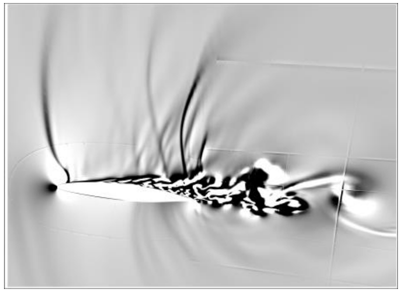

t*=2.46

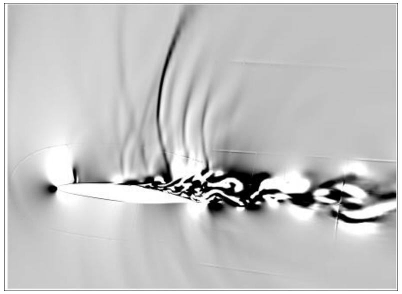

t*=3.28

t*=4.10

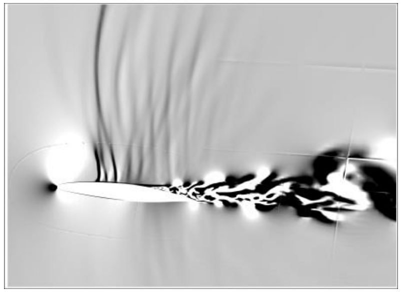

t*=4.92

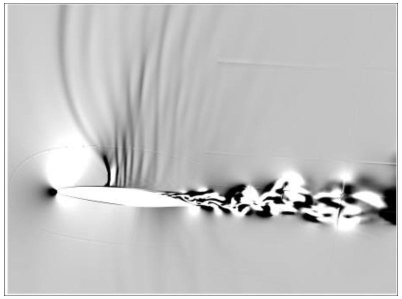

t*=5.74

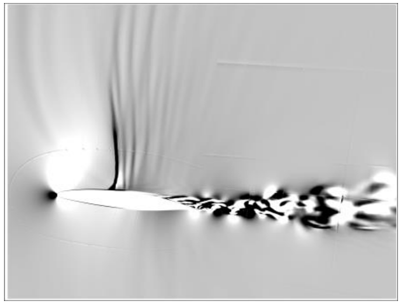

43

Buffet Fluctuations

URANS vs DDES (medium mesh)

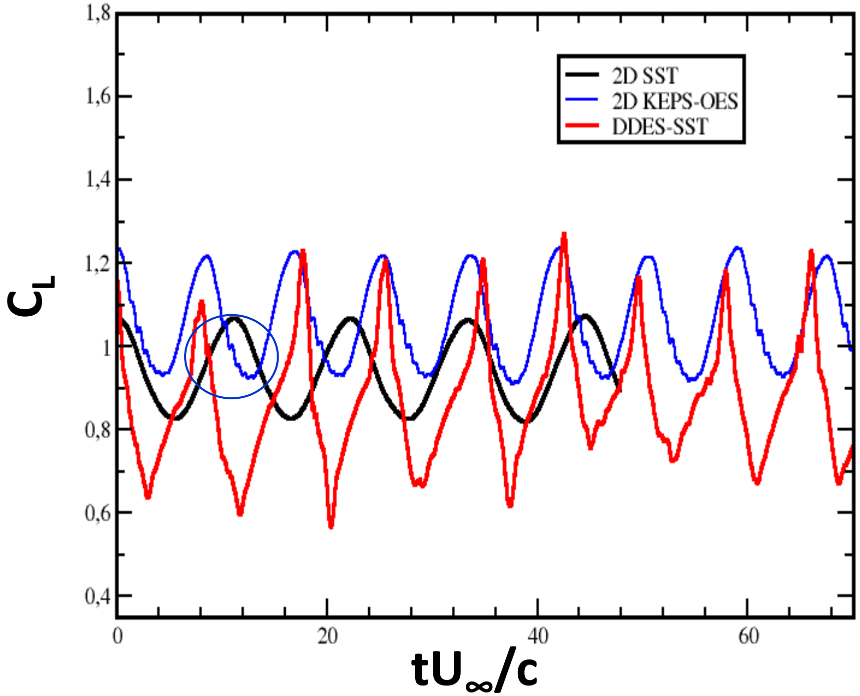

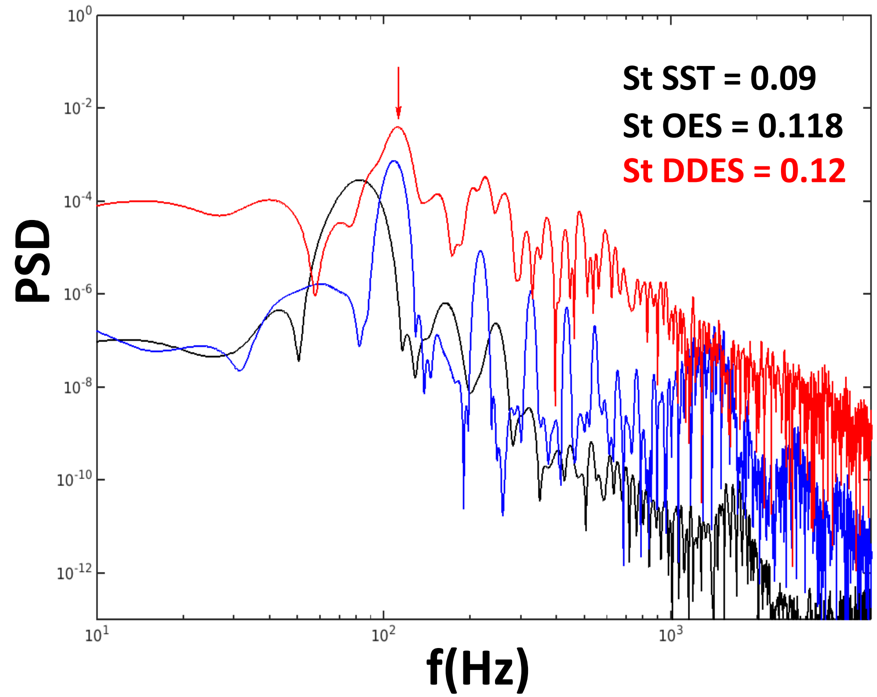

	<C$_L$>	<C$_D$>
SST 2D	0.942	0.062
OES 2D	1.059	0.081
DDES SST	0.875	0.090

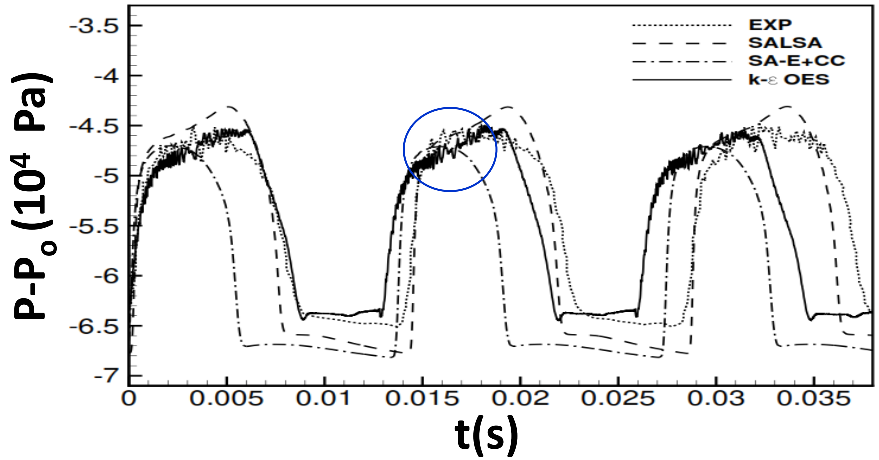

- Re = $3x10^6$
- Mach = 0.70
- AoA = 3.5°
- **x/C=0.45**

ATAAC EU PROJECT

Exps by ONERA
Jacquin et al, AIAA 2005, 09

3D Laminar Wing

Simulation details	Steady	Unsteady
SA, Re=4.35e6, M=0.725, a=5deg	X	
SA, Re=4 .47e6, M=0.745, ↑=5deg	X	
SA, Re=4.5e6, M=0.75, ↑=5deg	X	
SA, Re=4.56e6, M=0.76, ↑=5deg	X	
k-⊭Chien, Re=4.47e6, M=0.745, ↑=5deg	X	
k-⊭Chien, Re=4.47e6, M=0.745, ↑=5deg , imposed transition		X
k-▫ SST, Re=4.47e6, M=0.745, ↑=5deg	X	
k-▫ SST, Re=4.47e6, M=0.745, ↑=5deg , imposed transition		X
k-▫ SST + γ-R_{θ}, Re=4.47e6, M=0.745, ↑=5deg		X

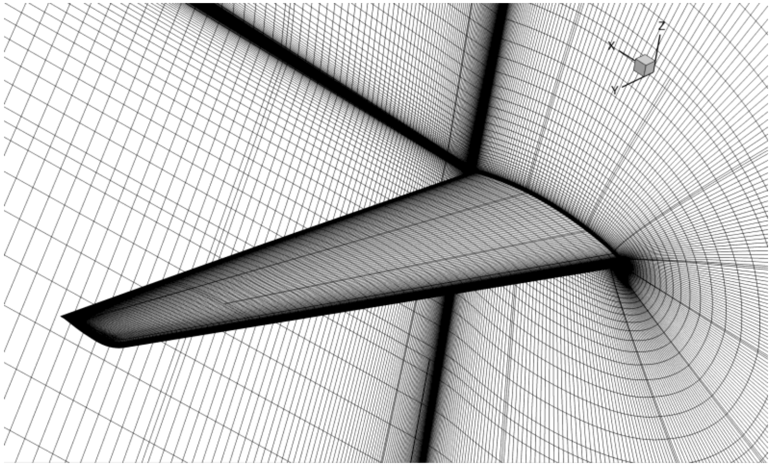

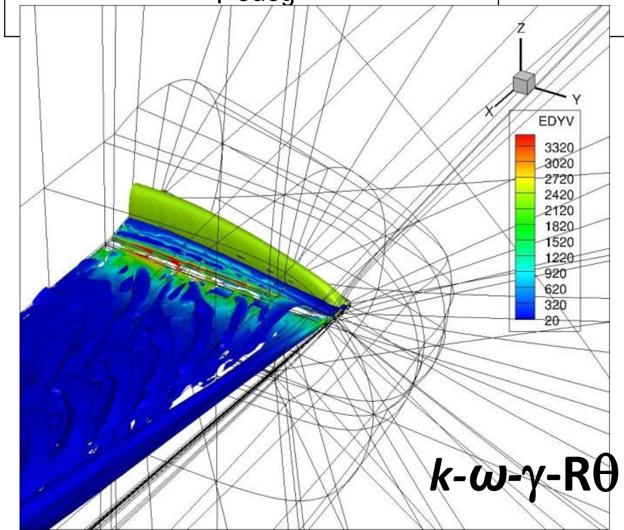

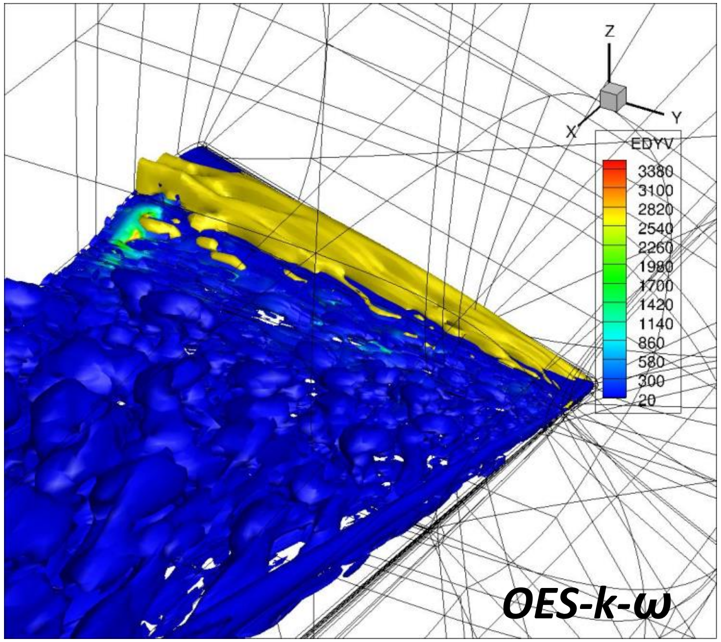

Computations with k-ω and and γ-Rθ

Prediction of the unsteady aerodynamic loads for the problem of acoustic noise

in a generic configuration of a landing gear

‘The tandem cylinders’

Reynolds number 165,000

A test-case of the European research program ATAAC:

***Advanced Turbulence Simulations for Aerodynamic Application Challenges*, April 2009- August 2012**

coordinated by DLR - Germany

Experimental setup at Nasa Langley Rsearch Center

- *Subcritical* flow regime
- Experiments force transcritical flow with **transition strips** Q= 50° - 60°

<u>Re = 166.000</u>
M∞ = 0.128
L =3.7D

Experiments performed at <u>NASA-Langley Research Center</u>

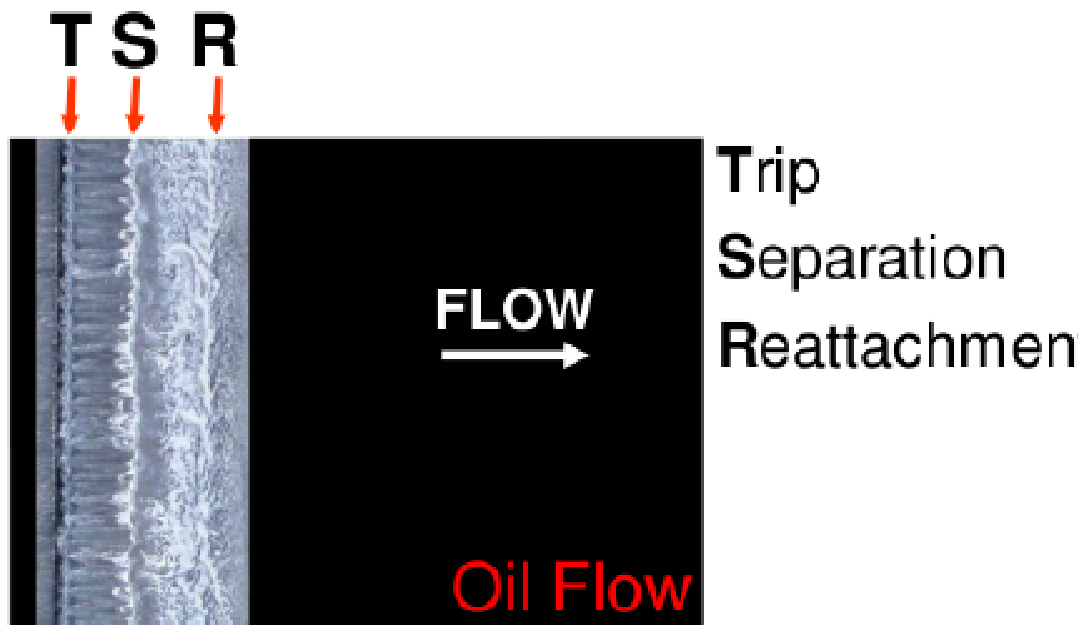

L.N. Jenkins, M.R. Khorrami, M.M. Choudhari, C. B. McGinley 2005, 2006, AIAA Conf. Reno

Numerical Approach

Pilot EU project PRACE – CINES - CEA

- **Computational domain**

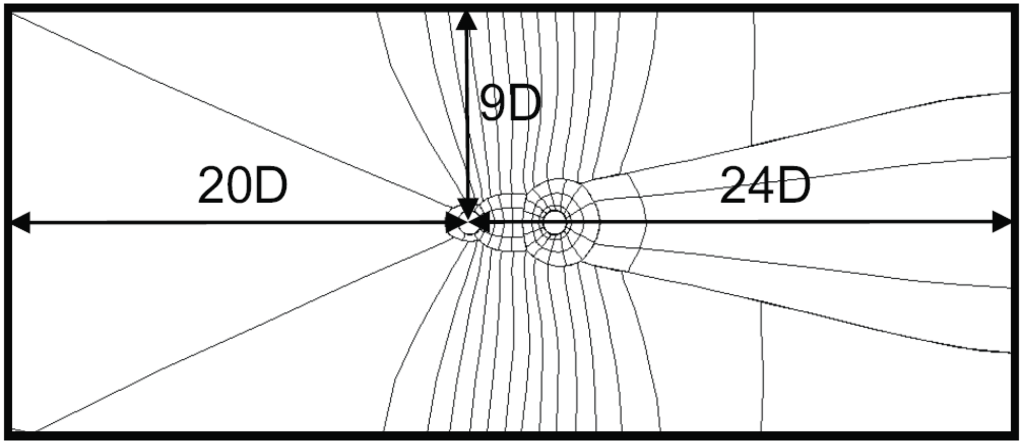

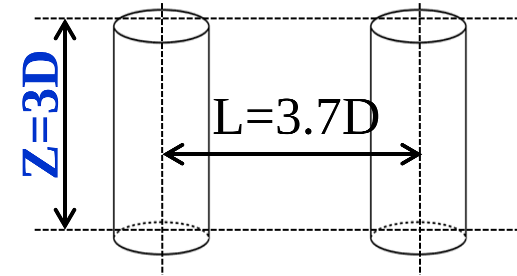

Grid size: 12,5 mio. points

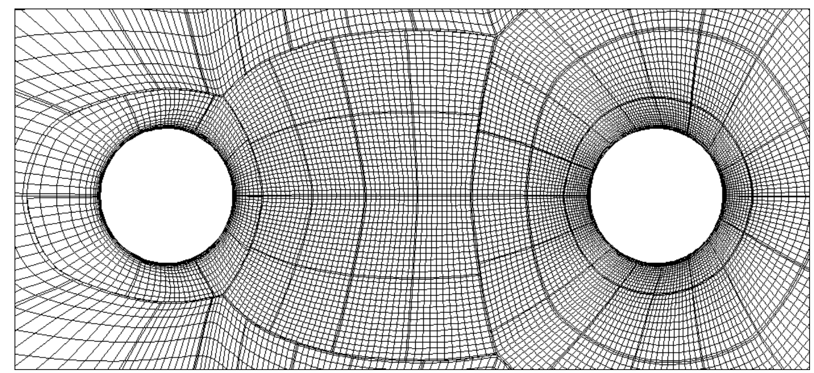

Grid provided by **NTS** (New Technologies and Services), St. Petersburg, Russia- M. Strelets – M. Shur

Code: NSMB - Navier Stokes Multi Block

Numerical Scheme:	Central- 2nd Order
Time Steps:	$\Delta t = 0.01$ and $\Delta t = 0.0005$
MPI-Architecture:	SGI ALTIX ICE
Number of CPUs:	512, 1024, 4096

Simulations performed in supercomputers **JADE of the CINES** Centre Informatique National de l'Enseignement Supérieur, Montpellier, France and on **CURIE** –CEA (**PRACE** MPI European initiative)

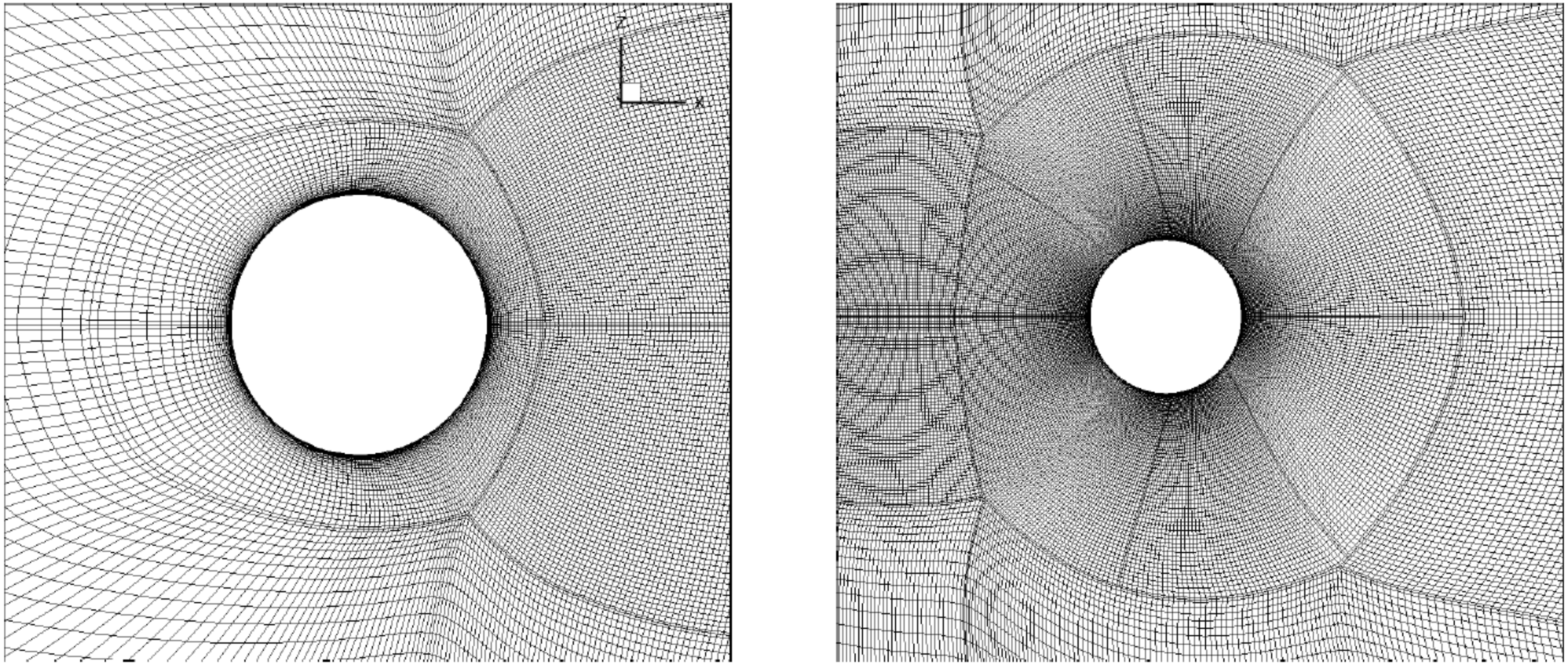

Zoom of the grid near the bodies

Mandatory grid provided by NTS - M. Strelets St - Petersbourg - partner in the ATAAC European program and coordinator of test-case

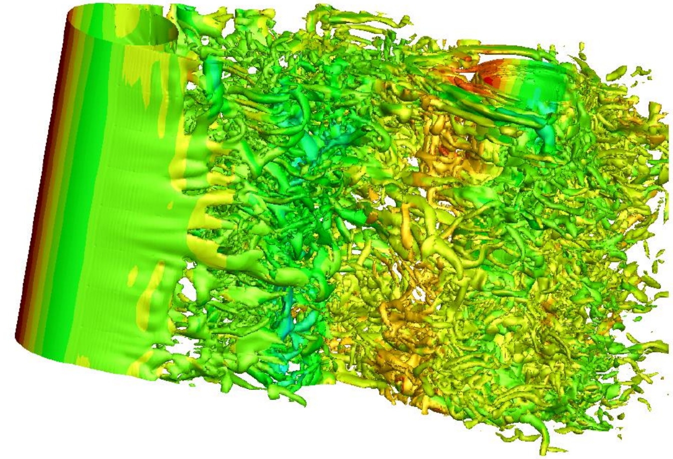

Figure 7.1: Isovorticity $\Omega/D = 15$ with pressure flood (red = high pressure, blue = low pressure)

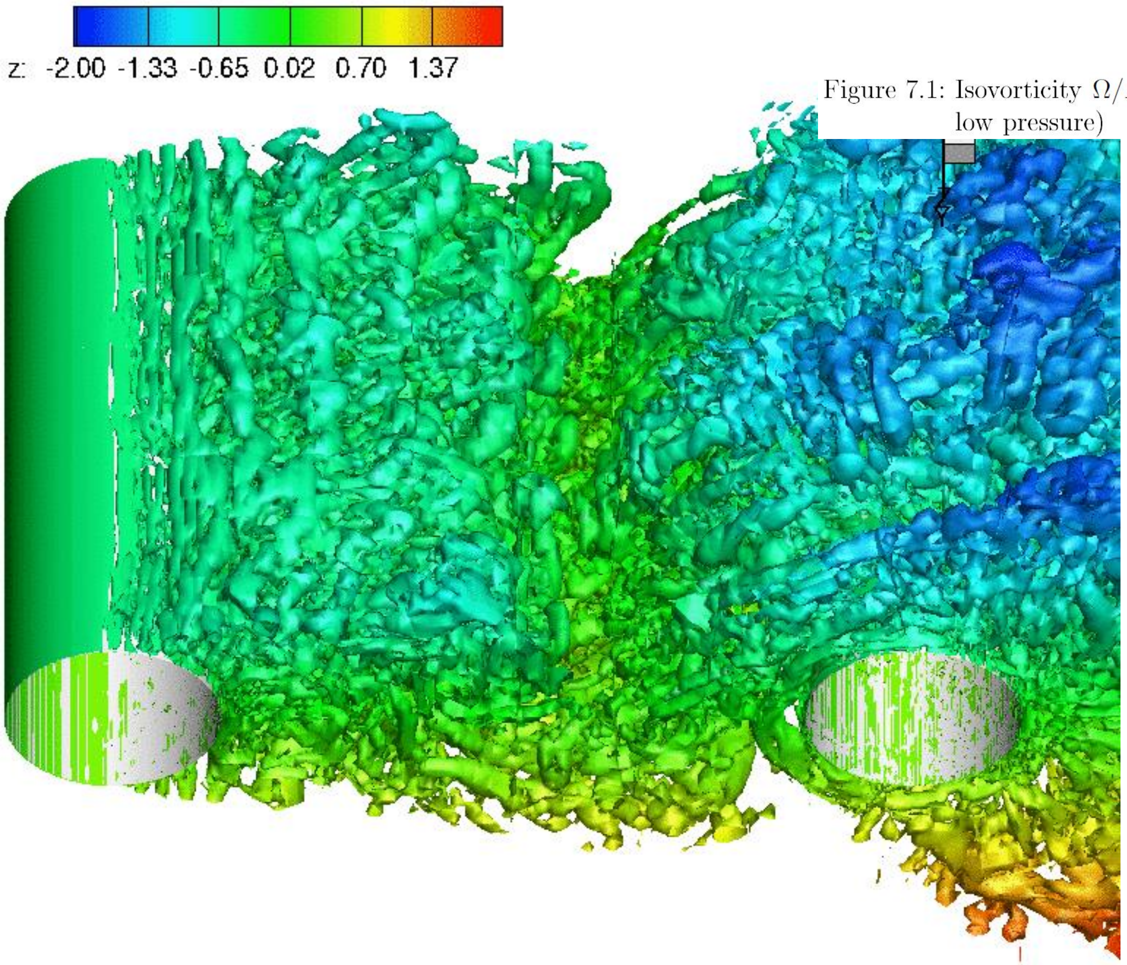

T. Deloze

The shear-layer instability :

source of aerodynamic noise. Tandem Cylinders – landing gear

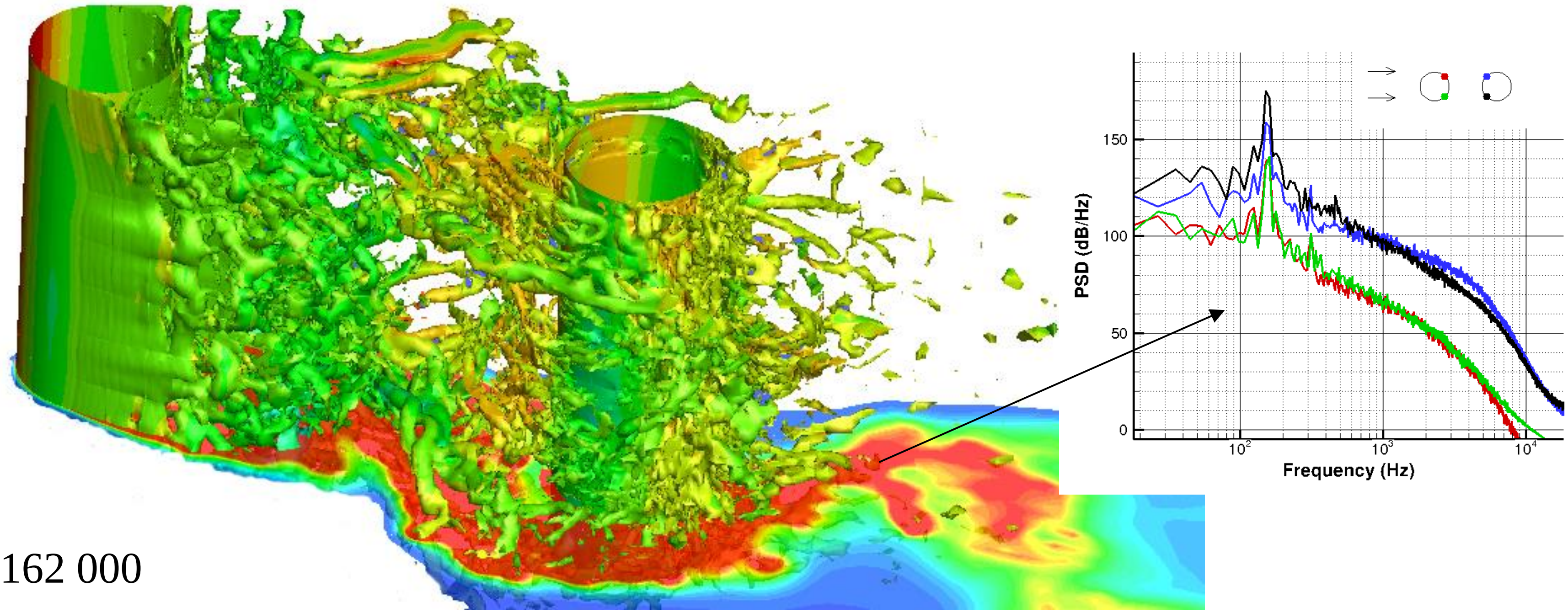

Re= 162 000

DDES ***k***-*ω*-OES modelling – NSMB code 6.4

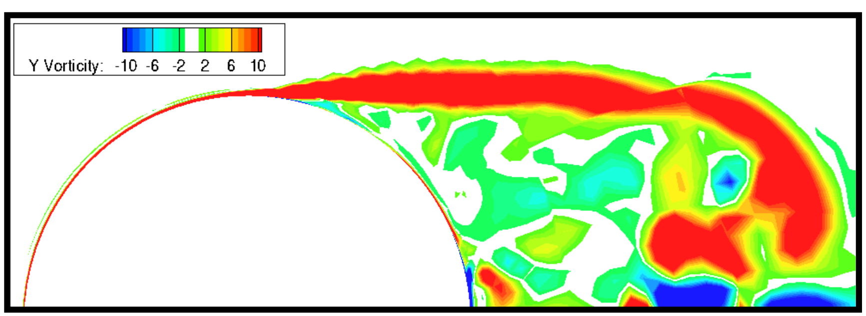

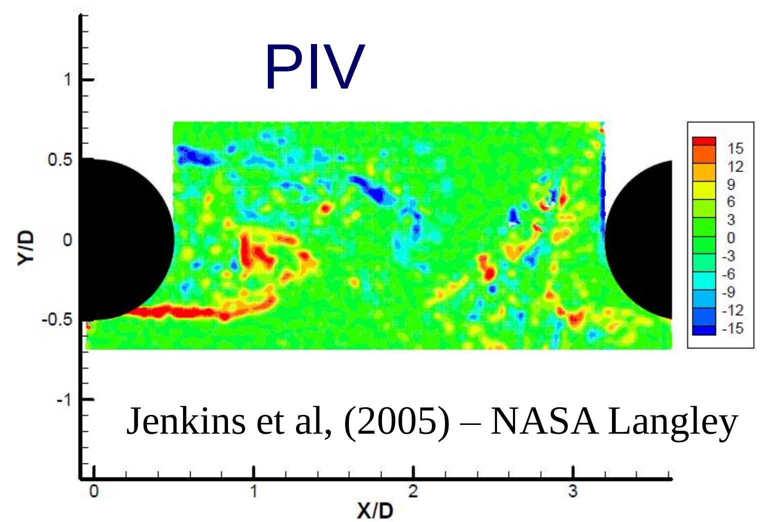

Jenkins et al, (2005) – NASA Langley

Overview of the iso-velocity contours field and of velocity profiles and spectra

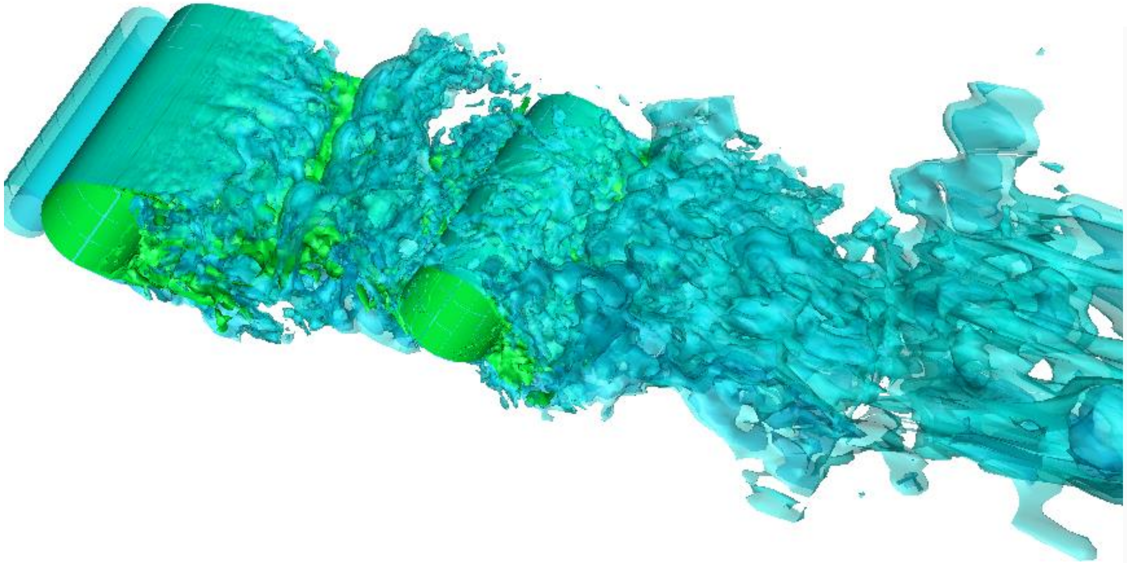

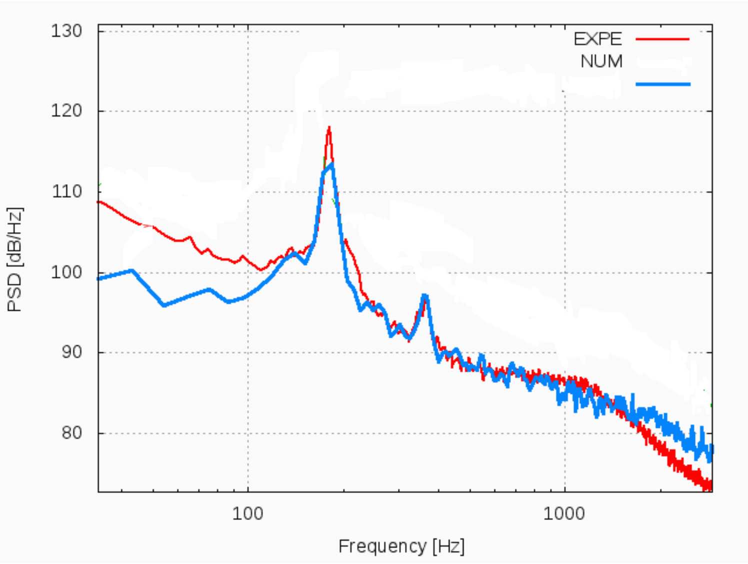

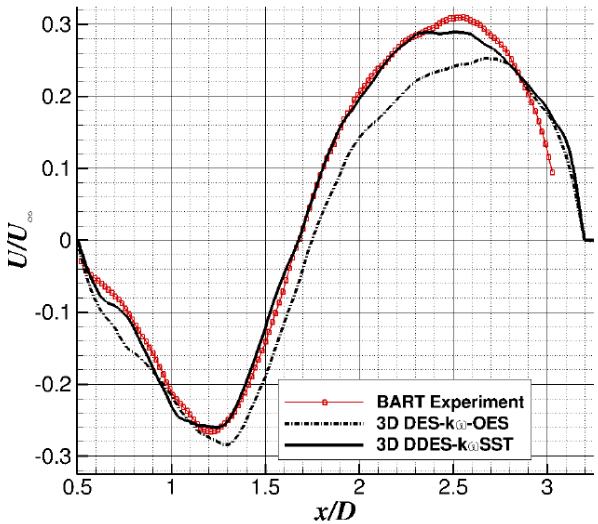

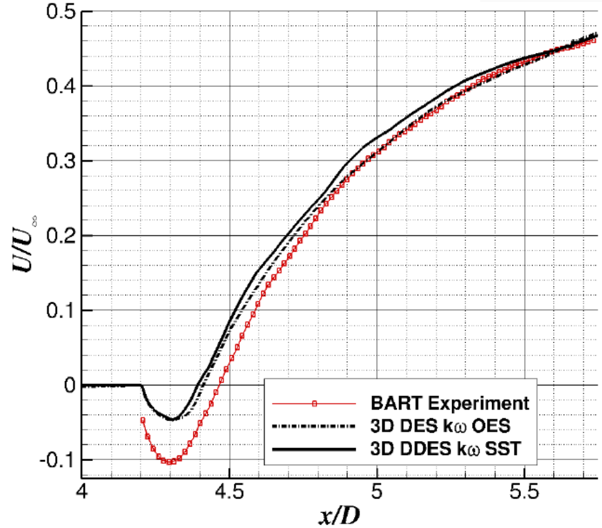

Results

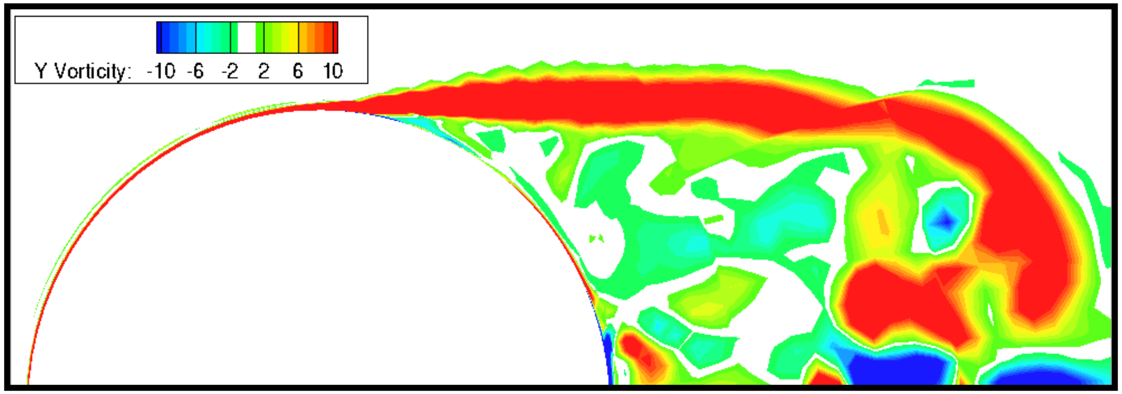

- thin boundary layer dynamics
- turbulence wraps around 2nd cylinder
- high unsteadiness

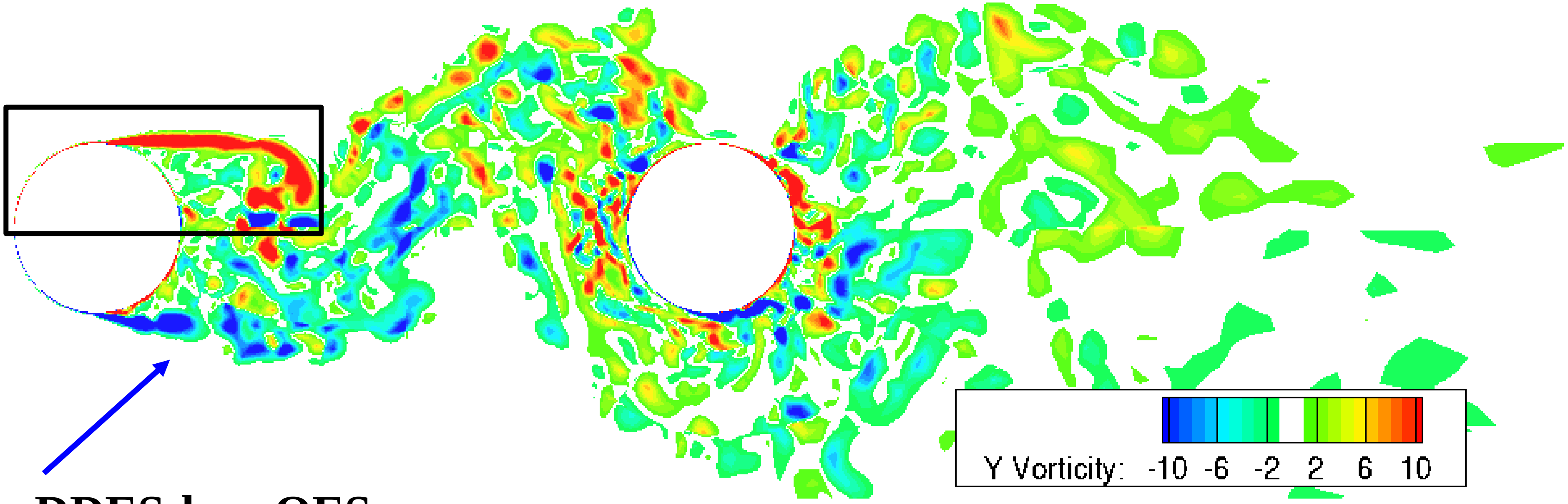

DDES-k-ω-OES

Mean velocity streamlines in comparison with exp. field

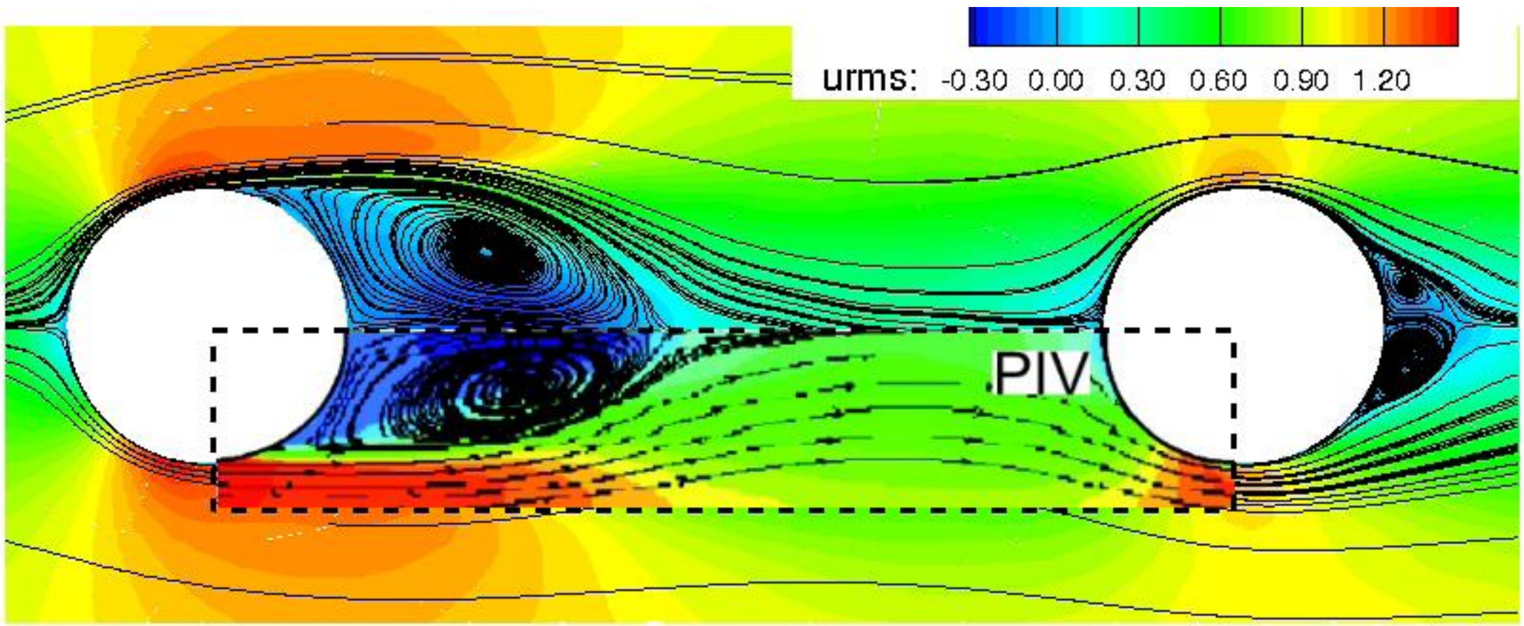

Good agreement **PIV- CFD**
DDES-OES

CPU-time:
~ 100.000 CPUh

„Real“ time:
~ 1.5 weeks

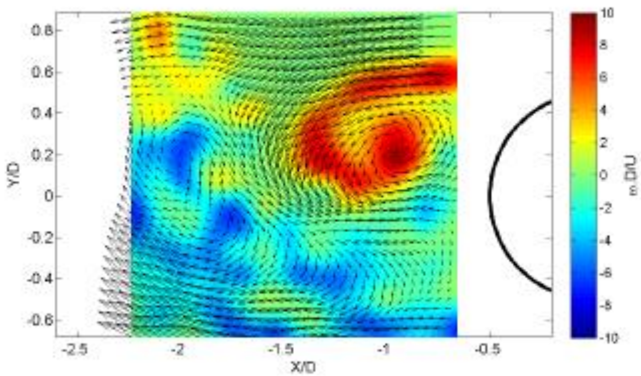
Y/D
X/D
ω.D/U

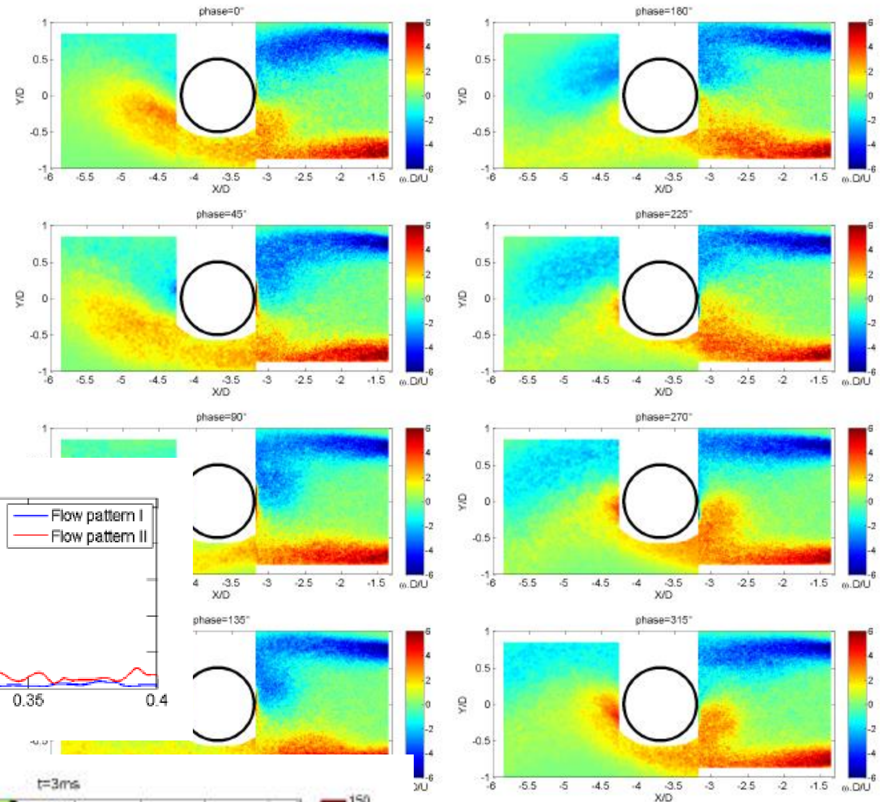
phase=0°
phase=45°
phase=90°
phase=135°
phase=180°
phase=225°
phase=270°
phase=315°
Y/D
X/D
ω.D/U

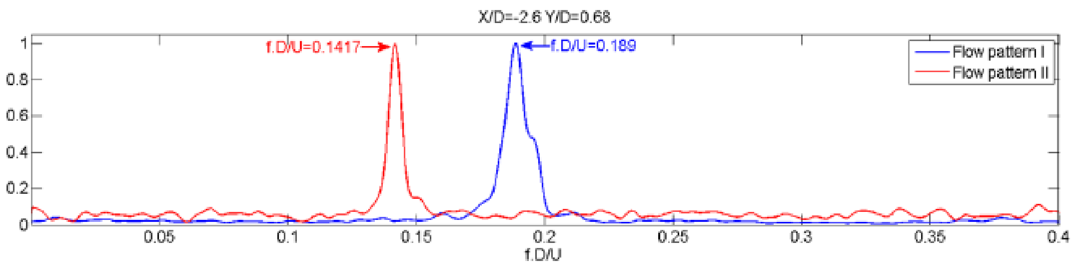
X/D=-2.6 Y/D=0.68
f.D/U=0.1417
f.D/U=0.189
Flow pattern I
Flow pattern II
f.D/U

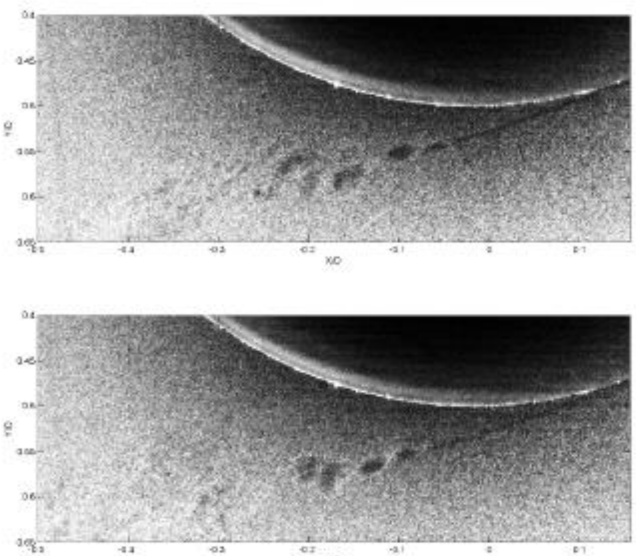

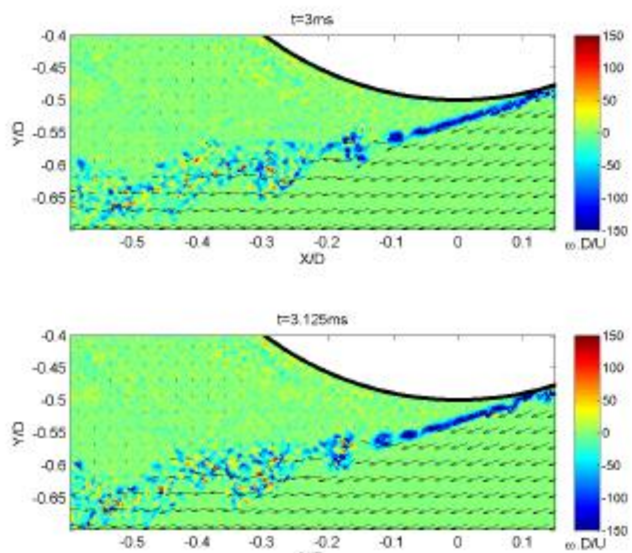
t=3ms
t=3.125ms
Y/D
X/D
ω.D/U

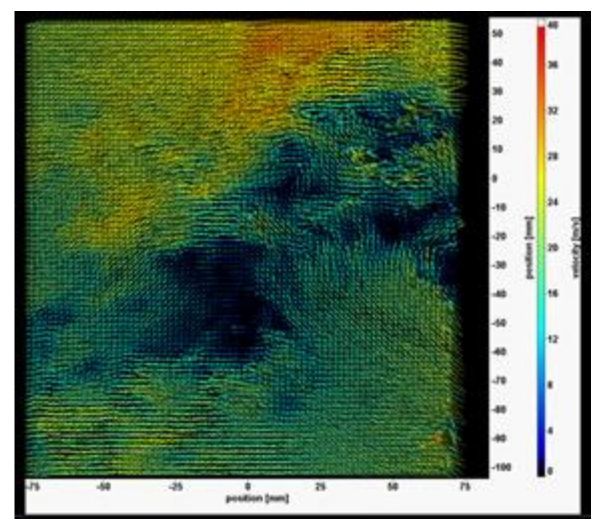

DYNAMIC CASE : 2nd CYLINDER FREELY MOVING

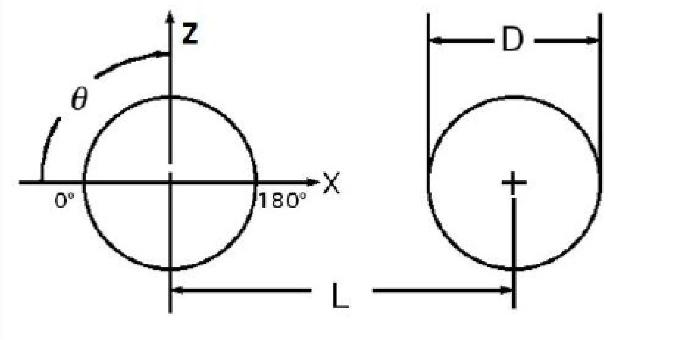

FIGURE: ATAAC configuration : $L = 3.7d$ and $Re = 166000$

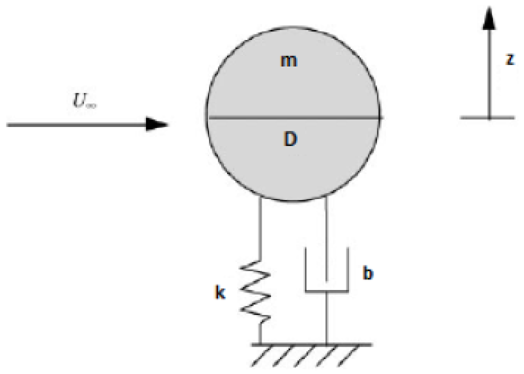

FIGURE: Free vibration of the downstream cylinder

ALE approach for coupling

In NSMB code

$$m^* \ddot{y}^* + b^* \dot{y}^* + k^* y^* = c_y(t^*)$$

Equation de la dynamique

Pour 2 degrés de liberté :

$$\begin{cases} m\,\ddot{x}(t) + c\,\dot{x}(t) + k\,x(t) = F_x(t) \\ m\,\ddot{y}(t) + c\,\dot{y}(t) + k\,y(t) = F_y(t) \end{cases} \tag{6}$$

m la masse, c l'amortissement et k la raideur de la structure

$$\boxed{F_i(t) = C_i(t)\,\frac{1}{2}\,\rho\,D\,u_i(t)^2} \text{ avec } C_i(t) \text{ le coefficient de } \begin{cases} \text{trainée} \\ \text{portance} \end{cases} \tag{7}$$

Soit $q(t)$ le vecteur position, sous forme matricielle :

$$\boxed{[M]\,\ddot{q}(t) + [C]\,\dot{q}(t) + [K]\,q(t) = F(t)} \tag{8}$$

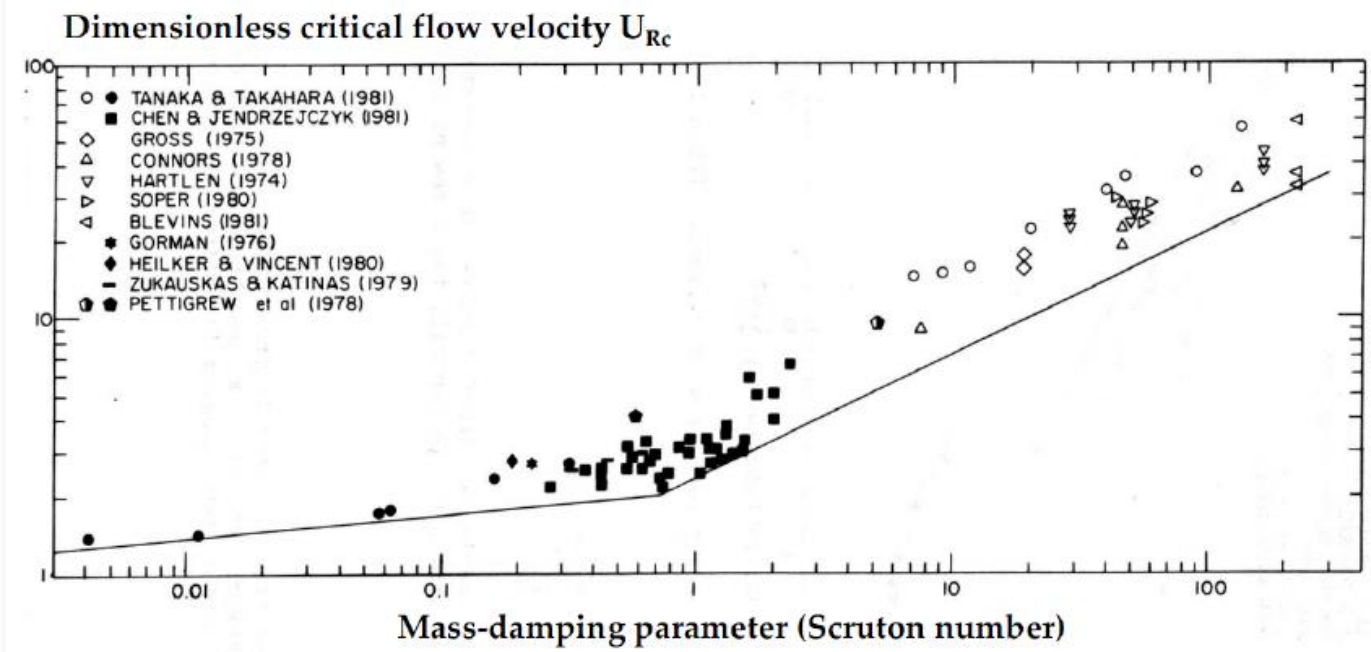

Scruton number (mass-damping) : $\boxed{Sc = \frac{2\,\pi\,\xi\,m}{\rho\,d^2\,l}}$ avec $\xi = \frac{a}{2\sqrt{m\,r}}$

Reduced velocity : $\boxed{u^* = \frac{u}{f_{s_0}\,d}}$ avec $f_{s_0} = \frac{1}{2\,\pi}\sqrt{\frac{r}{m}}$

m, mass, a, damping et r, stiffness of the tube of the bundle

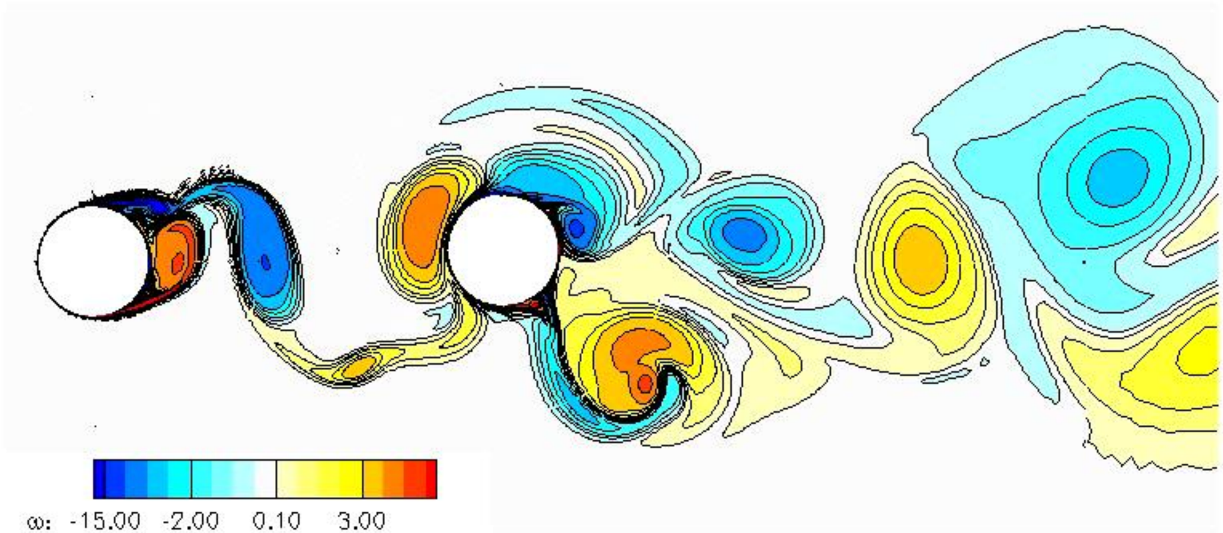

U*=2,
Scr=1

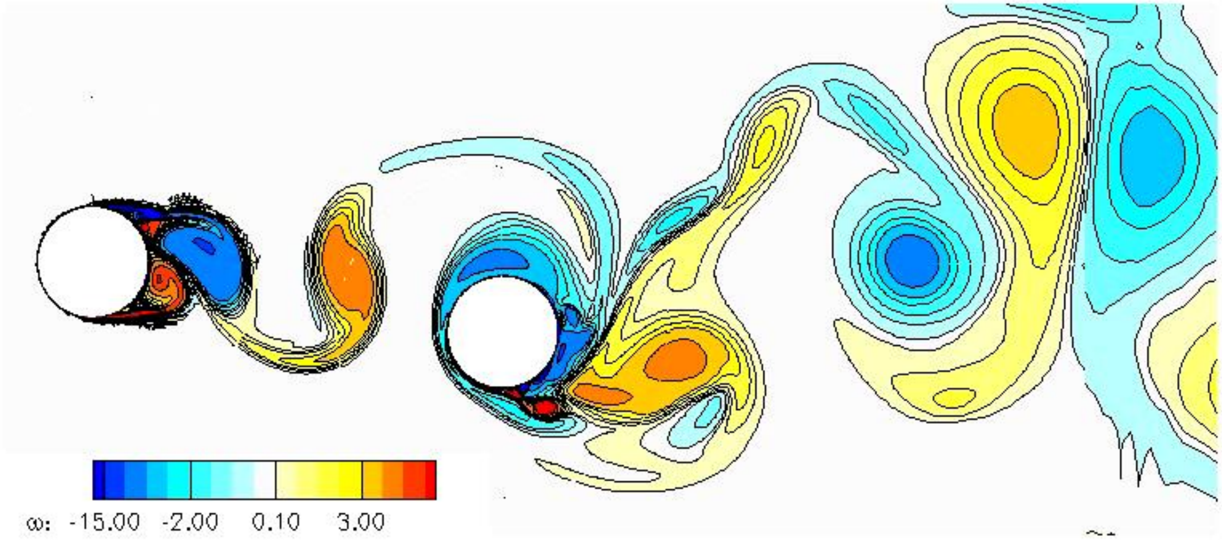

U*=5

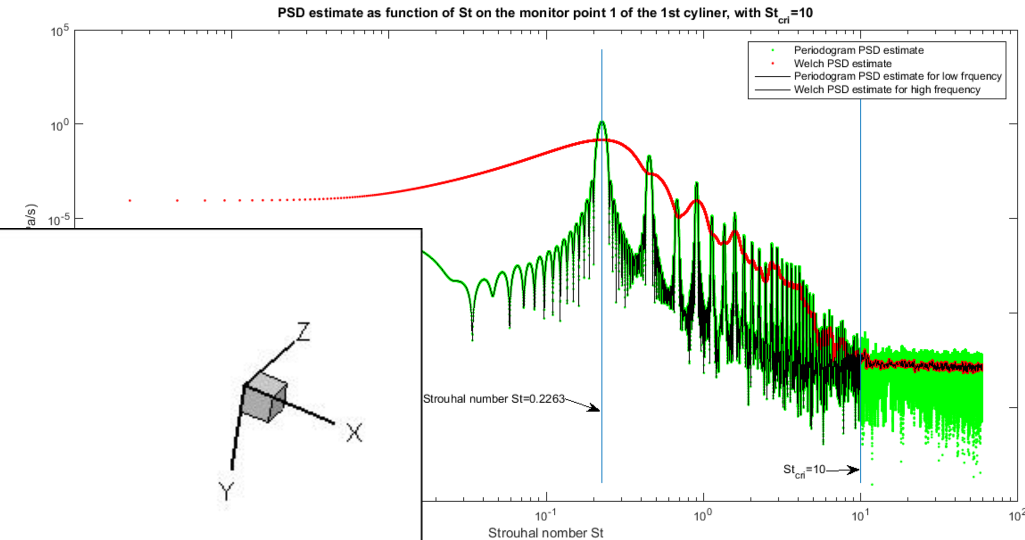
PSD estimate as function of St on the monitor point 1 of the 1st cyliner, with St_{cri}=10
Periodogram PSD estimate
Welch PSD estimate
Periodogram PSD estimate for low frquency
Welch PSD estimate for high frequency
Strouhal number St=0.2263
St_{cri}=10
10^{5}
10^{0}
10^{-5}
10^{-1}
10^{0}
10^{1}
10^{2}
Strouhal nomber St

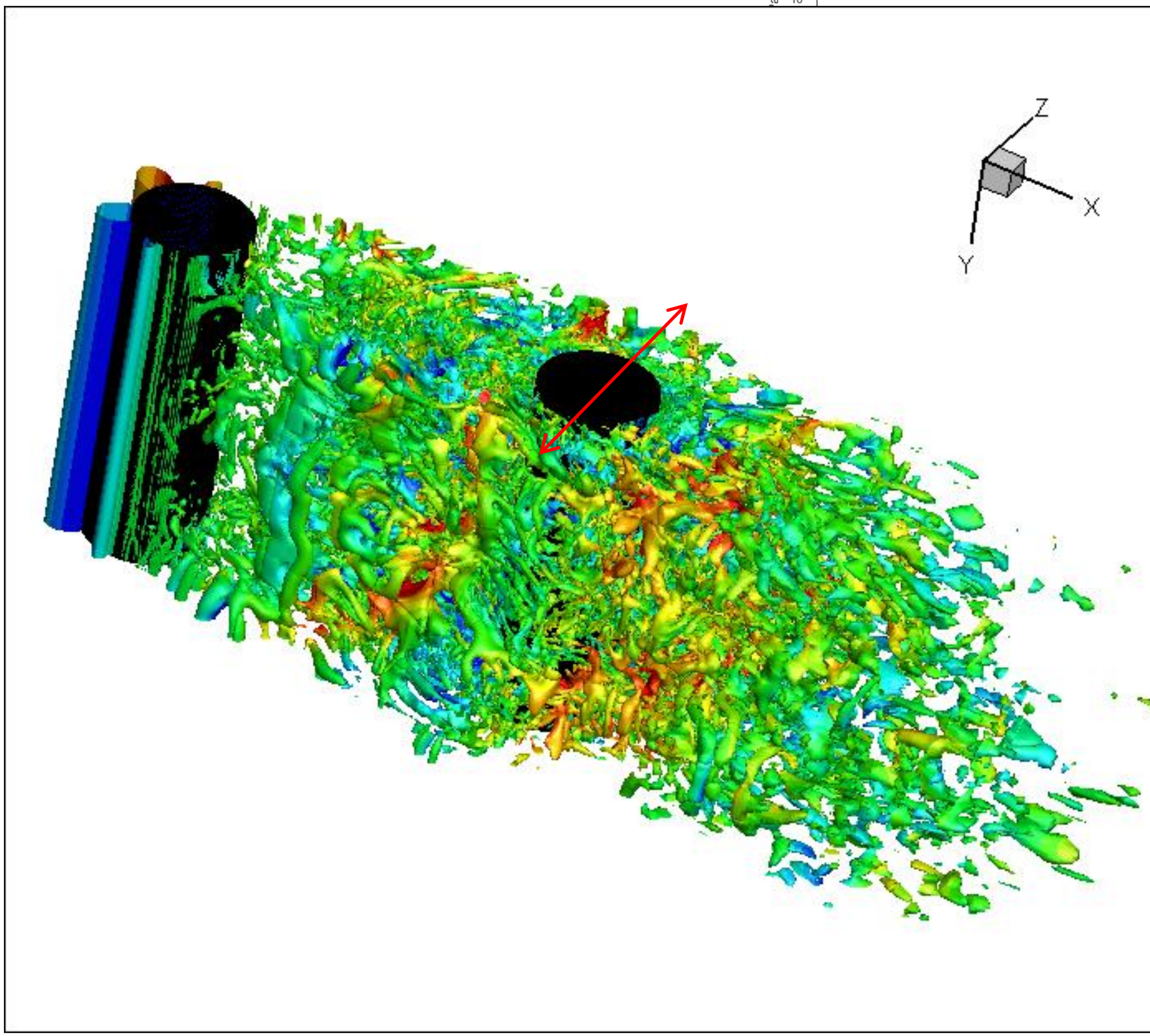
Z
X
Y

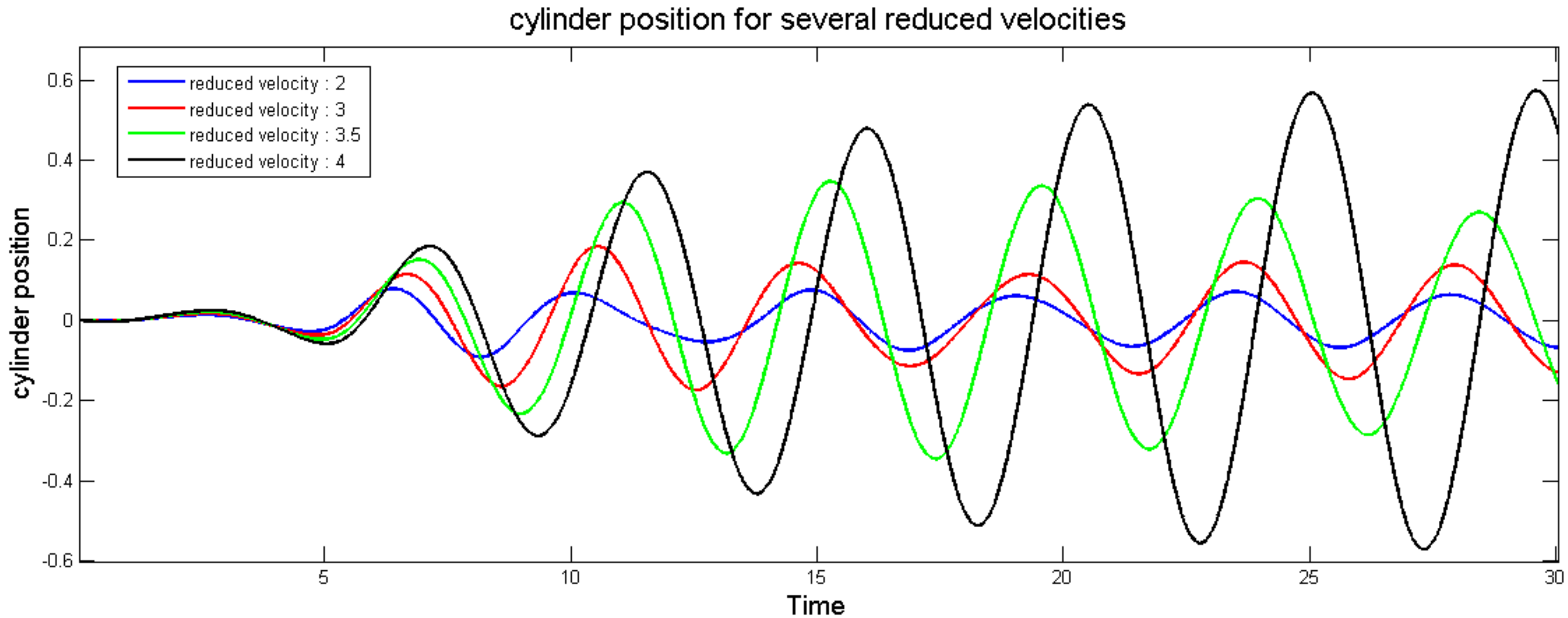
cylinder position for several reduced velocities
reduced velocity : 2
reduced velocity : 3
reduced velocity : 3.5
reduced velocity : 4
cylinder position
Time

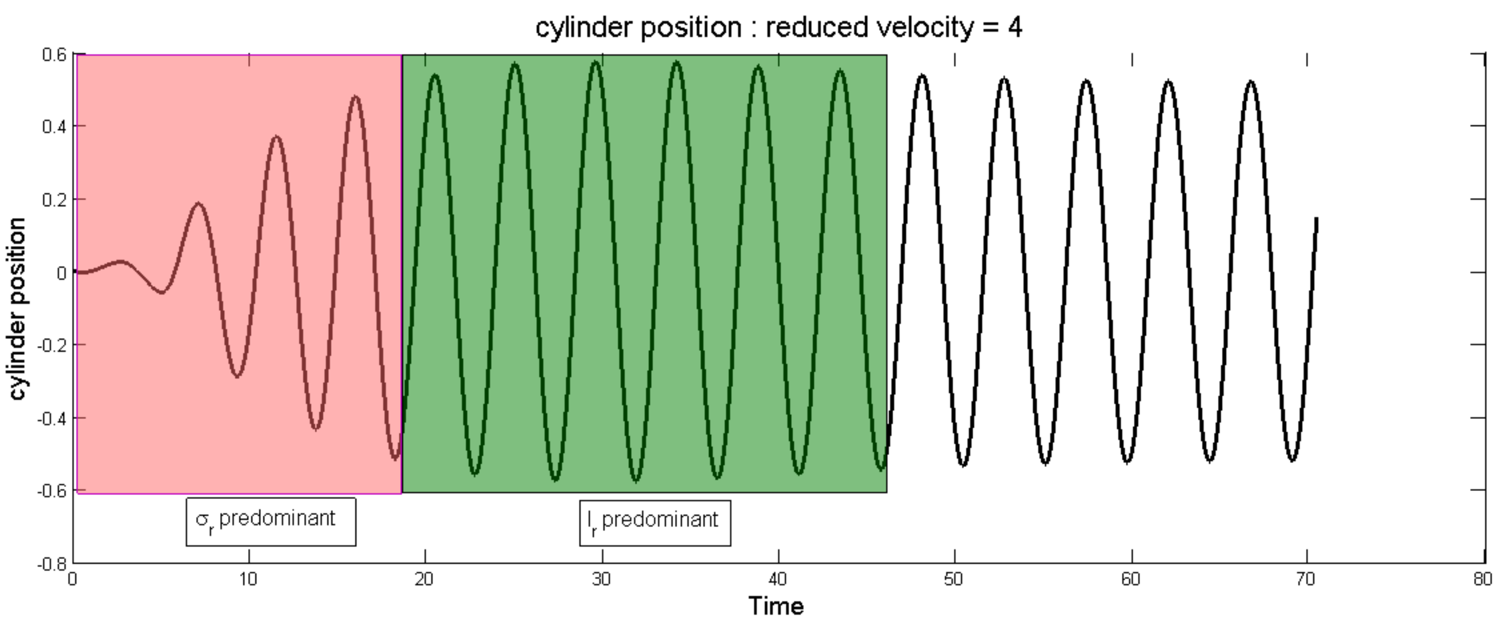
cylinder position : reduced velocity = 4
cylinder position
σr predominant
lr predominant
Time

POD reconstruction -Reduced Order Modelling
Vibratory motion of the second cylinder

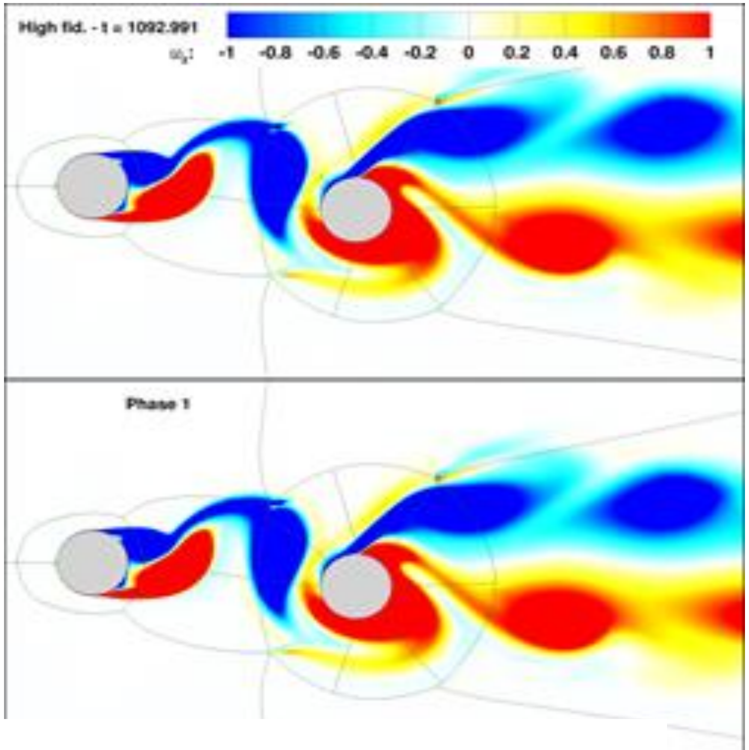

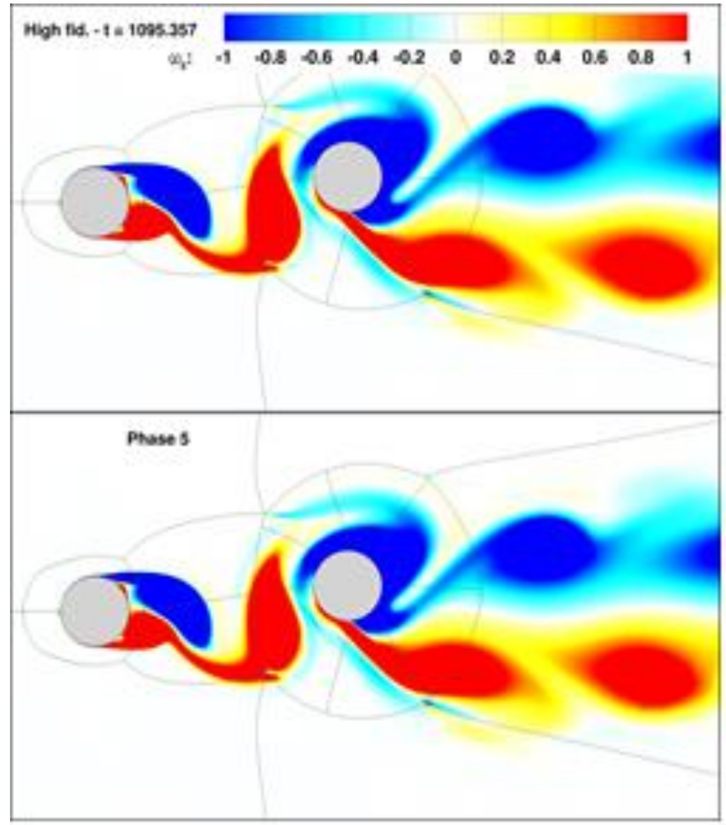

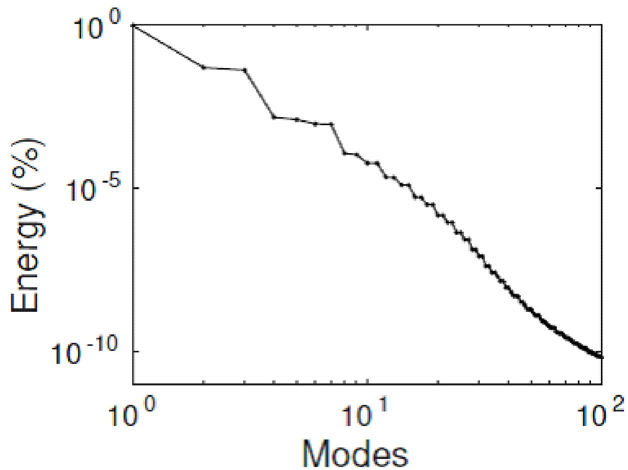

Prediction of fluid-elastic instability

at high Reynolds number

in a cylinders bundle

National research program ANR 'BARESAFE' :

Simulation of Safety Barrier Reliability

ANR : « Agence Nationale de Recherche » - France

Tuble bundle

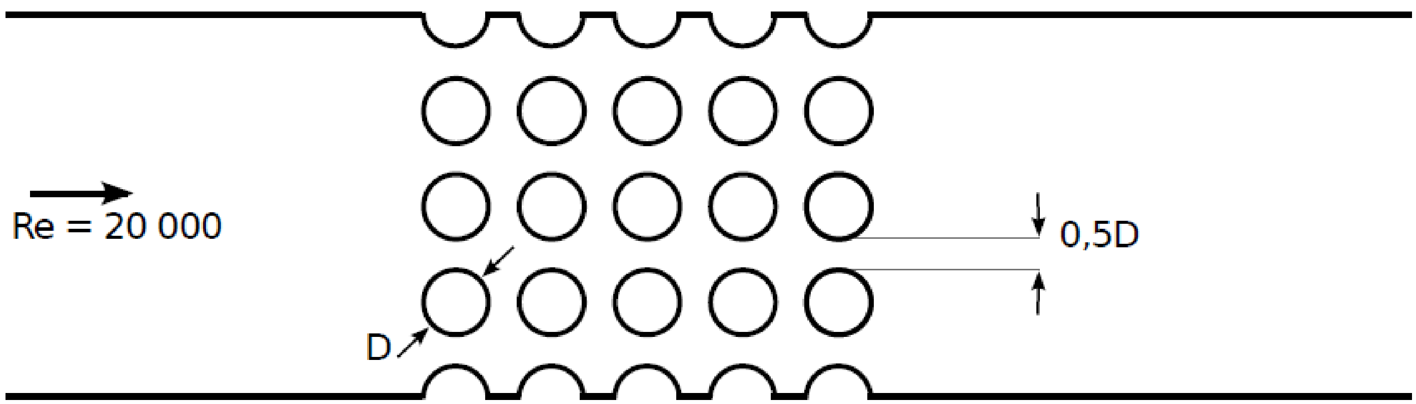

Results from the publication: Shinde, Braza, Longatte et al, JFS 2014, Vol. 47 - one of the most downloaded JFS articles

Characteristic

- 15 cylinders + 10 half-cylinders
- reduced step $P^* = 1{,}5$
- $Re_\infty = 20\ 000$, $Re_{it.} = 60\ 000$ (it=inter-tube)

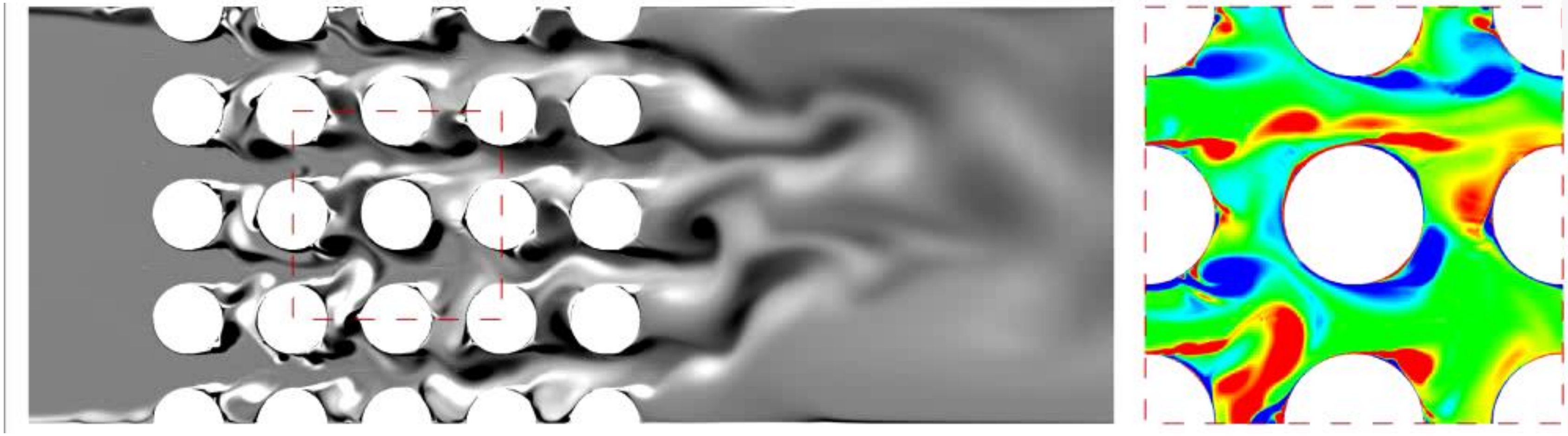

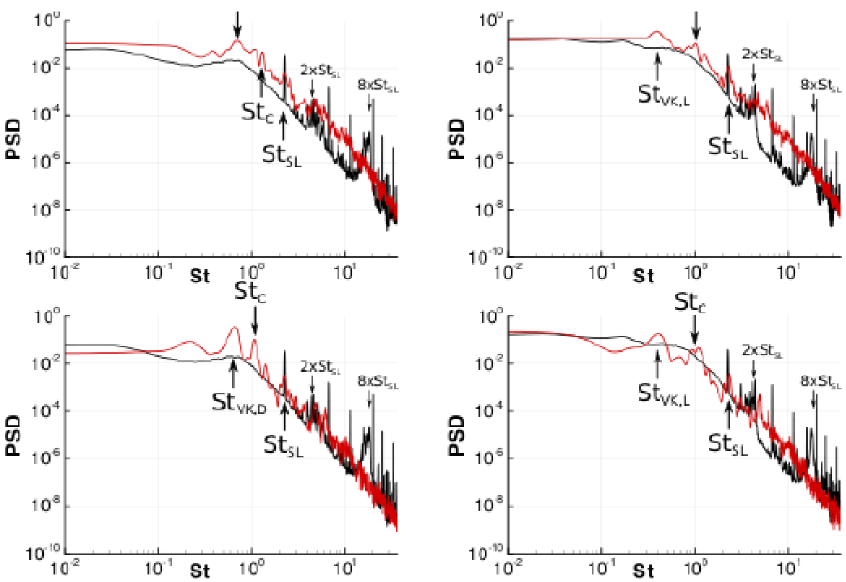

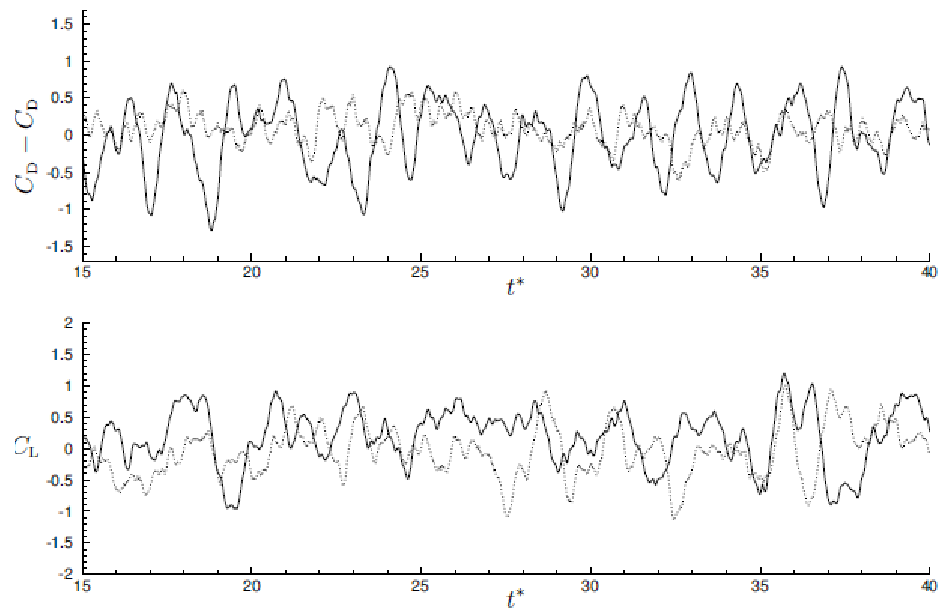

OES-k-ε – 2D

Drag and Lift coefficient (experimental data in dashed line)

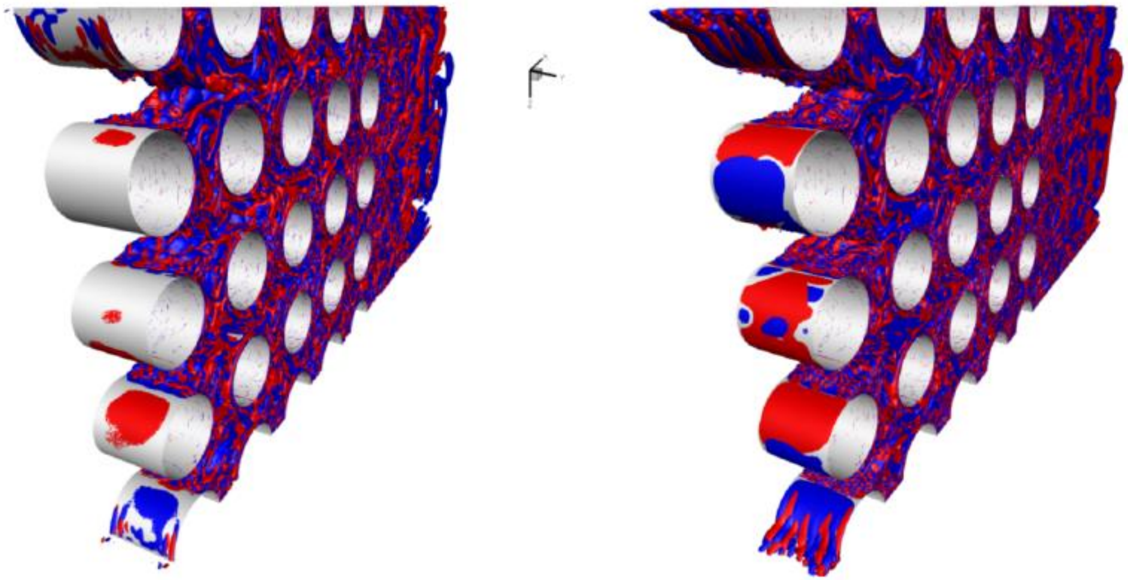

Iso-surface of vorticity (flow direction)

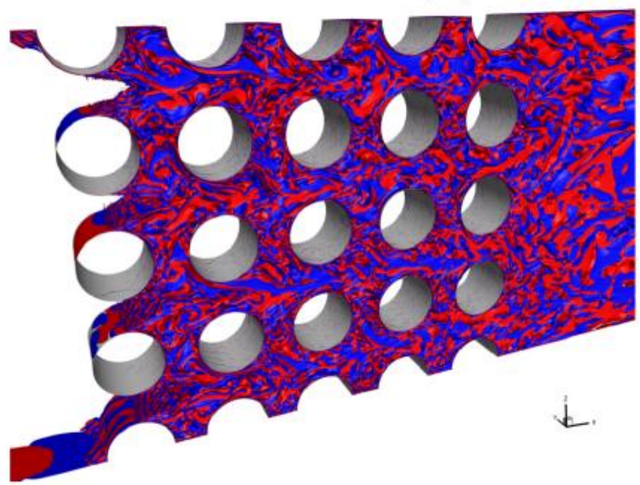

Iso-surface of vorticity (spanwise direction)

DDES-k-ω-OES

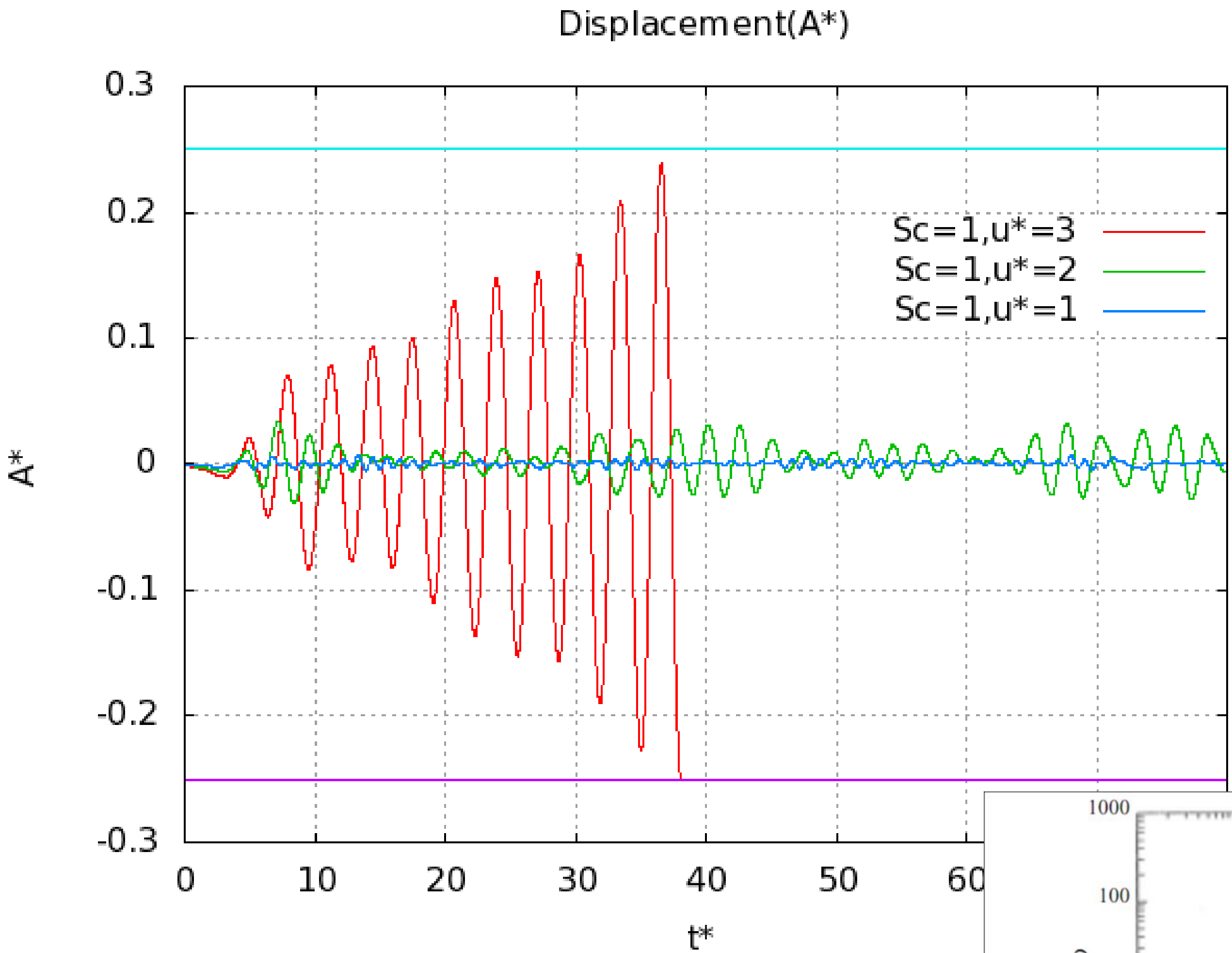

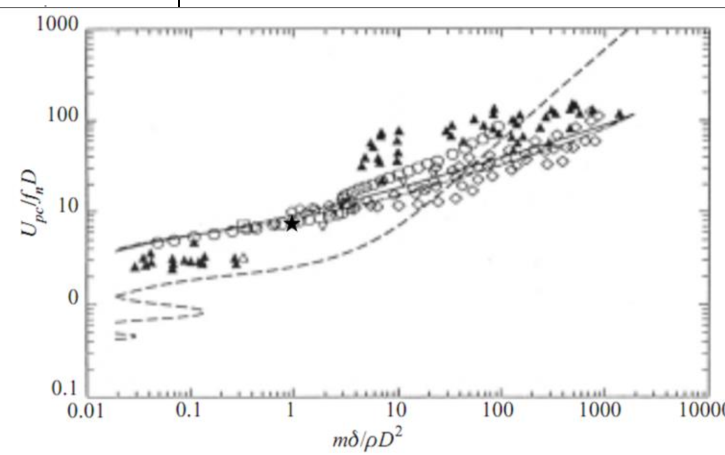

Figure 5.28. Stability boundaries for a single flexible cylinder in in-line square arrays [rep
duced from Granger & Païdoussis (1996)]: – –, Price & Païdoussis quasi-steady model; –
quasi-unsteady model ($N = 1$); – · –, quasi-unsteady model ($N = 2$). For experimental d
see Granger & Païdoussis (1996).

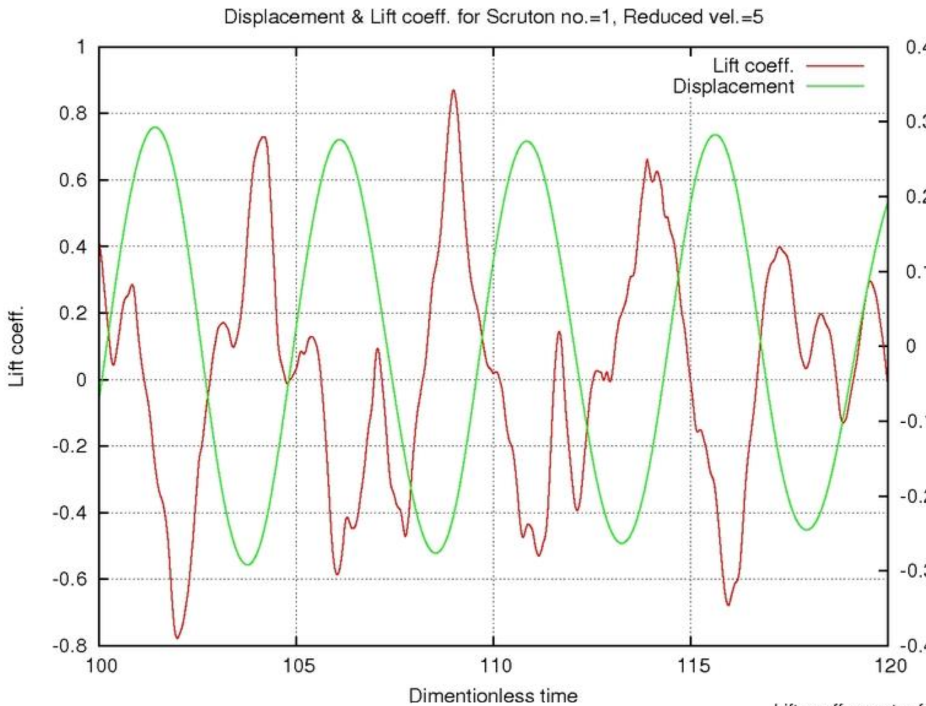

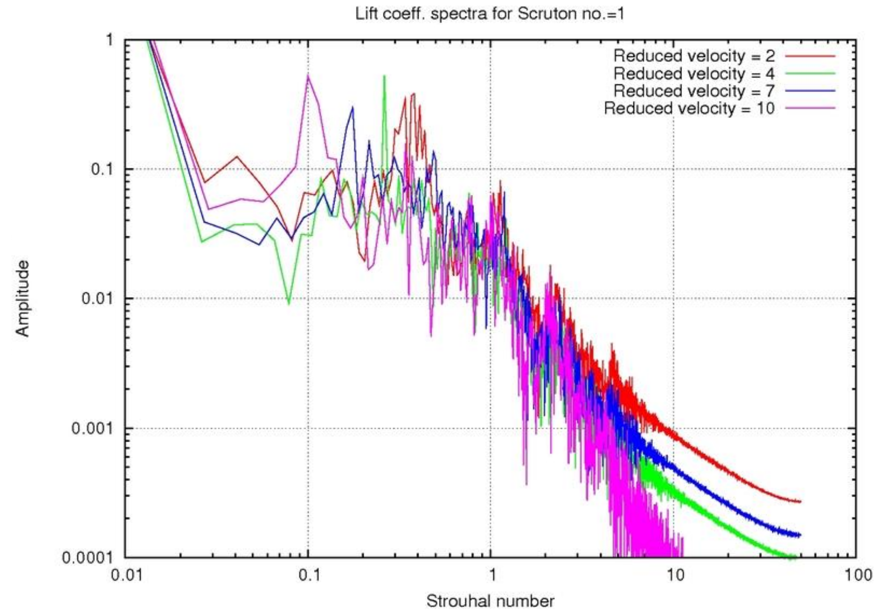

Influence du nombre de Scruton

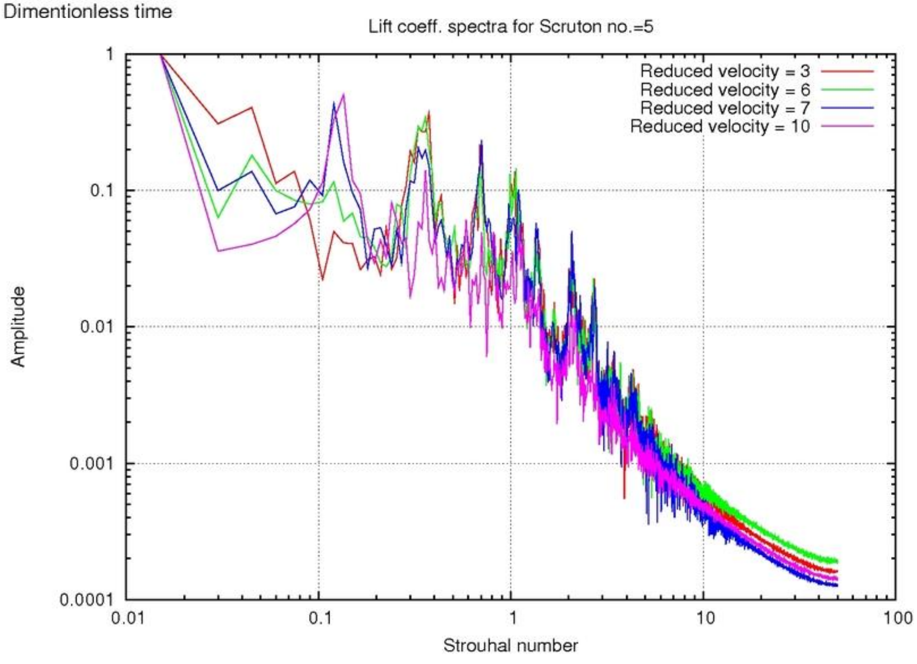

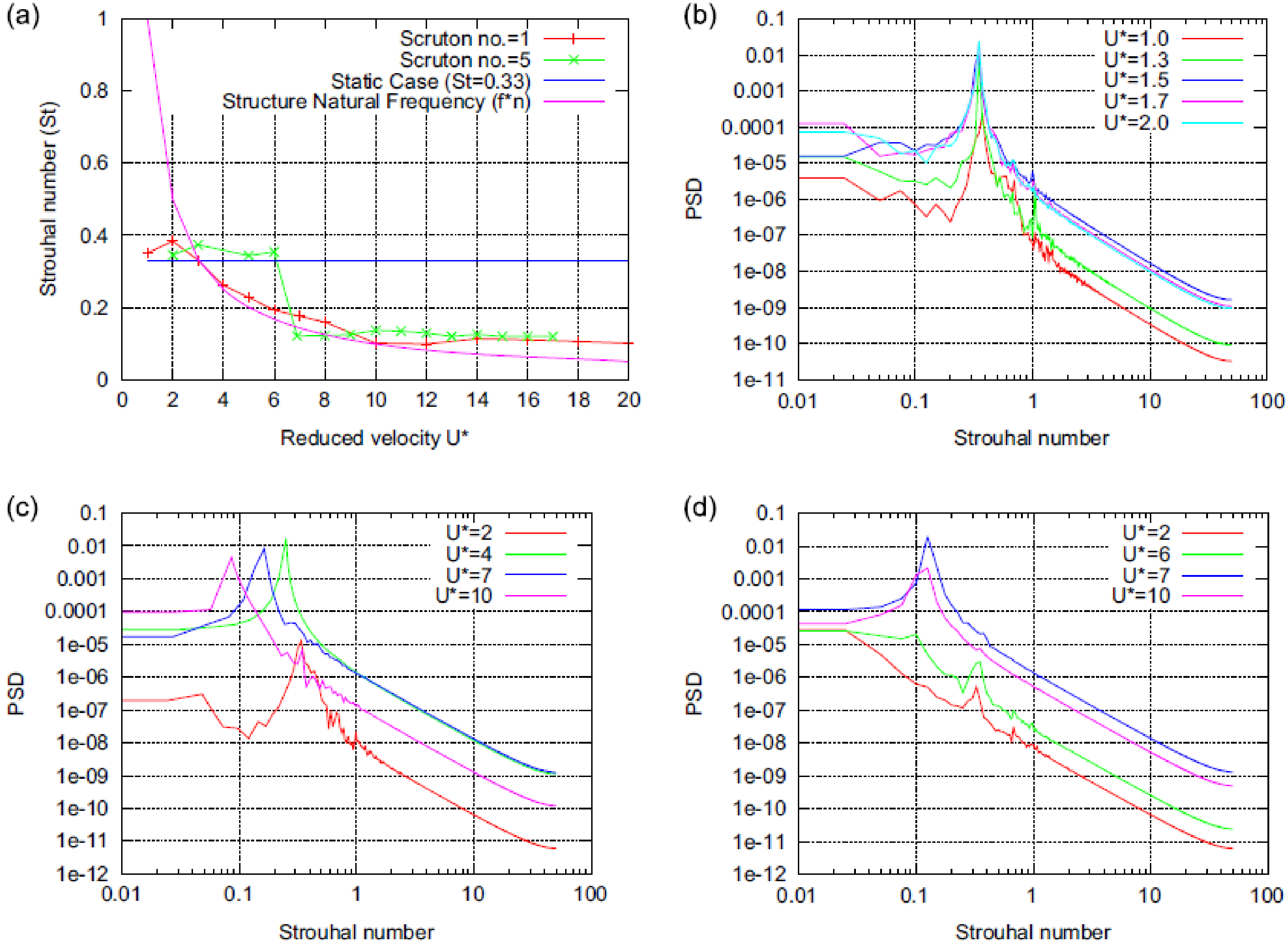

Fig. 13. 1-DOF response of the central cylinder for different values of Scruton number (Sc) and reduced velocity (U^*). (a) Variation of Strouhal number (St) in different cases, (b) frequency spectra of the central cylinder displacement for $Sc=0.0127$, (c) frequency spectra of the cylinder displacement for Scruton number $Sc=1$ and (d) frequency spectra of the displacement for Scruton number $Sc=5$. (For interpretation of the references to color in this figure caption, the reader is referred to the web version of this article.)

2D versus 3D simulations regarding comparison with exps (DIVA configuration - CEA

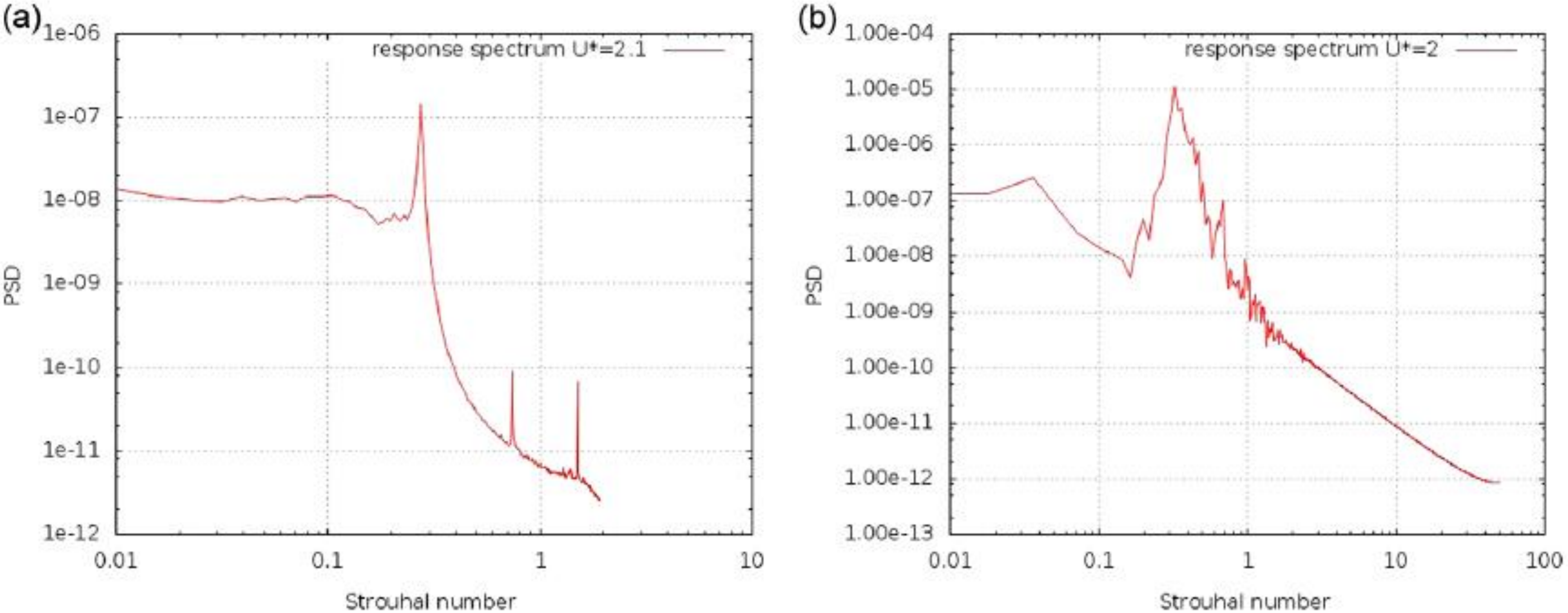

Fig. 14. Comparison of the dynamic response PSD between the experiment and the 2-D simulations, k–ω-BL-OES model.

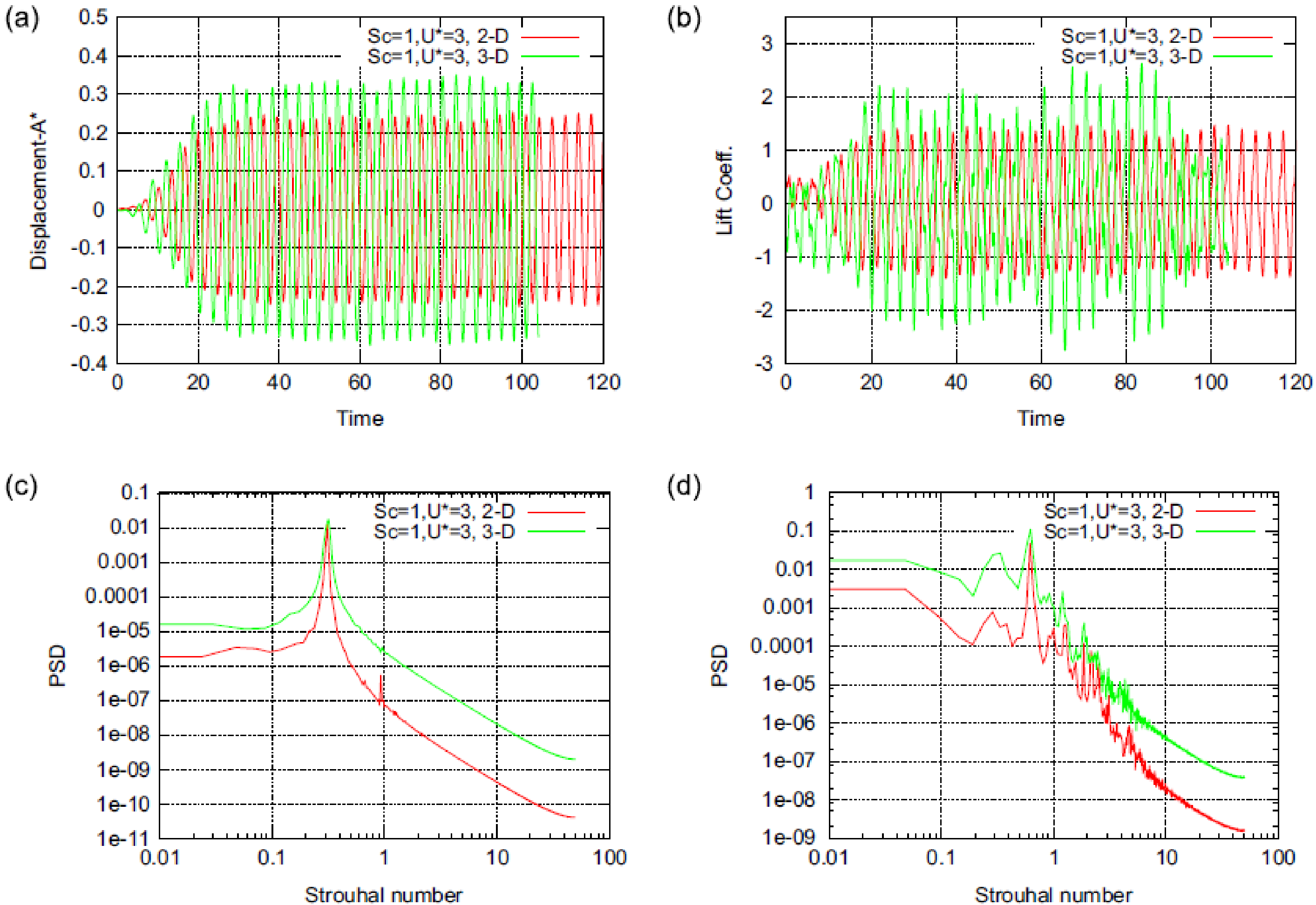

Fig. 15. Comparison between the 2D simulations carried out by the k–ω -OES model and 3D simulations carried out by the DDES-k–ω -OES model. (a) and (b) Time-histories of the cylinder displacement and of the lift coefficient respectively. (c) and (d) Spectra of the above time-histories. (For interpretation of the references to color in this figure caption, the reader is referred to the web version of this article.)

Conclusions

- Reliable prediction of the unsteady loads and fluid-elastic instabilities
- Providing good estimation even in 2D (usefulness for pre-design)
- Accurate prediction of the fluid forces and of their fluctuations in static and moving configurations
- Improvement of URANS and of DDES by OES modeling including stochastic forcing
- Hybrid URANS-LES: DDES approaches recommendable for more refined design
- Reliable Reduced order Modelling based on POD reconstruction applied to moving/deformable structures